

AD No. _____
DDC FILE COPY

ADA058110

✓
RADC-TR-78-69
Final Technical Report
March 1978

12

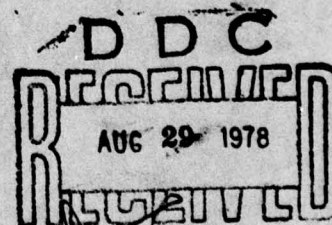


DETERMINATION OF RADAR PERFORMANCE
DEGRADATION DUE TO TROPOSPHERIC DUCTS

Raytheon Company

LEVEL #

Approved for public release; distribution unlimited



This research was supported by the Air Force In-House
Laboratory Independent Research Fund

ROME AIR DEVELOPMENT CENTER
AIR FORCE SYSTEMS COMMAND
GRIFFISS AIR FORCE BASE, NEW YORK 13441

78 08 28 012

This report has been reviewed by the RADC Information Office (OI) and is releasable to the National Technical Information Service (NTIS). At NTIS it will be releasable to the general public, including foreign nations.

RADC-TR-78-69 has been reviewed and is approved for publication.

APPROVED:

Koichi Mano

KOICHI MANO
Contract Monitor

APPROVED:

Terence J. Elkins

TERENCE J. ELKINS, Acting Chief
Propagation Branch
Electromagnetic Sciences Division

APPROVED:

Allan C. Schell

ALLAN C. SCHELL, Acting Chief
Electromagnetic Sciences Division

FOR THE COMMANDER:

John P. Huss

JOHN P. HUSS
Acting Chief

This effort was funded totally by the Laboratory Directors' Fund.

If your address has changed or if you wish to be removed from the RADC mailing list, or if the addressee is no longer employed by your organization, please notify RADC (EEP), Hanscom AFB MA 01730.

Do not return this copy. Retain or destroy.

UNCLASSIFIED

SECURITY CLASSIFICATION OF THIS PAGE (When Data Entered)

REPORT DOCUMENTATION PAGE		READ INSTRUCTIONS BEFORE COMPLETING FORM
1. REPORT NUMBER RADC-TR-78-69	2. GOVT ACCESSION NO.	3. RECIPIENT'S CATALOG NUMBER
4. TITLE (and Subtitle) DETERMINATION OF RADAR PERFORMANCE DEGRADATION DUE TO TROPOSPHERIC DUCTS	5. TYPE OF REPORT & PERIOD COVERED Final Technical Report 20 April - 31 October 1977	6. PERFORMING ORG. REPORT NUMBER BR-10101
7. AUTHOR(s) G. H. Joshi	8. CONTRACT OR GRANT NUMBER(s) F19628-77-C-0145	9. PROGRAM ELEMENT, PROJECT, TASK AREA & WORK UNIT NUMBERS 61101F 177702
10. CONTROLLING OFFICE NAME AND ADDRESS Raytheon Company, Missile Systems Division Hartwell Road Bedford MA 01730	11. REPORT DATE March 1978	12. NUMBER OF PAGES 153
13. MONITORING AGENCY NAME & ADDRESS (if different from Controlling Office) 1255 P.	14. SECURITY CLASS. (of this report) UNCLASSIFIED	15. DECLASSIFICATION/DOWNGRADING SCHEDULE N/A
16. DISTRIBUTION STATEMENT (of this Report) Approved for public release; distribution unlimited.		
17. DISTRIBUTION STATEMENT (of the abstract entered in Block 20, if different from Report)		
18. SUPPLEMENTARY NOTES This research was supported by the Air Force In-House Laboratory Independent Research Fund		
19. KEY WORDS (Continue on reverse side if necessary and identify by block number) Meteorological Ducts Radar Performance Degradation Wave Propagation Geometrical Optics Physical Optics Diffraction Zone		
20. ABSTRACT (Continue on reverse side if necessary and identify by block number) Wave propagation for anomalous meteorological conditions around Canton Island is studied by pursuing the geometrical optics and the physical optics approaches. The relative merits along with the limitations of these two approaches have been established. For ranges beyond line of sight the physical optics approach is applied to the bilinear and the tri-linear refractive index profiles. The numerical analysis to determine the real eigenvalues and the height gain functions has been carried out for the bilinear refractive index profile. This numerical analysis has been carried out for four bilinear		

DD FORM 1 JAN 73 1473 EDITION OF 1 NOV 65 IS OBSOLETE

UNCLASSIFIED

SECURITY CLASSIFICATION OF THIS PAGE (When Data Entered)

297620

UNCLASSIFIED

SECURITY CLASSIFICATION OF THIS PAGE(When Data Entered)

refractive index profiles and three wavelengths.

UNCLASSIFIED

SECURITY CLASSIFICATION OF THIS PAGE(When Data Entered)

EVALUATION

F19628-77-C-0145

1. This is the Final Report on the contract which over the period from 20 April to 31 October 1977 investigated analytically the radar performance degradation due to tropospheric ducts. With the case of low look-angle specially in mind, the physical-optics approach has been employed to study the wave propagation for the cases of bilinear and trilinear profiles of the atmospheric index of refraction.
2. The above work is of value to the Air Force since it will provide basic information which is needed for a proper evaluation of the radar performance related to the detection of low-altitude objects in the presence of the tropospheric ducts.

Koichi Mano
KOICHI MANO
Contract Monitor
Propagation Branch
Electromagnetic Sciences Division

ACCESSION FOR	
NTIS	White Section <input checked="" type="checkbox"/>
DOC	Out Section <input type="checkbox"/>
UNCLASSIFIED	<input type="checkbox"/>
JUSTIFICATION	
INSTRUMENTATION AVAILABILITY CODES	
TIME	AVAIL. AND IN SPECIAL
<i>A</i>	

PREFACE

The author would like to thank the project officers Dr. E. Altshuler, Dr. K. Mano, and Mr. M. Wong of Rome Air Development Center, for their continued interest and support throughout the project. He would also like to thank Mr. R. Roy of Raytheon for assistance in computing the solutions of the transcendental equation.

TABLE OF CONTENTS

	<u>Page</u>
1. INTRODUCTION	7
1.1 Statement of Problem	7
1.2 Report Outline	11
2. METEOROLOGICAL DATA FROM CANTON ISLAND	13
2.1 Data Format	13
2.2 Data Evaluation & Classification	13
3. GEOMETRICAL VERSUS PHYSICAL OPTICS APPROACH	28
3.1 Geometrical Optics Or Ray Trajectory Approach	28
3.2 Physical Optics Or Guided Mode Approach	34
3.3 Ray Trajectories For Four Refractive Index Profiles	36
4. GUIDED MODE APPROACH - PHYSICAL OPTICS	42
4.1 Propagation Through Stratified Media	42
4.1.1 Propagation Through the Meteorological Duct With Bilinear M-Profile	44
4.1.2 Trilinear Refractive Index Profile	51
4.1.3 Propagation Through Ducts with Trilinear Profiles	54
4.2 Solutions of the Transcendental Equation - The Bilinear Refractive Index Profile	57
4.2.1 Newton-Raphson Technique	58
4.2.2 Secant Method	59
4.2.3 Zero Crossing Technique	59
4.3 Numerical Analysis for Bilinear M-Profile	60
4.3.1 The Zero Crossing Technique For Trapped Modes	61
4.3.2 The Leaky Modes	75
4.4 Height Gain Functions For The Trapped Modes	76

TABLE OF CONTENTS (CONT.)

	<u>Page</u>
5. CONCLUSION/RECOMMENDATIONS	115
5.1 Summary	115
5.2 Recommendations	116
6. REFERENCES	117 - 118
7. APPENDIXES I and II - COMPUTER PROGRAMS	119 - 151
I-1 thru I-17	119 - 136
II-1 thru II-14	137 - 151

LIST OF ILLUSTRATIONS

		<u>Page</u>
Fig. (1-1)	M and N Profiles For Normal Atmosphere	9
Fig. (1-2)	M Profiles For (1) Normal, (2) Subrefractive and (3) Superrefractive Conditions	10
Figure (3-1) thru (3-4)	Typical Ray Trajectories	30 - 33
Fig. (3-5)	Tropospheric Duct Propagation	35
Fig. (3-6) thru (3-9)	Ray Trajectories For Canton Island - 1973	37 - 40
Fig. (4-1)	Canton Island Refractive Index Profiles For Four Days	43
Fig. (4-2)	Surface Duct - Bilinear Profile	52
Fig. (4-3)	Elevated Surface Duct - Trilinear Profile	52
Figure (4-4)	Elevated Duct - Trilinear Profile	52
Fig. (4-5) thru (4-16)	Plots of ϕ (°) as a Function of z	62 - 73
Fig. (4-17) thru (4-53)	Height Gain Functions For January, April, September and December	77 - 113

LIST OF TABLES

Table (2-1) thru (2-12)	Refractive Index Profiles For Canton Island For 1973	14 - 25
Table (4-1)	Trapped Wavelengths	60
Table (4-2)	Eigenvalues For Leaky Modes	76

1. INTRODUCTION

1.1 Statement of the Problem

The frequently occurring meteorological anomalies in certain geographical areas of the world can modify significantly the electromagnetic propagation. The modification in propagation affects the performance of the communication systems in such a fashion as to be able to communicate for distances significantly larger than what is expected during normal meteorological conditions. For ground based tactical missile systems and the long range surveillance radars, the impact is more significant. The radar systems experience range and angular errors for look angles which are greater than a couple of degrees. For elevation angles less than a couple of degrees, the systems can detect targets at significantly large distances. However the signals corresponding to these long ranges of detection are contaminated with the clutter, the primary and multiple time around. Further along with the extended detection ranges, for slightly higher elevation angles the target detection is impaired due to the existence of holes or the shadow zones.

The existence of regions of extended detection ranges, and of regions of shadow zones, are dependent on the meteorological conditions which tend to modify the refractive index profile and hence the propagation behavior. The refractive index n is related to the atmospheric pressure P , absolute temperature T , and the partial water vapor pressure e . The refractive index n is given in terms of different parameters such as N , M , and B units, etc. In this report we use only the N and M units to describe the refractive index and they are defined as follows:

$$N = (\eta - 1) \times 10^6 = \frac{k_1}{T} P + \frac{k_2 e}{T^2}$$

Here the constants k_1 and k_2 have the following empirical values.

$$k_1 = 77.6, \quad k_2 = 3.73 \times 10^5$$

For normal atmosphere N decreases uniformly with height imparting a downward bending for a ray path. On the other hand, the earth's curvature gives the appearance that the rays tilt upwards. This apparent upward tilt can be nullified by incorporating the curvature of the earth in the refractive index profile which leads to a straight trajectory for a flat earth. The media dependent bending of the ray then is described in terms of modified refractive index profile $\hat{\eta}$ or in terms of M - units, and they are defined as follows:

$$\hat{\eta} = \eta + \frac{z}{a}$$

and

$$M = (\hat{\eta} - 1) \times 10^6 = \left(\eta + \frac{z}{a} - 1\right) \times 10^6$$

Here z is the height and a is the radius of curvature of earth, ($a = 6.4 \times 10^6$ m).

Thus M and N units are related to each other in the following fashion:

$$M = \left(N + \left(\frac{z}{a} \times 10^6 \right) \right)$$

For normal meteorological conditions, the plots of M and N units as a function of height reveal that there is a steady increase of M units with height as contrast to steady decrease of N units with height and this is displayed in Fig. (1-1).

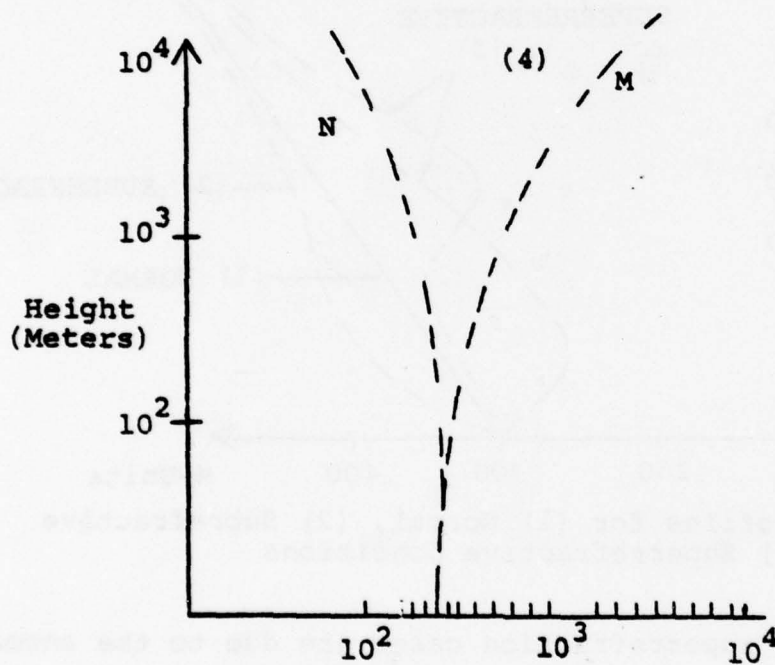


Figure (1-1) - M and N Profiles For Normal Atmosphere

During anomalous meteorological conditions the temperature and the water vapor content change in such a fashion as to cause significant deviations in the refractive index profiles and thus in the profiles of M and N as a function of height.

Some representative plots of M profiles have been reproduced in Fig. (1-2) and they, in general, fall in three major categories:

1. Normal refraction
2. Subrefraction
3. Superrefraction

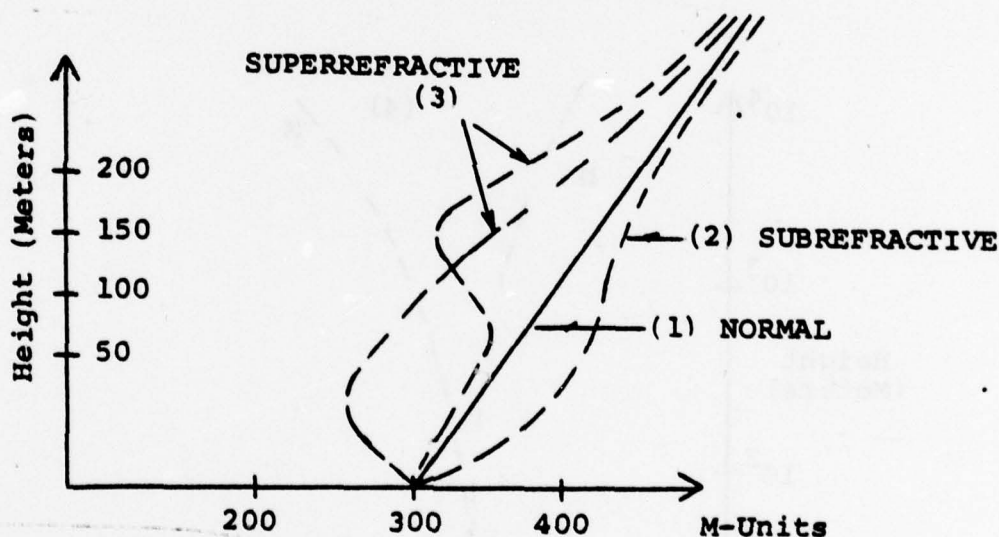


Figure (1-2) - M - Profiles for (1) Normal, (2) Subrefractive and (3) Superrefractive Conditions

The subrefraction and superrefraction cases are due to the anomalous meteorological conditions and this report deals with the electromagnetic propagation through such an anomalous medium.

1.2 The Outline of the Report

This section, Section 1, has identified the main topic of this report, namely, the determination of propagation through meteorological ducts.

For the propagation studies, the meteorological data for Canton Island was provided by ESD and Section 2 evaluates the data and classifies it in an appropriate fashion.

The electromagnetic propagation through the medium around Canton Island can be studied by geometrical optics which provides a reasonable characterization of the line of sight propagation. Section 3 discusses this approach and its limitations. The alternate approach, namely the physical optics, is also discussed in this section in order to highlight its application to the diffraction region. Section 3 further provides the ray trajectories for four days of meteorological conditions so chosen as to cover the broad spectrum of variations in the characteristic parameters of the duct such as the duct width and the lapse rate of the M units.

The primary purpose of this investigation is to develop the physical optics approach for propagation through meteorological ducts and hence details of the analytical formulation of the guided mode approach is provided in Section 4 for two refractive index profiles, bilinear and trilinear. The numerical analysis based on several techniques such as Newton-Raphson to determine the characteristic wave numbers has been carried out for the bilinear case and is

discussed in Section 4. Also, the height-gain functions which describe the dependence of electromagnetic field with height for different modes have been included in Section 4 for the bilinear refractive index profile.

Finally, the conclusions and recommendations, the references, and the different appendixes are provided in Sections 5, 6 and 7, respectively.

2. METEOROLOGICAL DATA FROM CANTON ISLAND

For the purpose of analysis, it was decided during the early stages of the contract that Raytheon will be provided with sample meteorological data from Canton Island (28°S, 171.6°W).

2.1 Data Format

The data was provided by U.S. Air Forces Environmental Technical Applications Centre at Scott Air Force Base, Illinois and was in terms of the meteorological parameters (T, P, e). Here T, P, e, respectively, stand for the temperature, the atmospheric pressure and the partial water vapor pressure. The data provides for the typical refractive index profiles for the year 1973. This data is translated into N units, M units and the rate of change of N with height in tables (2-1) through (2-12). These tables are for twelve months, with two profiles per month. The criterion that is used to determine the presence or absence of a duct is based on the condition that the rate of change of N units with height is less than $10^6/r$ where r is the radius of the earth ($r = 6.4 \times 10^6\text{m}$).

2.2 Data Evaluation and Classification

Based on this criterion, the following observations are made regarding the nature of the refractive index profile:

1. The meteorological duct was present for all the days for which the data has been provided.

2 JAN M	12 N	17 M	DN/DN
.003	387.400	387.871	
.040	378.900	385.176	-229.730
1.137	293.800	472.209	-77.5752
1.473	278.400	509.531	-45.8333
3.121	228.700	718.422	-30.1578
4.386	189.000	877.216	-31.3834
4.972	174.300	954.466	-25.0853
5.250	161.900	985.688	-44.6043
5.850	155.500	1073.44	-10.6667
6.587	141.700	1175.28	-18.7246
6.742	138.500	1196.40	-20.6452
7.590	123.700	1314.66	-17.4528
9.720	95.500	1620.68	-13.2394
11.010	83.000	1810.60	-9.68992
12.500	70.100	2031.50	-8.65772
14.300	56.500	2300.34	-7.55556
16.610	42.300	2648.61	-6.14719

3 JAN M	0 N	22 M	DN/DN	TABLE (2-1)-Jan. 1973
.003	396.100	396.571		
.042	365.400	371.990	-787.179	
.784	301.600	424.619	-85.9838	
1.470	256.200	486.861	-66.1808	
2.550	211.900	612.026	-41.0185	
3.125	207.100	697.450	-8.34783	
4.424	175.300	869.479	-24.4808	
5.455	155.500	1011.45	-19.2047	
5.860	147.900	1067.40	-18.7658	
7.590	120.600	1311.56	-15.7803	
9.730	94.800	1621.55	-12.0561	
11.070	82.300	1811.47	-9.68992	
11.358	79.400	1861.61	-8.57988	
12.520	69.600	2034.14	-8.43373	
14.330	56.500	2305.05	-7.23757	
16.161	43.300	2579.15	-7.20918	
16.703	40.600	2661.50	-4.98155	
17.495	34.200	2779.37	-8.08081	
18.774	26.600	2972.47	-5.94214	
19.986	21.600	3157.64	-4.12581	
20.660	18.800	3260.60	-4.15430	
22.026	14.700	3470.84	-3.00146	

TABLES (2-1) thru (2-12) - Refractive Index Profiles for Canton
Island For 1973

3FEB M	0 N	24 M	DN/DH
.003	344.900	395.371	
.076	351.600	363.525	-593.151
1.263	277.400	475.580	-62.5105
1.498	264.900	499.054	-53.1915
3.140	210.600	703.304	-33.0694
4.715	179.400	919.240	-19.8095
5.890	151.800	1076.01	-23.4894
7.620	121.700	1317.37	-17.3988
9.750	95.500	1625.39	-12.3005
11.030	82.800	1813.54	-9.92188
12.530	69.700	2035.81	-8.73333
14.340	56.100	2306.22	-7.51381
16.731	39.800	2645.09	-6.81723
18.240	30.000	2892.07	-6.49437
18.802	26.700	2976.96	-5.87189
20.640	19.100	3260.90	-4.09042
22.825	12.900	3594.42	-2.86374
23.192	11.900	3651.00	-2.72480
23.790	10.800	3743.74	-1.83946

5FEB M	0 N	29 M	DN/DH
.003	397.800	398.271	
.081	353.300	366.010	-570.513
1.363	257.300	471.171	-74.8830
1.403	257.100	477.247	-5.00000
1.500	250.600	485.968	-67.0103
1.872	236.900	530.639	-36.8280
2.681	209.400	630.081	-33.9926
3.146	202.300	695.945	-15.2688
5.870	148.200	1069.27	-19.8605
6.662	134.900	1180.25	-16.7929
7.610	121.200	1315.30	-14.4515
9.750	95.600	1625.49	-11.9626
11.030	82.900	1813.64	-9.92188
12.520	69.700	2034.24	-8.85906
14.340	56.200	2306.32	-7.41758
16.710	40.400	2662.40	-6.66667
17.892	32.900	2840.37	-6.34518
18.032	32.200	2861.64	-5.00000
18.325	29.900	2905.31	-7.84983
18.723	27.200	2965.06	-6.78392
20.730	19.000	3271.79	-4.08570
21.775	15.900	3432.66	-2.96651
23.860	10.700	3754.62	-2.49400
24.530	9.700	3858.75	-1.49254
25.023	8.800	3935.21	-1.82556
26.450	7.100	4157.42	-1.19131
26.778	6.700	4208.49	-1.21951
27.311	6.100	4291.52	-1.12570
30.379	3.800	4770.63	-0.749674

TABLE (2-2) - Feb. 1973

2MAR	0	29	
M	N	M	DN/DH
.003	375.100	375.571	
.062	328.500	338.229	-789.831
1.479	258.100	490.173	-49.6824
2.179	229.600	571.511	-40.7143
3.124	201.600	691.793	-29.6296
5.860	147.800	1067.30	-19.6637
6.601	135.200	1170.98	-17.0040
7.600	120.900	1313.43	-14.3143
8.357	110.700	1422.01	-13.4742
9.740	95.300	1623.62	-11.1352
11.020	82.800	1811.97	-9.76563
12.520	69.600	2034.14	-8.80000
14.330	56.300	2304.85	-7.34807
16.249	43.600	2593.26	-6.61803
16.680	40.600	2657.89	-6.96056
17.590	34.500	2794.58	-6.70330
18.679	28.400	2959.36	-5.60147
19.822	22.300	3132.61	-5.33683
20.600	18.800	3251.19	-4.49871
22.130	14.100	3486.56	-3.07190
23.175	12.000	3648.43	-2.00957
23.770	10.600	3740.40	-2.35294

3MAR	0	15		
M	N	M	DN/DH	TABLE (2-3) - March 1973
.003	391.700	392.171		
.075	373.200	384.968	-256.944	
1.494	286.000	520.426	-61.4517	
3.142	220.400	713.417	-39.8058	
4.613	185.400	909.235	-23.7933	
5.870	155.800	1076.87	-23.5481	
7.610	122.900	1317.00	-18.9080	
9.750	94.900	1624.79	-13.0841	
11.050	81.800	1815.68	-10.0769	
11.625	76.800	1900.90	-8.69565	
12.560	69.000	2039.81	-8.34225	
14.390	55.800	2313.76	-7.21311	
15.912	46.100	2542.88	-6.37319	
16.757	40.100	2669.47	-7.10059	
16.929	39.300	2695.66	-4.65116	

3 APR M	0 N	27 M	DN/DH
.003	394,900	395.371	
.075	349,000	360.768	-637.500
1.495	267,000	501.583	-57.7465
3.145	206,100	699.588	-36.9091
4.307	179,500	855.320	-22.8916
4.788	167,100	918.395	-25.7796
5.880	148,500	1071.14	-17.0330
7.610	121,400	1315.50	-15.6647
9.154	102,700	1539.07	-12.1114
9.740	95,500	1623.82	-12.2867
11.010	83,400	1811.00	-9.52756
12.500	69,900	2031.30	-9.06040
14.310	56,100	2301.51	-7.62431
16.680	40,400	2657.69	-6.62447
17.663	33,800	2805.34	-6.71414
17.871	31,700	2835.87	-10.0962
18.469	29,100	2927.11	-4.34783
18.700	27,500	2961.75	-6.92641
19.810	21,900	3130.33	-5.04505
20.700	18,800	3266.88	-3.48315
21.081	17,100	3324.96	-4.46194
23.950	10,400	3768.44	-2.33531

5 APR M	0 N	20 M	DN/DH	TABLE (2-4) - April, 1973
.003	383,600	384.071		
.085	331,300	344.638	-637.805	
1.505	251,200	487.353	-56.4085	
3.153	201,900	696.643	-29.9150	
5.262	159,000	984.671	-20.3414	
5.890	147,600	1071.81	-18.1529	
7.630	121,300	1318.54	-15.1149	
9.760	95,700	1627.16	-12.0188	
11.030	83,200	1813.94	-9.84252	
12.530	69,600	2035.71	-9.06667	
14.340	56,100	2306.22	-7.45856	
16.730	39,800	2664.94	-6.82008	
18.760	28,000	2971.67	-5.81281	
18.925	27,200	2996.76	-4.84848	
20.380	20,100	3217.97	-4.87973	
20.730	18,400	3271.19	-4.85714	
23.960	10,500	3770.11	-2.44582	
26.610	6,900	4182.33	-1.35849	
27.898	5,500	4383.03	-1.08696	
29.515	4,400	4635.66	-0.680272	

9MAY	0	32	
H	N	M	DN/DH
.003	374.000	374.471	
.084	343.400	356.581	-377.778
.887	312.200	451.381	-38.8543
1.126	274.700	451.383	-156.904
1.504	258.200	494.196	-43.6508
2.186	220.000	563.010	-56.0117
3.158	197.200	692.728	-23.4568
4.348	187.800	870.053	-7.89916
4.789	170.700	922.151	-38.7755
5.890	152.500	1076.71	-16.5304
7.620	120.400	1316.07	-18.5549
9.740	95.300	1623.62	-11.8396
11.020	83.300	1812.47	-9.37500
12.500	70.300	2031.70	-8.78378
14.300	56.600	2300.44	-7.61111
15.563	48.000	2490.02	-6.80918
16.660	34.900	2654.05	-7.38377
17.786	33.000	2823.84	-6.12789
18.700	27.000	2961.25	-6.56455
19.515	23.300	3085.44	-4.53988
19.819	21.600	3131.44	-5.59211
20.730	18.400	3271.19	-3.51262

10MAY	0	23	
H	N	M	DN/DH
.003	372.400	372.871	
.085	348.100	361.438	-296.341
.787	333.300	450.513	-22.3565
.972	300.600	453.118	-145.333
1.500	279.500	514.868	-39.9621
1.839	252.900	541.061	-78.4661
3.150	204.400	698.673	-36.9947
3.527	189.100	742.529	-40.5836
4.586	168.100	887.698	-19.8300
5.900	145.800	1071.58	-16.9711
7.620	120.400	1316.07	-14.7674
9.740	95.700	1624.02	-11.6509
11.010	83.300	1810.90	-9.76378
12.490	70.400	2030.23	-8.71622
15.281	49.500	2447.27	-7.48836
16.654	40.200	2653.41	-6.77349
19.681	22.000	3110.18	-6.01255
20.800	18.700	3282.47	-2.94906
24.026	10.400	3780.37	-2.57285
26.697	6.900	4195.98	-1.31037
30.167	3.900	4737.46	-0.864553
31.433	3.300	4935.51	-0.473934
32.904	2.600	5165.63	-0.475867

TABLE (2-5) - May, 1973

3JUN H	0 N	15 M	DN/DH
.003	364.600	365.071	
.083	336.700	349.724	-348.750
1.114	296.100	470.900	-39.3792
1.497	248.800	483.697	-123.499
1.814	237.800	522.438	-34.7003
1.950	246.200	572.178	208.824
3.136	216.400	708.476	-41.9899
3.231	195.500	702.483	-220.000
5.559	151.300	1023.57	-18.9863
5.850	155.200	1073.14	13.4021
6.282	147.600	1133.32	-17.5926
6.600	140.000	1175.62	-23.8994
7.580	120.600	1309.99	-19.7959
9.680	96.000	1614.91	-11.7143
9.799	94.400	1631.98	-13.4454

5JUN H	0 N	23 M	DN/DH
.003	371.600	372.071	
.071	344.200	355.341	-402.941
.789	320.000	443.804	-33.7047
1.486	266.300	499.471	-77.0445
1.993	224.200	536.926	-83.0375
2.974	221.200	687.856	-3.05810
3.131	207.700	698.091	-85.9873
3.794	183.500	778.824	-36.5008
4.642	175.100	903.485	-9.90566
5.212	160.800	978.625	-25.0877
5.496	164.700	1027.09	13.7324
5.850	145.900	1063.84	-53.1073
6.105	149.700	1107.65	14.9020
6.368	143.000	1142.22	-25.4753
7.580	122.400	1311.79	-16.9967
8.247	115.400	1409.45	-10.4988
9.690	96.900	1617.38	-12.8205
10.960	83.500	1803.26	-10.5512
12.440	70.300	2022.28	-8.91892
14.230	57.000	2289.86	-7.43017
14.767	53.000	2370.12	-7.44879
15.446	47.600	2471.26	-7.95287
16.590	40.400	2643.57	-6.29371

TABLE (2-6) - June, 1973

3JUL	O	34	
M	N	M	DN/DH
.003	353.300	353.771	
.075	328.600	340.364	-343.056
1.481	254.400	486.787	-52.7738
1.682	239.600	503.526	-73.6318
1.941	225.300	529.866	-55.2124
3.124	197.300	687.493	-23.6686
3.954	185.100	805.530	-14.6988
4.637	166.600	894.201	-27.0864
5.860	145.900	1065.40	-16.9256
6.905	131.000	1214.48	-14.2584
7.570	121.500	1309.32	-14.2857
8.033	115.100	1375.57	-13.8229
8.605	108.400	1458.63	-11.7133
8.883	104.700	1498.55	-13.3094
9.670	96.000	1613.34	-11.0546
10.802	84.900	1779.86	-9.80565
10.940	83.500	1800.12	-10.1449
12.420	70.700	2019.55	-8.64865

4JUL	O	31	
M	N	M	DN/DH
.003	370.300	370.771	
.067	345.900	356.413	-381.250
.888	307.800	447.138	-46.4068
1.479	237.300	469.373	-119.289
2.070	222.100	546.908	-25.7191
2.563	210.200	612.365	-24.1379
3.122	197.400	687.279	-22.8980
5.140	157.400	963.928	-19.8216
5.860	146.300	1065.80	-15.4167
7.570	121.200	1309.02	-14.6784
8.799	105.600	1486.27	-12.6932
9.680	96.400	1615.31	-10.4427
10.940	84.100	1800.72	-9.76190
12.410	71.000	2018.28	-8.91156
14.200	56.900	2265.05	-7.87709
16.006	44.300	2555.83	-6.97674
16.540	39.900	2635.22	-8.23970
17.077	36.400	2715.99	-6.51769
17.338	33.300	2753.84	-11.8774
18.640	26.200	2951.04	-5.45315
20.001	20.800	3159.20	-3.96767
20.710	18.000	3267.65	-3.94922
23.147	12.300	3684.34	-2.33898
23.950	10.500	3768.54	-2.24159

TABLE (2-7) - July, 1973

2AUG M	0 N	32	M	DN/DH
.003	371.600		372.071	
.093	347.100		361.693	-272.222
.910	303.100		445.890	-53.8556
1.500	267.200		502.568	-60.8475
1.570	235.400		481.752	-454.286
1.826	228.700		515.221	-26.1719
2.635	209.100		622.563	-24.2274
3.133	197.500		689.105	-23.2932
3.337	192.900		716.515	-22.5490
5.538	152.500		1021.46	-18.3553
5.850	147.000		1064.94	-17.6282
7.560	121.200		1307.45	-15.0877
9.660	96.900		1612.67	-11.5714
10.521	88.200		1739.07	-10.1045
10.920	83.700		1797.18	-11.2782
12.390	70.900		2015.04	-8.70748
13.595	61.400		2194.62	-7.88382
14.170	56.800		2280.24	-8.00000
15.531	47.100		2484.10	-7.12711

5AUG M	0 N	32	M	DN/DH
.003	360.700		361.171	
.084	335.300		348.481	-313.580
.549	321.000		407.145	-30.7527
1.223	278.700		470.603	-62.7596
1.483	256.200		488.900	-86.5385
3.111	196.100		686.253	-35.6860
3.620	186.800		754.821	-22.2004
4.627	167.800		893.832	-18.8679
5.820	146.800		1060.03	-17.6027
7.530	121.400		1302.95	-14.8538
8.974	103.300		1511.43	-12.5346
9.630	96.400		1607.46	-10.5183
10.600	86.800		1750.07	-9.89691
10.890	83.700		1792.47	-10.6897
12.360	71.000		2010.43	-8.63946
13.417	62.500		2167.79	-8.04163
14.150	56.700		2277.00	-7.91269
15.318	48.600		2452.18	-6.93493
16.235	41.000		2588.47	-8.28790
16.510	39.100		2629.72	-6.90909
16.992	36.400		2702.65	-5.60166
17.814	30.200		2825.43	-7.54258
18.630	26.200		2949.47	-4.90196

TABLE (2-8) - Aug., 1973

4SEP H	0 N	42 M	DN/DH
.003	391,500	391,971	
.094	370,200	384,950	-234,066
.343	355,800	409,621	-57,8313
.707	321,500	432,437	-94,2308
1.501	293,400	528,925	-35,3904
1.905	262,700	561,617	-75,9901
2.515	223,700	618,334	-63,9344
2.876	210,800	662,079	-35,7341
3.125	219,800	710,150	36,1446
3.473	205,600	750,555	-40,8046
3.986	196,400	821,851	-17,9337
4.116	199,600	845,650	26,1538
4.380	176,500	863,774	-88,2576
5.380	159,600	1003,79	-16,9000
5.650	162,500	1049,05	10,7407
5.830	153,000	1067,80	-52,7778
6.457	146,400	1159,58	-10,5263
7.530	122,300	1303,85	-22,4604
8.330	111,600	1418,68	-13,3750
8.494	112,800	1445,61	7,31707
8.599	109,500	1458,79	-31,4286
8.726	109,300	1478,51	-1,57480
8.920	104,400	1504,05	-25,2577
9.620	96,600	1606,09	-11,1429
10.561	87,300	1744,45	-9,88310

5SEP H	0 N	17 M	DN/DH
.003	386,700	389,171	
.102	353,900	369,905	-351,515
.819	301,900	430,411	-72,5244
1.151	286,700	467,306	-45,7831
1.997	246,700	560,053	-47,2813
2.232	242,700	592,928	-17,0213
2.484	223,900	613,669	-74,6032
3.139	197,600	690,147	-40,1527
4.799	164,800	917,821	-19,7590
5.809	146,900	1064,68	-17,0476
6.464	136,000	1150,88	-16,7480
7.565	121,300	1308,34	-13,8945
9.690	96,500	1616,98	-11,6786
10.607	87,200	1751,57	-10,1418
10.950	84,000	1802,19	-9,32945
12.420	70,800	2019,65	-8,97959
14.165	57,300	2279,96	-7,73639

TABLE (2-9) - Sept., 1973

7OCT	0	37	
M	N	M	DN/DH
.003	385.000	385.471	
.078	357.900	370.139	-361.333
.699	320.500	430.181	-60.2254
1.094	282.200	453.862	-96.9620
1.485	267.200	500.214	-38.3632
2.264	217.300	572.549	-64.0565
3.118	197.600	686.852	-23.0679
3.715	196.500	770.428	-1.84255
4.021	178.800	809.743	-57.8431
5.840	145.900	1062.27	-18.0869
6.290	139.600	1126.58	-14.0000
6.541	134.900	1161.26	-18.7251
7.560	121.500	1307.75	-13.1501
8.103	113.900	1385.36	-13.9963
9.670	96.000	1613.34	-11.4231
10.749	85.400	1772.05	-9.82391
10.940	83.700	1800.32	-8.90052
12.410	70.800	2018.08	-8.77551
14.200	57.000	2285.15	-7.70950
15.132	50.400	2424.79	-7.08155
15.458	47.400	2472.95	-9.20245
16.004	44.200	2555.42	-5.86061

TABLE (2-10) Oct., 1973

8OCT	0	19	
M	N	M	DN/DH
.003	375.100	375.571	
.084	353.700	366.881	-264.198
.649	317.500	419.336	-64.0708
1.488	283.100	516.585	-41.0012
2.134	259.800	594.650	-36.0681
2.262	238.800	593.735	-164.062
2.480	212.300	601.442	-121.560
3.108	210.500	698.182	-2.86624
5.830	146.300	1061.10	-23.5856
7.550	121.000	1305.69	-14.7093
9.660	96.000	1611.77	-11.8483
10.686	85.900	1762.66	-9.84405
10.920	83.600	1797.08	-9.82906
12.400	70.500	2016.21	-8.85135
14.184	57.100	2282.74	-7.51121
14.806	52.700	2375.94	-7.07395
16.530	40.500	2634.25	-7.07657
16.762	38.000	2668.16	-10.7759
18.274	28.600	2896.01	-6.21693

5 NOV M	0 N	20 M	DN/DH
.003	371.900	372.371	
.067	347.100	357.613	-387.500
.696	317.000	426.211	-47.8537
1.468	274.700	505.047	-54.7927
1.938	239.700	543.795	-74.4681
3.107	197.400	684.925	-36.1848
5.830	146.300	1061.10	-18.7661
7.550	121.900	1306.59	-14.1860
8.883	104.400	1498.25	-13.1283
9.650	96.400	1610.60	-10.4302
10.727	85.500	1768.69	-10.1207
10.910	83.700	1795.61	-9.83607
12.390	70.600	2014.74	-8.85135
14.180	56.900	2281.91	-7.65363
16.530	40.300	2634.05	-7.06383
17.324	34.300	2752.64	-7.55668
18.592	27.000	2944.31	-5.75710
18.902	24.800	2990.75	-7.09677
20.590	18.800	3249.62	-3.55450
21.516	15.700	3391.82	-3.34773

TABLE (2-11) - Nov., 1973

6 NOV M	0 N	17 M	DN/DH
.003	363.600	364.071	
.067	342.500	353.013	-329.688
1.468	269.600	499.947	-52.0343
1.698	246.600	513.037	-100.000
2.429	218.700	599.839	-38.1669
3.095	204.900	690.543	-20.7207
5.810	150.200	1061.86	-20.1473
6.163	143.400	1110.45	-19.2635
7.530	121.000	1302.55	-16.3862
9.640	96.600	1609.23	-11.5640
10.715	85.600	1766.91	-10.2326
10.900	84.000	1794.34	-8.64865
12.380	70.500	2013.07	-9.12162
13.298	63.400	2150.02	-7.73420
14.170	56.400	2274.84	-8.02752
14.457	54.400	2322.88	-6.96864
16.540	40.100	2635.42	-6.86510

30 DEC	0	27	
M	N	M	DN/DN
0.003	374.000	374.471	
0.084	355.200	368.381	-232.099
1.489	287.500	521.142	-48.1851
2.092	244.200	572.460	-71.8076
3.114	206.800	695.424	-36.5949
3.935	191.700	809.149	-18.3922
4.418	175.700	868.937	-33.1263
5.379	154.100	998.129	-22.4766
5.810	149.900	1061.56	-9.74478
6.845	130.600	1211.80	-14.5024
7.131	126.700	1245.64	-20.6992
7.520	121.400	1301.38	-13.6247
9.610	97.400	1605.32	-11.4833
10.499	87.900	1735.32	-10.6862
10.870	84.100	1789.73	-10.2426
12.340	71.300	2007.59	-8.70748
13.283	63.800	2148.06	-7.95334
14.110	57.300	2271.33	-7.85973

TABLE (2-12) - Dec., 1973

4 DEC	0	33	
M	N	M	DN/DN
0.003	366.400	366.871	
0.075	351.900	363.668	-201.389
0.956	299.200	449.208	-59.8184
1.476	272.100	503.702	-52.1154
1.872	260.800	554.539	-28.5354
2.328	231.000	596.291	-65.3509
3.101	216.800	703.384	-18.3700
4.295	182.800	856.737	-28.4757
4.456	183.000	882.200	1.24224
4.980	161.800	943.222	-40.4580
5.780	152.500	1059.45	-11.6250
6.223	145.500	1121.96	-15.8014
6.338	138.200	1132.71	-63.4783
7.490	123.700	1298.97	-12.5868
8.500	108.600	1442.35	-14.9505
9.580	96.700	1599.92	-11.0185
10.442	88.300	1726.77	-9.74478
10.840	84.600	1785.53	-9.29648
12.300	71.200	2001.22	-9.17808
12.963	66.100	2100.15	-7.69231
14.080	57.200	2266.52	-7.96777
15.819	45.200	2527.39	-6.90052
16.400	40.100	2613.46	-8.77797

2. Eighty percent of the time there existed surface ducts.
3. Twenty percent of the time the duct profiles were more complex with possible existence of elevated ducts.
4. The limited number of data points (M-units versus altitude) force to characterize the surface ducts as bilinear.
5. The duct width, under the circumstances, is inaccurately determined. For the available data, the duct width is most likely the maximum value rather than the likely value.
6. The duct intensity, as determined by the rate of change of N with height, varies from $-201/\text{km}$ to $-789/\text{km}$. The minimum intensity occurring in December and the maximum in March. The refractive index profiles based on the radiosonde data are not corrected for different measurement errors. The errors could either be sensor-related or could be the timelag in temperature and humidity measurements. Finally, the most conspicuous error is the lack of correlation between the first radiosonde data point at some altitude which is different than mean sea level and the sea level measurement.

7. The duct widths for the surface ducts, defined as the height at which the minimum for M occurs, varies from 40 meters for January 2nd to 102 meters for September 5th.
8. For the largest duct width of 102 meters, the minimum frequency that is trapped is approximately 350 MHz, and the minimum for the smallest duct of 40 meters, it is 1.43 GHz. This is based on a crude relationship between the maximum wave length trapped and the duct width.

$$\lambda_{\text{max}} \approx 0.014d^{3/2}$$

\downarrow
cm

\downarrow
feet

3. GEOMETRICAL VERSUS PHYSICAL OPTICS APPROACH

The electromagnetic propagation through a medium is governed by the refractive index profile of the medium; and it can be characterized either by the geometrical optics that is the ray treatment, or the physical optics that is the wave treatment. The distinction in the two approaches which was highlighted for optics originally, is equally valid for electromagnetic propagation.

3.1 Geometrical Optics or Ray Trajectory Approach

The geometrical optics approach is primarily based on the Fermat's principle which states that the line integral of the refractive index between two points is stationary. This leads to the well know Snell's law which states that $n_1 r_1 \cos \theta_1 = n_2 r_2 \cos \theta_2$. Here, n_1 is the refractive index at r_1 and θ_1 is the angle of inclination of the ray with the horizontal, and n_2 is the refractive index at r_2 and θ_2 is the angle of inclination at r_2 .

Based on this, a set of ray trajectories for actual refractive index profiles has been plotted to highlight the salient features of the geometrical optics approach. The ray trajectories are for a specific location for four different days in the month of August at local noon. The antenna height is 50 meters, and the elevation angle is between 0 and 1 degree. All the four ray trajectories reveal most of the features of the ground duct, namely, the trapping of the rays at angles less than 1° , the shadow regions beyond 40 km range, and the modest refraction at or above 1° elevation.

These ray trajectories reveal the cases when the geometrical optics approach is not valid. It is well established that the geometrical optics or ray treatment is valid when two conditions are satisfied and those are:

$$\frac{1}{kn} \frac{\Delta n}{n} \ll 1, \quad \frac{1}{kn} \frac{|\Delta J^{1/2}|}{J^{1/2}} \ll 1$$

Here J is the Jacobian and for detail explanation see Ref. (2), (Paes 52 - 58).

The first condition states that the relative variation of the refractive index per wavelength is smaller than unity. The second condition states that the relative density of the rays in a bundle, or the relative spacing between the rays, is less than a constant. This second condition is quite often not adequately emphasized when the geometrical optics approach is pursued. This second condition is often violated when the duct is present as is evident in the ray trajectories shown in Figures (3-1) thru (3-4). Further, the ray trajectories indicate that there exists a complete blank region with no electromagnetic energy at all, which in practice is not the case. Lastly, the geometrical optics approach is independent of frequency and polarization. This aspect prevents the geometrical optics approach from treating any scattering problems and thus the clutter which is dependent on frequency, polarization and roughness of ground or sea surface. For both communication and radar systems these considerations are of great importance, and the preferred approach is that based on physical

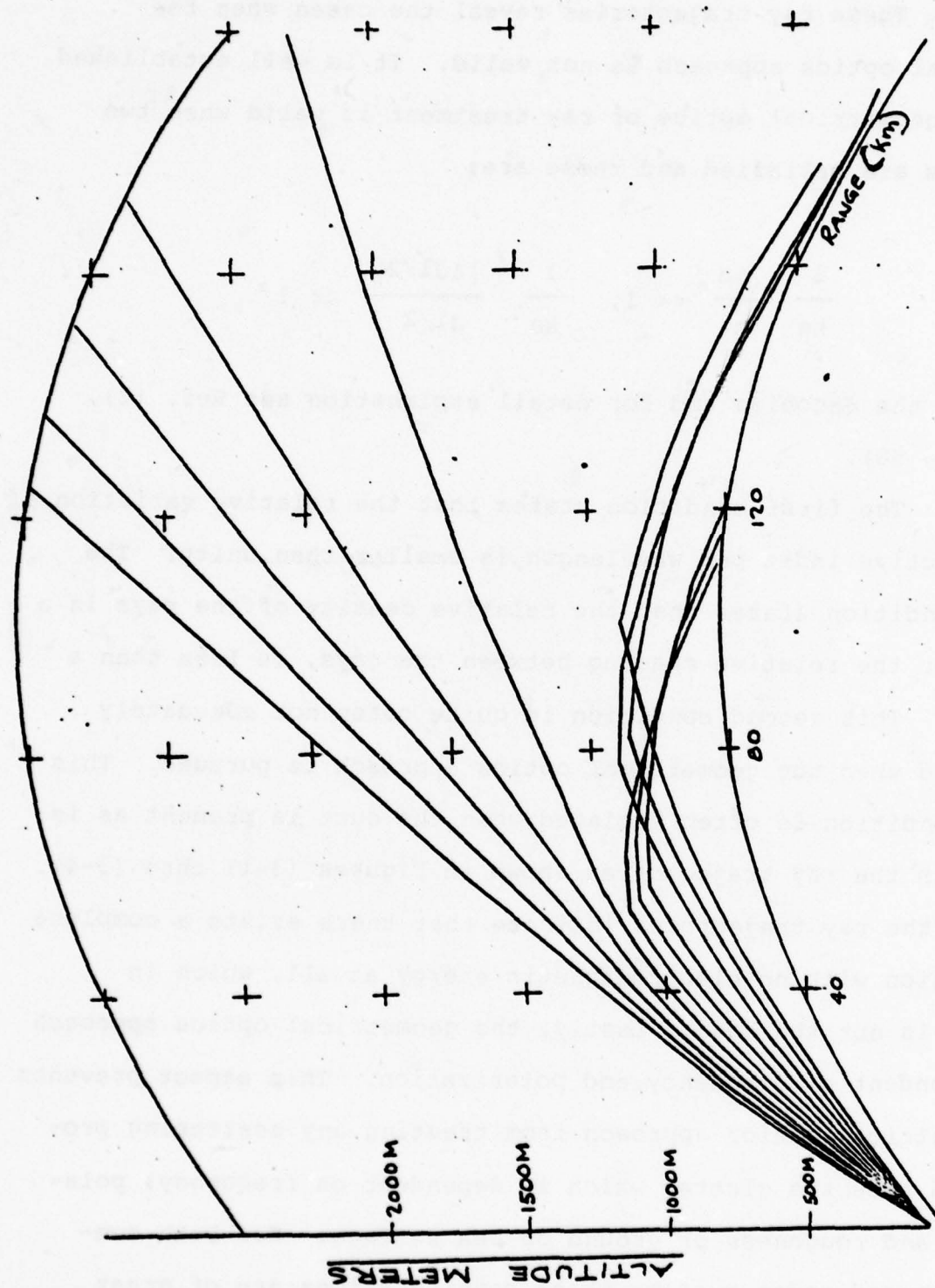


Figure (3-1) Typical Ray Trajectories for August 26

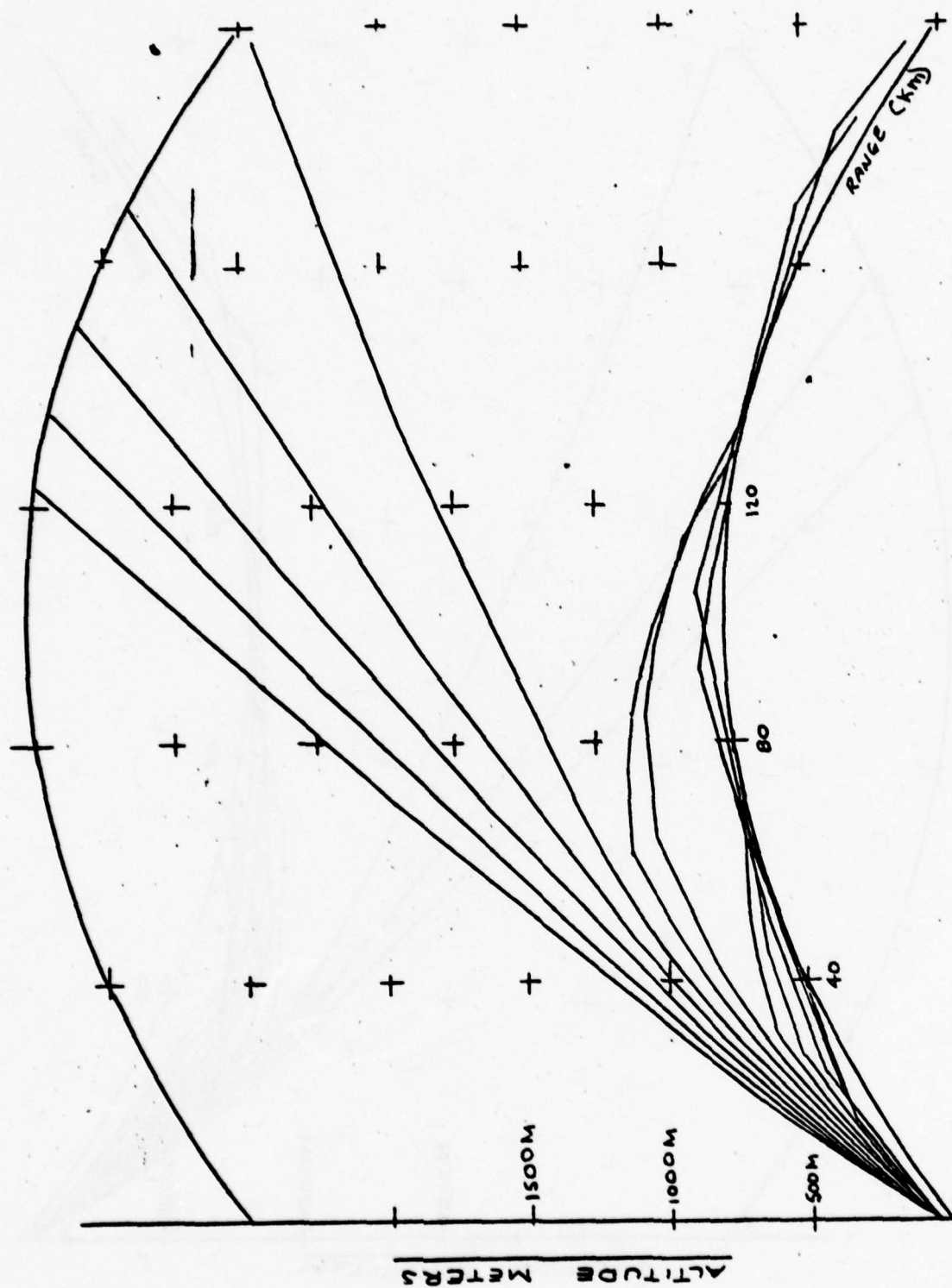


Figure (3-2) Typical Ray Trajectories for August 28

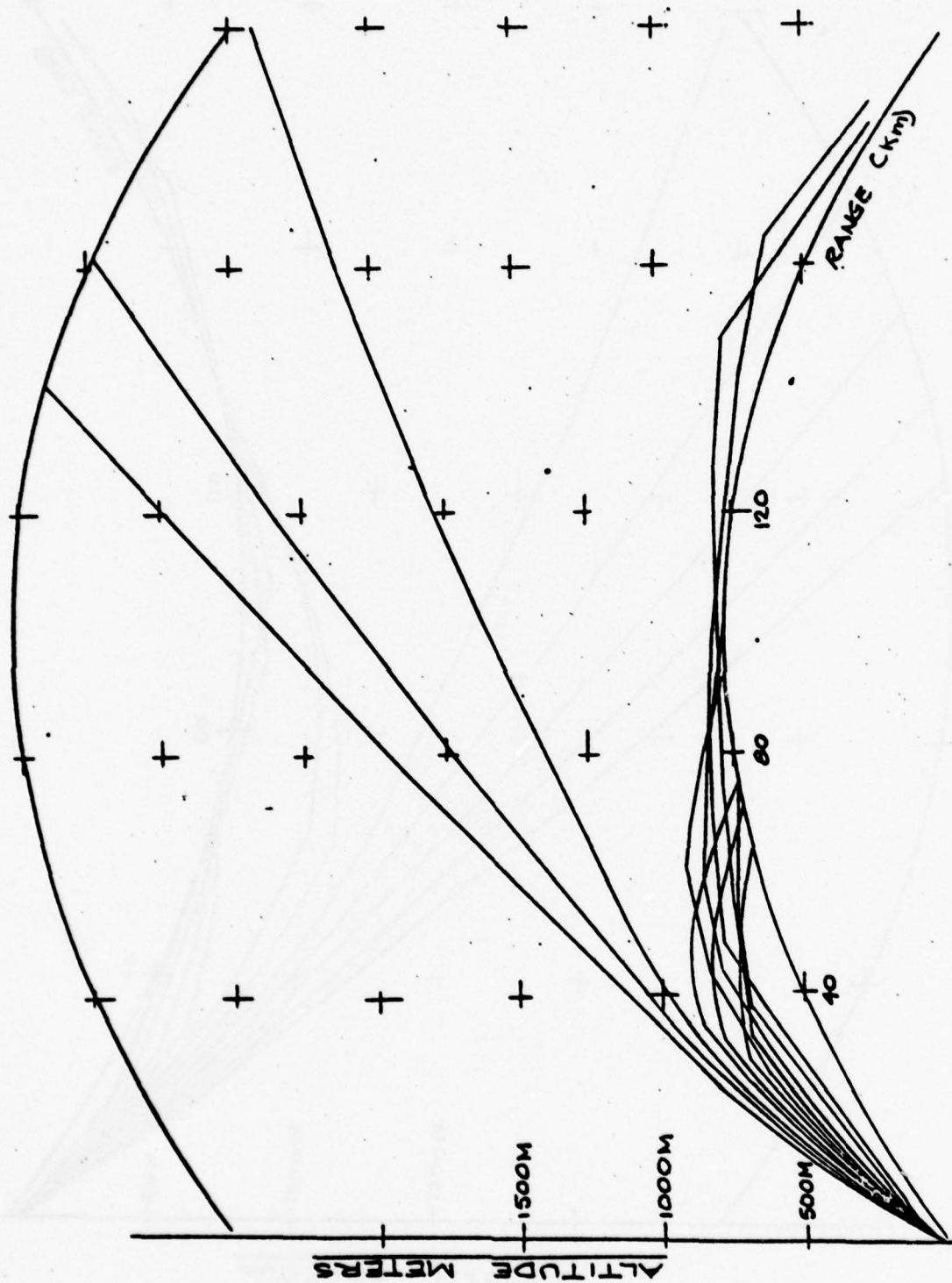


Figure (3-3) Typical Ray Trajectories for August 30

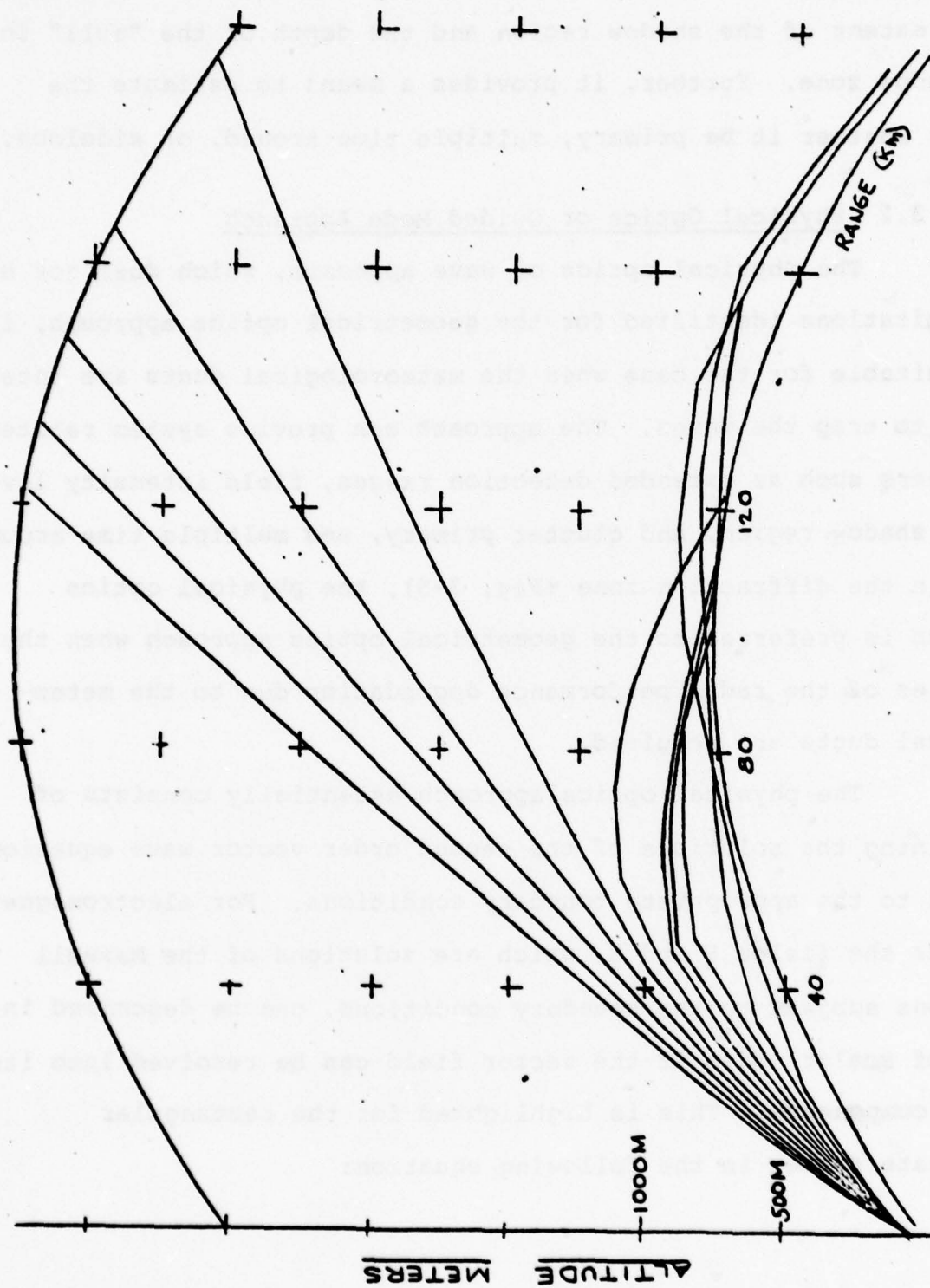


Figure (3-4) Typical Ray Trajectories for August 31

optics. The physical optics approach provides important information on the extent of the shadow region and the depth of the "null" in the shadow zone. Further, it provides a means to estimate the clutter whether it be primary, multiple time around, or sidelobe.

3.2 Physical Optics or Guided Mode Approach

The physical optics or wave approach, which does not have the limitations identified for the geometrical optics approach, is most suitable for the case when the meteorological ducts are intense enough to trap the waves. The approach can provide system related parameters such as extended detection ranges, field intensity levels in the shadow region, and clutter primary, and multiple time around. Thus, in the diffraction zone (Fig. 3-5), the physical optics approach is preferred to the geometrical optics approach when the estimates of the radar performance degradation due to the meteorological ducts are required.

The physical optics approach essentially consists of determining the solutions of the second order vector wave equation subject to the appropriate boundary conditions. For electromagnetic problems the fields \underline{E} and \underline{H} , which are solutions of the Maxwell equations subject to the boundary conditions, can be described in terms of scalar modes if the vector field can be resolved into its scalar components. This is highlighted for the rectangular coordinate system in the following equation:

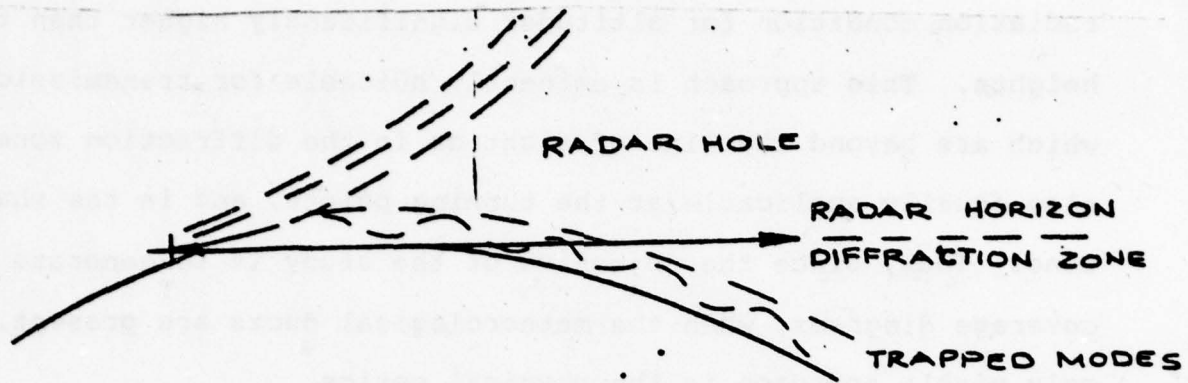


Figure (3-5) - Tropospheric Duct Propagation

$$\bar{\Phi}(\underline{r}) = \sum_i a_i \phi_i(\underline{r}) = \sum_i a_i \phi_i(T) e^{jk_{xi} \cdot x}$$

Here, $\bar{\Phi}(\underline{r})$ is the total vector electromagnetic field and is described in terms of the summation of the characteristic modes, $\phi_i(T)$; and T stands for the transverse coordinates y and z which are orthogonal to x , the direction of propagation. The longitudinal wave numbers k_{xi} are the characteristic values. The modes $\phi_i(T)$ are functions of the transverse coordinate, and they form a complete orthonormal set. The amplitude coefficient a_i thus are determined from the source conditions with the help of the orthogonality condition. Thus implicit in this approach are the characteristics of the source generating field such as frequency, polarization, antenna height, etc. Application of the boundary condition implies

the statement of the field characteristics (a) at the ground, (b) at the different regions of the M profile, and (c) the Sommerfeld radiation condition for altitudes significantly higher than the duct heights. This approach is eminently suitable for transmission paths which are beyond the line of sight or in the diffraction zone and also equally applicable at the turning points, and in the shadow zone. Thus, since the objective of the study is to generate radar coverage diagrams, when the meteorological ducts are present, the only viable approach is the physical optics.

3.3 Ray Trajectories For Four Refractive Index Profiles

The geometrical optics or the ray trajectory approach involves the use of Snell's Law to identify the propagation paths. Typical ray trajectories for four days of refractive index profiles from Canton Island are shown in Figs. (3-6 to 3-9). For January and April meteorological conditions, the existence of shadow zones are clearly noticeable. This should be evident from the strength of the duct as measured by dN/dz .

For the September and December meteorological conditions, the duct has been weak and a weak shadow zone is evident. It is to be noticed that the shadow zones of January and April will not be as pronounced as is displayed if finer intervals in the trajectory angles are chosen. Based on these trajectories, one would conclude that in the shadow zone there will be a total absence of propagation paths and hence a total absence of electromagnetic power. The question which is very pertinent for system performance evaluation is how valid is this interpretation;

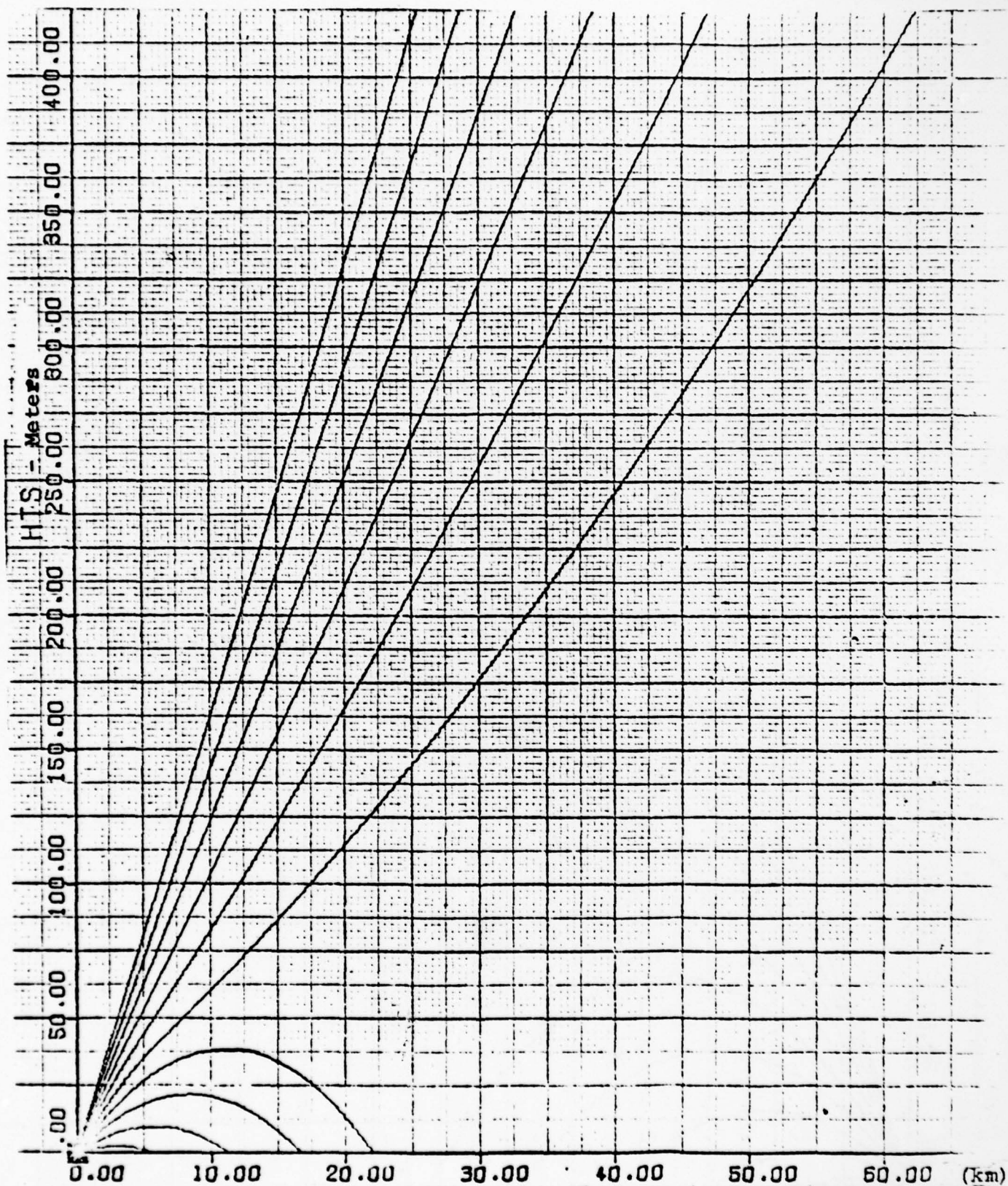


Fig. (3-6) Ray Trajectories for Canton Island - January, 1973

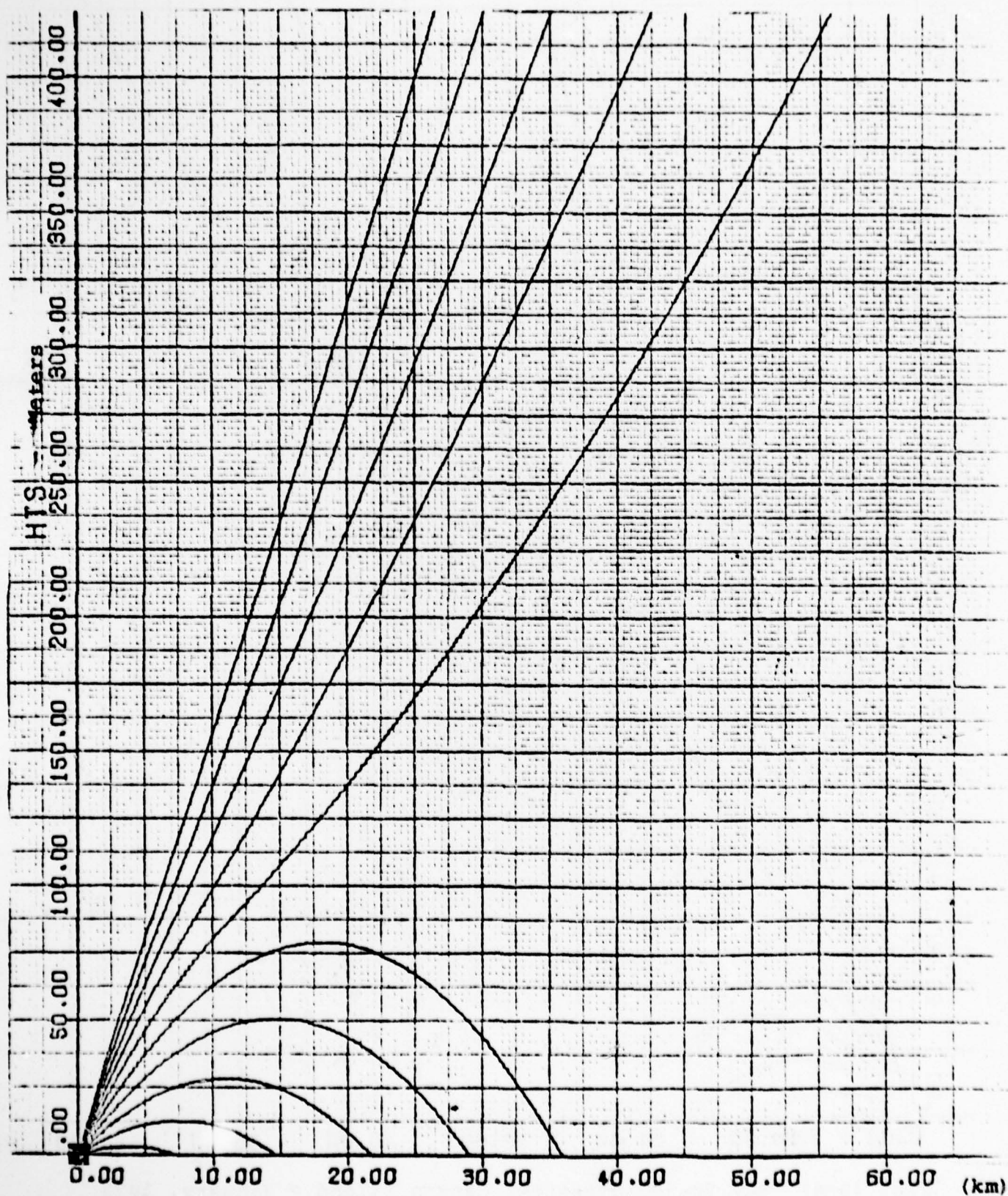


Fig. (3-7) Ray Trajectories For Canton Island - April, 1973

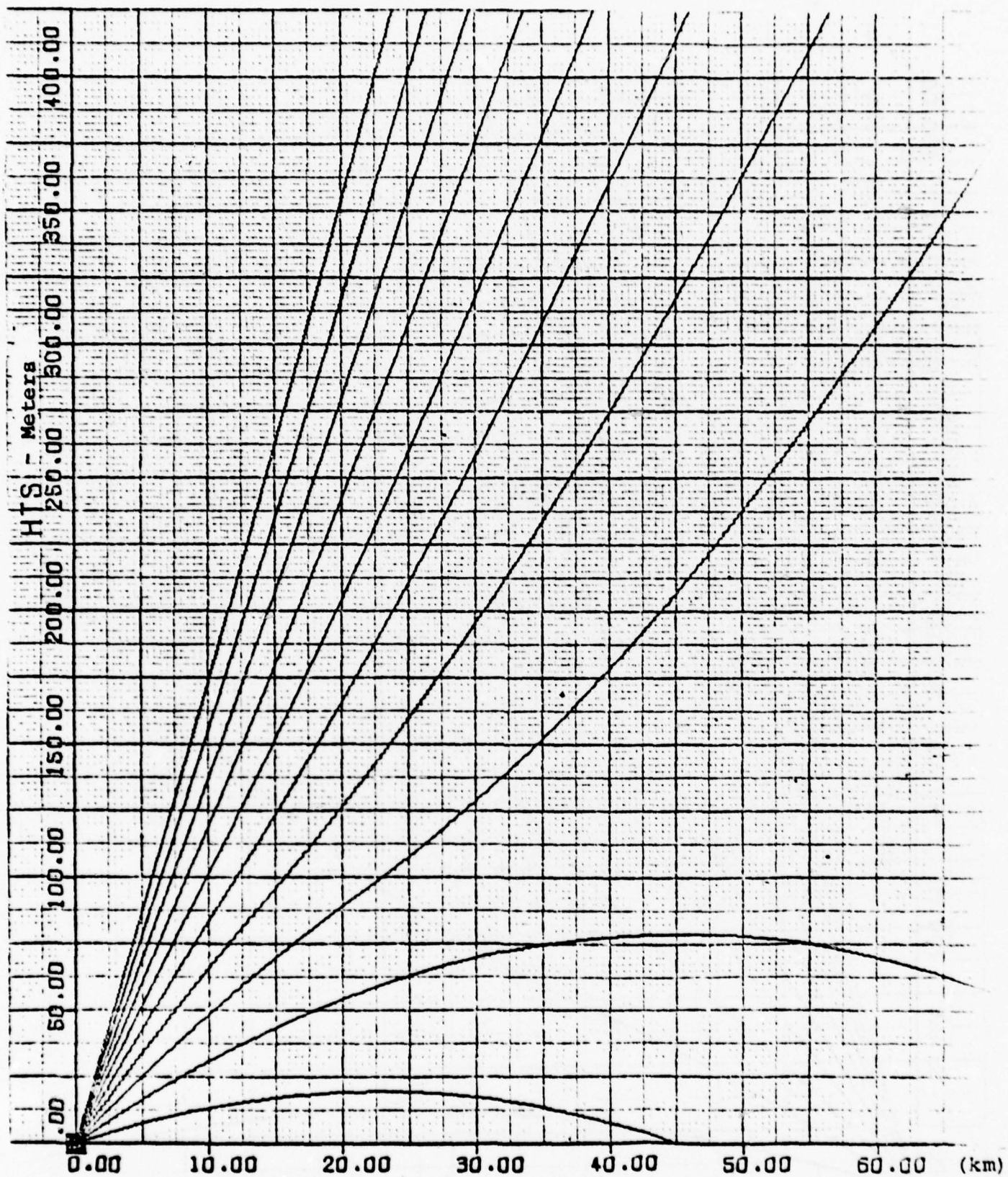


Fig. (3-8) Ray Trajectories For Canton Island - September, 1973

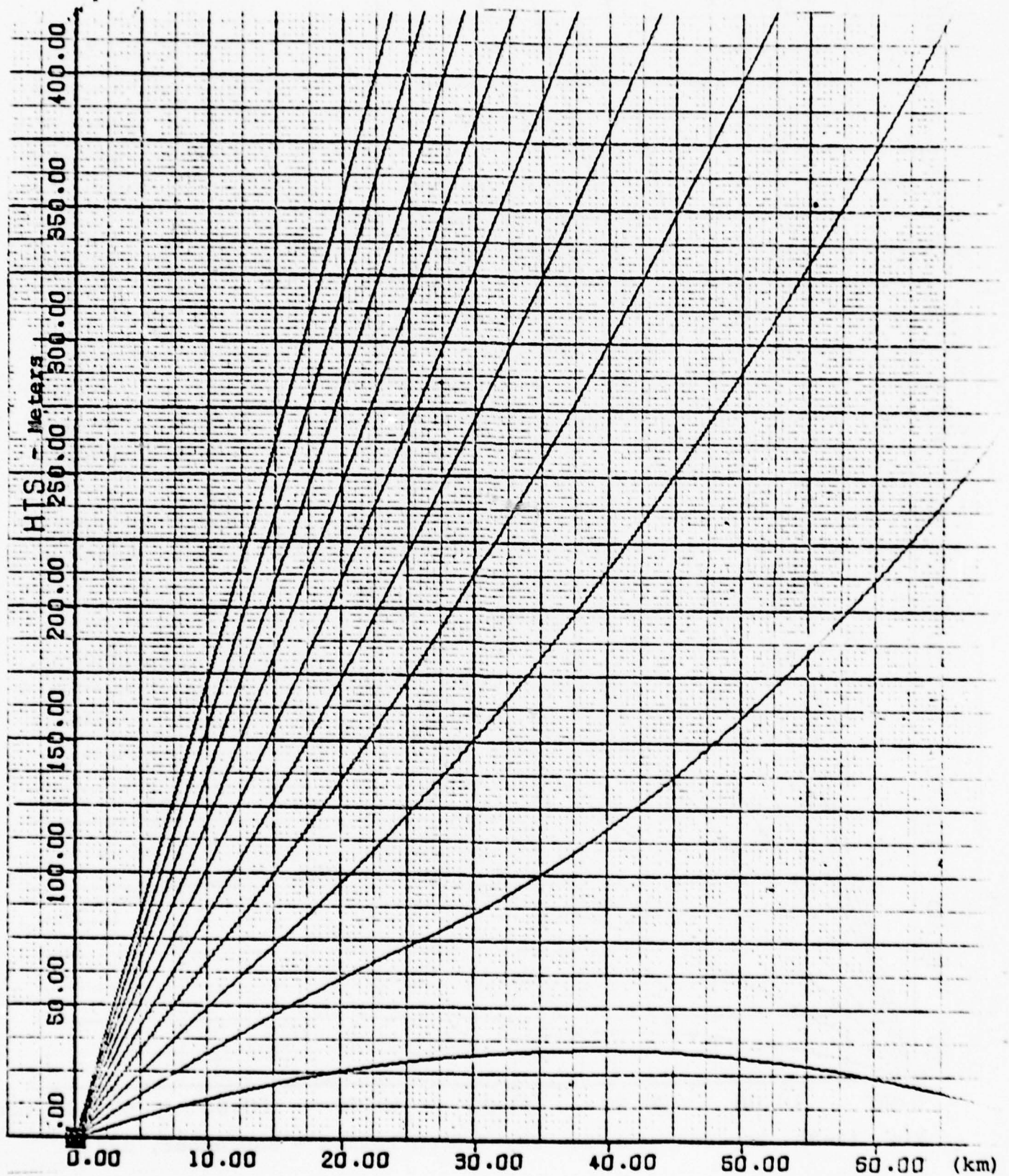


Fig. (3-9) Ray Trajectories For Canton Island - December, 1973

and is there a better way to estimate the field strength in the shadow zone.

In conclusion, it has been established that;

- a. the geometrical optics approach is not valid in the diffraction zone;
- b. it is inapplicable when the relative spacial variation of the refractive index per wavelength is larger than one;
- c. when the fractional change in the spacing between the neighboring rays in a wavelength is not less than unity, then it is not applicable.

4. GUIDED MODE APPROACH - PHYSICAL OPTICS

It is thus evident that the guided mode approach is the most viable approach to establish radar performance in the diffraction zone and in the presence of meteorological ducts. The measure of the radar system performance is either (a) in terms of radar coverage diagrams depicting signal strengths or path loss as a function of ground range and altitude, or (b) the signal to noise ratio as a function of slant range. Such a performance evaluation is mandatory for the judicious hardware/software modifications to alleviate or minimize the deleterious effects of propagation degradation. Recognizing this, the goal of this phase of the program is to determine propagation behavior in the presence of bilinear and trilinear types of refractive index profiles. The important milestone of the next phase of the program is to establish the radar coverage diagrams for different meteorological conditions and for different systems parameters.

4.1 Propagation Through Stratified Medium

For the propagation analysis, it was assumed that the medium is stratified in the vertical z direction. The stratification of the medium dictated by temperature, pressure and partial water vapor pressure variations with altitude is described in terms of the refractive index profile, which in turn is represented by the N-profile or the M-profile. The profiles which have been considered are the bilinear and trilinear. This is based on the evaluation of the Canton Island meteorological data for 1973.

The M-profile for January, April, September and December are produced in Fig. (4-1) and they will be considered in the numerical analysis.

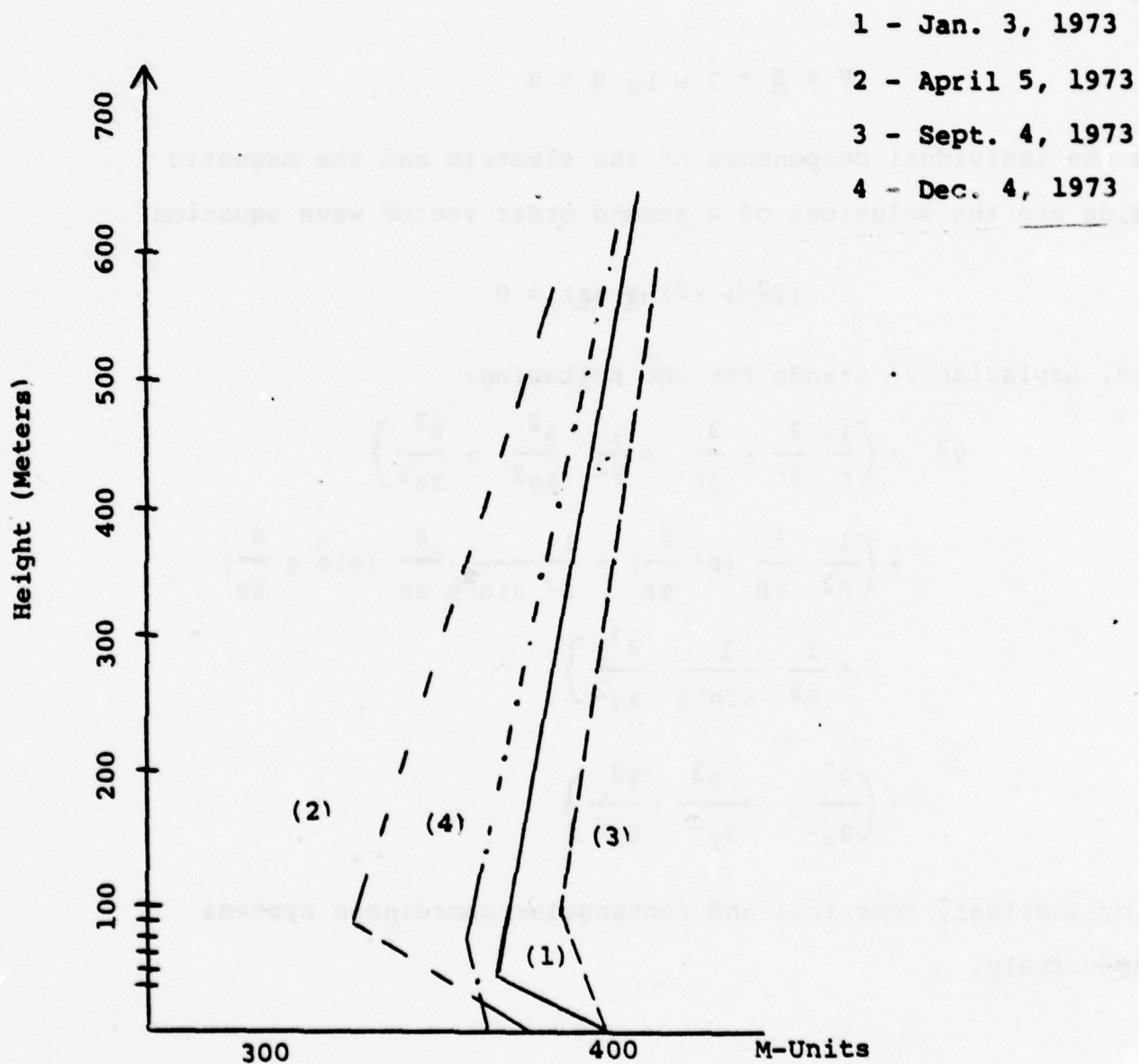


Fig. (4-1) - Canton Island Refractive Index Profiles for Four Days

4.1.1 Propagation Through The Meteorological Duct With Bilinear M Profile

The electromagnetic propagation through any medium is governed by Maxwell's equations.

$$\nabla \times \underline{H} - j \omega \epsilon_0 \underline{E} = 0$$

and

$$\nabla \times \underline{E} + j \omega \mu_0 \underline{H} = 0$$

and the individual components of the electric and the magnetic fields are the solutions of a second order vector wave equation

$$(\nabla^2 + k^2) \underline{\phi}(\underline{r}) = 0$$

Here, Laplacian ∇^2 stands for the following:

$$\begin{aligned} \nabla^2 \rightarrow & \left\{ \frac{1}{r} \frac{\partial}{\partial r} r \frac{\partial}{\partial r} + \frac{1}{r^2} \frac{\partial^2}{\partial \theta^2} + \frac{\partial^2}{\partial z^2} \right\} \\ & + \left\{ \frac{1}{R^2} \frac{\partial}{\partial R} (R^2 \frac{\partial}{\partial R}) + \frac{1}{R^2 \sin^2 \theta} \frac{\partial}{\partial \theta} (\sin \theta \frac{\partial}{\partial \theta}) \right. \\ & \left. + \frac{1}{R^2} \frac{1}{\sin \theta} \frac{\partial^2}{\partial \phi^2} \right\} \\ & + \left\{ \frac{\partial^2}{\partial x^2} + \frac{\partial^2}{\partial y^2} + \frac{\partial^2}{\partial z^2} \right\} \end{aligned}$$

in cylindrical, spherical and rectangular coordinate systems respectively.

The wave number $k = k_0 \eta$, k_0 is the free space wave number, $k_0 = \omega/c$, ω is the angular frequency and c is the velocity of light in free space. η is the refractive index of the medium.

The vector field $\underline{\Phi}$ stands for the \underline{E} and \underline{H} field

$$\underline{\Phi} = \begin{pmatrix} \underline{E}(\underline{r}) \\ \underline{H}(\underline{r}) \end{pmatrix} e^{j\omega t}$$

For a point source above ground, such as the dipole, the wave equation is more suitably described in terms of the spherical coordinate system. For the homogeneous atmosphere the mode solution of the wave equation was first obtained by Watson (18) and is given by

$$E_y = e^{j\omega t} \sum_m \frac{A_m}{x^{1/2}} e^{-jk_{xm} \cdot x} u_{m1}(z) u_{m2}(z)$$

Here, $u_{m1}(z)$ and $u_{m2}(z)$ are the height gain functions at the transmitter and the receiver, respectively; the subscript 1 stands for transmitter and 2 for the receiver. The transmitter and receiver locations have been left unspecified. For a ground radar system, the transmitter position is fixed at h and then $u_{m1}(z) \equiv u_m(h)$ is the specified antenna characteristics.

A_m are the amplitude coefficients of the modes; x is the horizontal range. Finally, the height gain function $u_m(z)$ is the solution of the one dimensional wave equation.

$$\left\{ \frac{d^2}{dz^2} + k_0^2 \hat{n}^2 - k_x^2 \right\} E_y(z) = 0$$

The x dependence has been assumed as $e^{-jk_x \cdot x}$ and $E_y(z) \equiv u_m(z)$.
The z dependence will be deleted from hereon.

The refractive index \hat{n} is assumed to be stratified only in the vertical z direction. For the chosen four days of M profile

$$\begin{aligned} \frac{dM}{dz} &= -p & z < d \\ &= +q & z > d \end{aligned}$$

d is the duct width.

The scalar wave equation for E_y is thus given by

$$\left\{ \frac{d^2}{dz^2} + k_0^2 (1 + 2M(z)) - k_x^2 \right\} E_y = 0$$

Thus for the M-profile, the wave equation takes the following form:

$$M(z) = M_0 - pz \quad z < d$$

$$M_{\min} + q(z-d) \quad z > d$$

$$\left\{ \frac{d^2}{dz^2} + B_1 - C_1 z \right\} E_y = 0 \quad z < d$$

$$\left\{ \frac{d^2}{dz^2} + B_2 + C_2 z \right\} E_y = 0 \quad z > d$$

Here $B_1 = k_0^2 (1 + 2 M_0) - k_x^2$

$$C_1 = 2k_0^2 p$$

$$B_2 = k_0^2 (1 + 2 (M_0 - pd - qd)) - k_x^2$$

$$C_2 = 2k_0^2 q$$

The wave equations are further transformed by the following change of variables

$$\xi_{<} = \frac{B_1}{C_1^{2/3}} - C_1^{1/3} z$$

$$\xi_{>} = \frac{B_2}{C_2^{2/3}} + C_2^{1/3} z$$

Thus substituting for $\xi_{<}$ in the wave equations, we have a well known Stokes equation

$$\left\{ \frac{d^2}{d\xi^2} + \xi \right\}_{<} E_{y<} = 0$$

$$\xi_{<}d = \xi_{1d} \quad , \quad \xi_{>}d = \xi_{2d}$$

$$\xi_{1d} = \frac{B_1}{C_1^{2/3}} - C_1^{1/3} d$$

$$\xi_{2d} = \frac{B_2}{C_2^{2/3}} + C_2^{1/3} d$$

$$\xi_{<} = \xi_{1d} - C_1^{1/3} (z-d)$$

$$\xi_{>} = \xi_{2d} + C_2^{1/3} (z-d)$$

and since

$$(B_1 - C_1 d) = (B_2 + C_2 d) \quad , \quad z = d$$

$$C_1^{2/3} \xi_{1d} = C_2^{2/3} \xi_{2d}$$

Finally,

$$\xi_{<0} = \xi_{10} = \frac{B_1}{C_1^{2/3}}$$

The Stokes equation now has to be solved with the help of the following boundary conditions:

$$E_{y<} = E_{y>} , \frac{dE_y}{dz} \Big|_{<} = \frac{dE_y}{dz} \Big|_{>} \quad z = d$$

For perfectly conducting earth

$$E_y = 0 \quad z = 0$$

E_y for $z \gg d$ is an outgoing wave. This condition represents the Sommerfeld radiation condition. The Stokes equation is well known and it has solutions in terms of Airy Integral Functions $A_i(\xi)$ and $B_i(\xi)$ and they are given by

$$E_{y<} = a A_i(-\xi_{<}) + b B_i(-\xi_{<})$$

$$E_{y>} = C (A_i(-\xi_{>}) + j B_i(-\xi_{>}))$$

Here, a , b and c are the coefficients to be determined by applying the boundary conditions. Note that up until now, we have not introduced any modal designate.

Application of the boundary conditions lead to the following transcendental equation

$$\frac{\left\{ A_i (-\xi_{1d}) - \frac{A_i (-\xi_{10})}{B_i (-\xi_{10})} \cdot B_i (-\xi_{1d}) \right\} \left\{ A_i' (-\xi_{2d}) + j B_i' (-\xi_{2d}) \right\}}{A_i (-\xi_{2d}) + j B_i (-\xi_{2d})}$$

$$= - \left(\frac{p}{q} \right)^{1/3} \left\{ A_i' (-\xi_{1d}) - \frac{A_i (-\xi_{10})}{B_i (-\xi_{10})} \cdot B_i' (-\xi_{1d}) \right\}$$

Here the prime refers to differentiation with respect to ξ , and

$$\frac{d}{dz} |< = \frac{d}{d\xi} \cdot \frac{d\xi}{dz} |< = - C_1^{1/3} \frac{d}{d\xi} |<$$

$$\frac{d}{dz} |> = \frac{d}{d\xi} \cdot \frac{d\xi}{dz} |> = + C_2^{1/3} \frac{d}{d\xi} |>$$

The solutions of the transcendental equations are the eigenvalues and for the fixed frequency, the wave number k_{xi} is related to the i th eigenvalue ξ_{1di} by

$$k_{xi}^2 = k_0^2 (1 + 2 M_{\min}) - \xi_{1di} \cdot C_1^{2/3}$$

$$k_{xi} \approx \left(k_0 (1 + M_{\min}) - \left(\frac{p}{q} \right)^{2/3} \cdot \frac{\xi_{1di}}{L} \right)$$

and

$$L = \left(\frac{2 k_0}{q^2} \right)^{1/3}$$

Thus, the solutions of the transcendental equation will enable one to determine the height gain functions and the eigenwave numbers along the x axis. Thus, the field corresponding to the wave numbers are completely determined with one exception, namely, the amplitude coefficients which are determined from the specification of excitation or antenna characteristics.

4.1.2 Trilinear Refractive Index Profiles

The selective meteorological data from Canton Island (Tables 2-1 through 2-12) has revealed that although, because of the nature of the measurements, majority of the cases were representable as having bilinear refractive index profiles; there were occasions when the profiles were more representable as trilinear and this in particular when the ducts were elevated. This necessitated developing an analytical propagation model for the trilinear refractive index profile. In principal, the approach is identical to the one developed for bilinear case and it entails additional boundary conditions representing matching of the transverse impedances at the intermediate regions of M-profile.

In order to display the basic features of the trilinear refractive index profile, we have reproduced in Figs. (4-2, 3, 4) some well known refractive index profiles. The Fig. (4-2) is obviously a surface duct with the bilinear M-profile, Fig. (4-3) and (4-4) are in general categorized as elevated ducts with trilinear M-profiles.

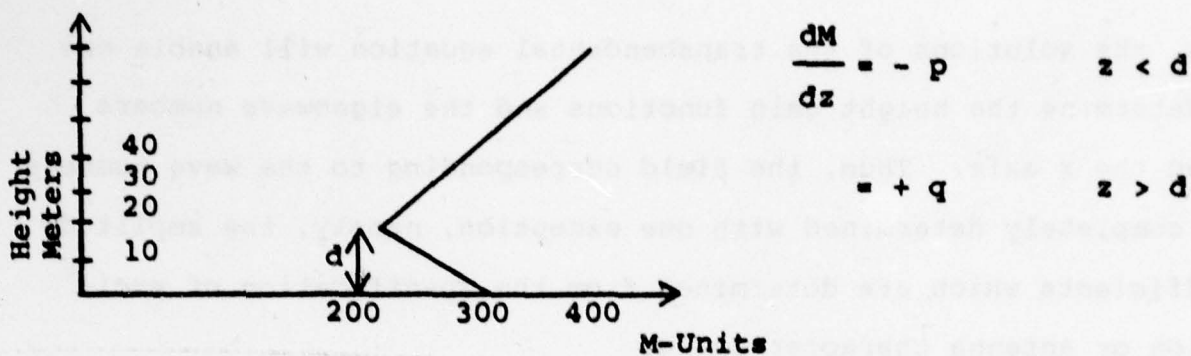


Fig. (4-2) - Surface Duct - Bilinear Profile

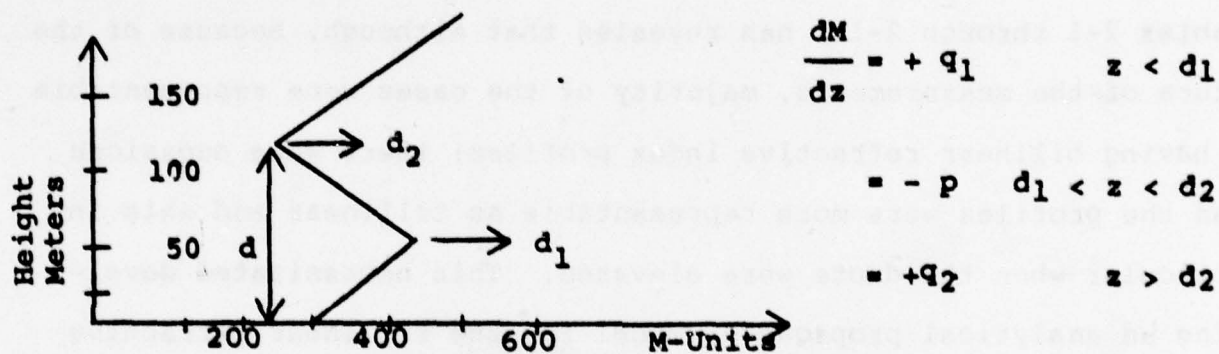


Figure (4-3) - Elevated Surface Duct - Trilinear Profile

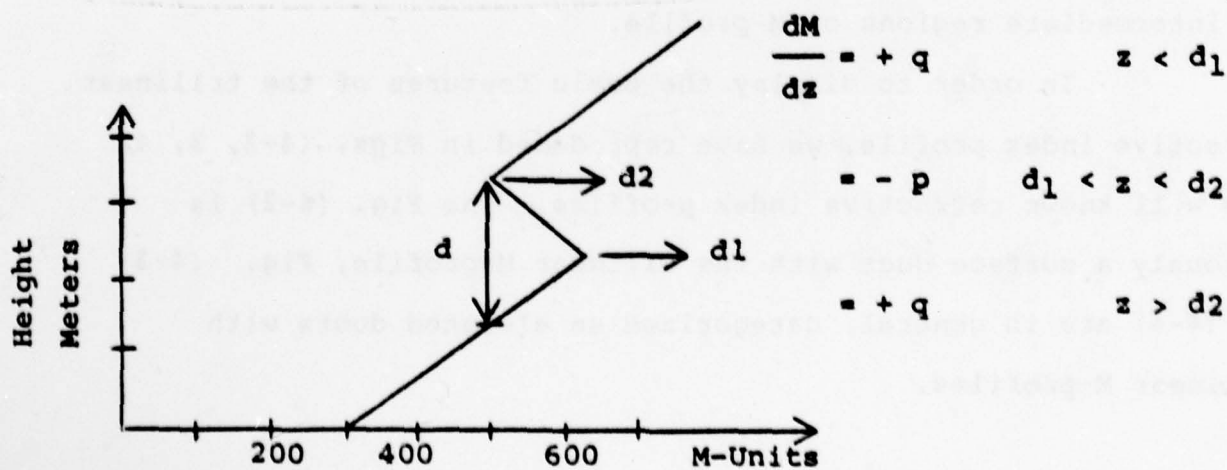


Figure (4-4) - Elevated Duct - Trilinear Profile

In all the three cases, the duct width is defined by d . In Figs. (4-3) and (4-4) note the difference in the elevated surface duct and the elevated duct. It is that at the duct apex the M_{\min} is less than the M at the surface for the elevated surface duct case, and M_{\min} is greater than M at the surface for the elevated duct. It is also to be recognized that in practice, the slope of the M -profile will not be that sharp, however, the measurement techniques perhaps would not provide closely spaced points to round off the M curves.

4.1.3 Propagation through Ducts with Trilinear Profiles

The scalar wave equation for E_y for the trilinear refractive index profiles is given by:

$$\left\{ \frac{d^2}{dz^2} + k_0^2 [1+2M(z)] - k_x^2 \right\} E_y = 0$$

$$M(z) \rightarrow M_0 + q_1 z \quad z < d_1$$

$$\rightarrow M_0 + q_1 d_1 - p(d_2 - d_1) + p(d_2 - z) \quad d_1 < z < d_2$$

$$\rightarrow M_0 + q_1 d_1 - p(d_2 - d_1) + q_2(z - d_2) \quad z > d_2$$

or

$$\left\{ \frac{d^2}{dz^2} + B_1 + C_1 z \right\} E_y = 0 \quad z < d_1$$

$$\left\{ \frac{d^2}{dz^2} + B_2 - C_2 z \right\} E_y = 0 \quad d_1 < z < d_2$$

and

$$\left\{ \frac{d^2}{dz^2} + B_3 + C_3 z \right\} E_y = 0 \quad z > d_2$$

Here B_1, C_1 ; B_2, C_2 ; and B_3, C_3 are given by

$$B_1 = k_0^2 (1 + 2M_0) - k_x^2$$

$$C_1 = 2k_0^2 q_1$$

$$B_2 = k_0^2 (1 + 2(M_0 + q_1 d_1 + p d_1)) - k_x^2$$

$$C_2 = 2k_0^2 p$$

$$B_3 = k_0^2 (1 + 2(M_0 + q_1 d_1 - p(d_2 - d_1) - q_2 d_2)) - k_x^2$$

$$C_3 = 2k_0^2 q_2$$

Let

$$\xi_{<1} = \frac{B_1}{C_1^{2/3}} + C_1^{1/3} z \quad \frac{d\xi}{dz} \Big|_{<} = +C_1^{1/3}$$

$$\xi_{<12>} = \frac{B_2}{C_2^{2/3}} - C_2^{1/3} z \quad \frac{d\xi}{dz} \Big|_{<12>} = -C_2^{1/3}$$

$$\xi_{>2} = \frac{B_3}{C_3^{2/3}} + C_3^{1/3} z \quad \frac{d\xi}{dz} \Big|_{>} = C_3^{1/3}$$

These substitutions in the wave equations lead to

$$\left\{ \frac{d^2}{d\xi^2} + \xi \right\} E_{y_1} = 0$$

$\begin{matrix} 1 & 1 & 1 \\ 2 & 2 & 2 \\ 3 & 3 & 3 \end{matrix}$

This again is the well known Spokes equation and has solutions in terms of Airy Integral functions.

Analogous to the bilinear case, the field description in the three different regions is as follows:

$$E_{y_1} = a_1 \left\{ A_i(-\xi_{<1}) - \frac{A_i(-\xi_{10})}{B_i(-\xi_{10})} B_i(-\xi_{<1}) \right\}$$

$$E_{y_2} = a_2 \{ A_i(-\xi_{<12}) + a_3 B_i(-\xi_{<12}) \}$$

$$E_{y_3} = a_4 \{ A_i(-\xi_{>2}) + j B_i(-\xi_{>2}) \}$$

The E field has to satisfy the following continuity relations:

$$\left. \begin{aligned} E_{y_1} &= E_{y_2} \\ \frac{dE_{y_1}}{dz} &= \frac{dE_{y_2}}{dz} \end{aligned} \right\} \quad \text{at } z = d_1$$

$$\left. \begin{aligned} E_{y_2} &= E_{y_3} \\ \frac{dE_{y_2}}{dz} &= \frac{dE_{y_3}}{dz} \end{aligned} \right\} \quad \text{at } z = d_2$$

These boundary conditions enable us to eliminate the different amplitude coefficients.

From now on we are specializing to the case of $q_1 = q_2 = q$. Consider first the continuity relations for field and its derivative at $z = d_1$ which lead to the following equations:

$$a_1 \left\{ A_i(-\xi_{1d1}) - \frac{A_i(-\xi_{10})}{B_i(-\xi_{10})} \cdot B_i(-\xi_{1d1}) \right\} =$$

$$a_2 \{ A_i(-\xi_{2d1}) + a_3 B_i(-\xi_{2d1}) \}$$

and

$$a_1 \left\{ A_i'(-\xi_{1d1}) - \frac{A_i(-\xi_{10})}{B_i(-\xi_{10})} \cdot B_i'(-\xi_{1d1}) \right\} =$$

$$-\left(\frac{p}{q}\right)^{1/3} \cdot a_2 \{ A_i'(-\xi_{2d1}) + a_3 B_i'(-\xi_{2d1}) \}$$

or

$$\left\{ \frac{A_i(-\xi_{1d1}) - \frac{A_i(-\xi_{10})}{B_i(-\xi_{10})} \cdot B_i(-\xi_{1d1})}{A_i'(-\xi_{1d1}) - \frac{A_i(-\xi_{10})}{B_i(-\xi_{10})} \cdot B_i'(-\xi_{1d1})} \right\} =$$

$$-\left\{ \left(\frac{p}{q}\right)^{-1/3} \cdot \frac{\{ A_i(-\xi_{2d1}) + a_3 B_i(-\xi_{2d1}) \}}{\{ A_i'(-\xi_{2d1}) + a_3 B_i'(-\xi_{2d1}) \}} \right\}$$

Let the L.H.S. $\equiv P/Q$.

then

$$a_3 = - \left\{ \frac{A_i(-\xi_{2d1}) + \frac{P}{Q} \left(\frac{p}{q}\right)^{1/3} \cdot A_i'(-\xi_{2d1})}{B_i(-\xi_{2d1}) + \frac{P}{Q} \left(\frac{p}{q}\right)^{1/3} \cdot B_i'(-\xi_{2d1})} \right\}$$

Likewise, the continuity relations at $z = d_2$ lead to the following

$$a_4 \{A_i(-\xi > d_2) + jB_i(-\xi > d_2)\} =$$

$$a_2 \{A_i(-\xi_2 d_2) + a_3 B_i(-\xi_2 d_2)\}$$

and

$$a_4 \{A_i'(-\xi > d_2) + jB_i'(-\xi > d_2)\} =$$

$$-a_2 \left(\frac{p}{q}\right)^{1/3} \cdot \{A_i'(-\xi_2 d_2) + a_3 B_i'(-\xi_2 d_2)\}$$

Thus the transcendental equation is given by

$$\left\{ \frac{A_i(-\xi > d_2) + jB_i(-\xi > d_2)}{A_i'(-\xi > d_2) + jB_i'(-\xi > d_2)} \right\} \cdot \left(\frac{q}{p}\right)^{-1/3} =$$

$$- \left\{ \frac{A_i(-\xi_2 d_2) + a_3 B_i(-\xi_2 d_2)}{A_i'(-\xi_2 d_2) + a_3 B_i'(-\xi_2 d_2)} \right\}$$

where

$$a_3 = - \frac{\left\{ A_i(-\xi_2 d_1) + \frac{p}{q} \left(\frac{p}{q}\right)^{1/3} \cdot A_i'(-\xi_2 d_1) \right\}}{\left\{ B_i(-\xi_2 d_1) + \frac{p}{q} \left(\frac{p}{q}\right)^{1/3} \cdot B_i'(-\xi_2 d_1) \right\}}$$

4.2 The Solutions of the Transcendental Equation - The Bilinear Refractive Index Profile

The transcendental equation which is arrived at by satisfying the boundary conditions at $z=d$, physically represents the matching of the transverse impedances at $z=d$.

$$Z_{z<} = Z_{z>}$$

or equivalently $\phi(Z) \equiv (Z_{z<} - Z_{z>}) = 0$

Here

$$\mathcal{Z}_z = H_x \frac{\frac{E_y}{Y} \propto \frac{E_y}{Y}}{\frac{dE_y}{dz}}$$

and $\mathcal{Z}_z<$, $\mathcal{Z}_z>$ are the transverse impedances for $z<d$ and $z>d$, respectively.

Because of the nature of the transcendental equation, a closed form solution does not exist and an iterative, numerical procedure to locate the zeros of the function $\phi(\mathcal{Z})$ has to be adopted. Three different approaches have been explored, and they are:

- a. The Newton-Raphson Method
- b. The Secant Method
- c. The Zero Crossing Method

4.2.1 The Newton-Raphson Technique

This technique, essentially, provides a procedure to obtain an approximate solution of the transcendental equation which, after several iterations, approaches the exact solution and it states

$$\mathcal{Z}_1 = \mathcal{Z}_0 - \frac{\phi(\mathcal{Z}_0)}{\phi'(\mathcal{Z}_0)}$$

Here, \mathcal{Z}_0 is the first trial solution of the transcendental equation $\phi(\mathcal{Z}) = 0$. $\phi'(\mathcal{Z}_0)$ is the derivative of ϕ with respect to \mathcal{Z}_0 and \mathcal{Z}_1 is the next better solution to be used for second iteration and so on. Thus, the i th solution is obtained from $(i-1)$ th and is

$$\mathcal{Z}_i = \mathcal{Z}_{i-1} - \frac{\phi(\mathcal{Z}_{i-1})}{\phi'(\mathcal{Z}_{i-1})}$$

If the transcendental equation has n solutions then this procedure has to be repeated n times.

The Newton-Raphson iterative technique to locate the zeros of the transcendental equation is effective only when the trial solution is reasonably close to the actual solution. The Newton-Raphson procedure thus has severe limitations.

4.2.2 The Secant Method

This iterative approach is analogous to the Newton-Raphson approach and the iterative solutions are given by

$$z_i = z_{i-1} - \frac{(z_i - z_{i-1})\phi(z_{i-1})}{\phi(z_i) - \phi(z_{i-1})}$$

Note that in the limit when z_i approaches the exact solution z_{i-1} , then this expression is identical to the Newton-Raphson expression. Alternatively, if $z_i - z_{i-1} \ll \delta$ and if $\phi(z_{i-1}) - \phi(z) \ll \epsilon$ then the technique is identical with the Newton-Raphson technique. Here δ and ϵ are very small quantities.

4.2.3 The Zero-Crossing Technique

Another technique which is applicable to determine the solutions of the transcendental equation is the zero crossing of $\phi(z)$, when $\phi(z)$ is plotted as a function of z . This procedure is extremely effective for the trapped modes or when the ξ_{ldi} are pure real, positive or negative numbers.

In any case, for all three cases, the computer programs for the Airy Integral Functions and the Hankel Functions are required.

4.3 Numerical Analysis For Bilinear M-Profile

It was decided that four meteorological profiles will be chosen in such a fashion that the two extremes of the characteristic parameters such as the duct height and duct intensity shall be chosen.

For the 3rd of January, the intensity of the duct was close to the maximum; for the 4th of December, the duct intensity was minimum. For the 4th of September the duct height was close to the largest while January 3rd it was close to the smallest. For the 5th of April the duct was moderately intense. For all four days, the profile was describable as bilinear. Finally, in order to extract the frequency dependence, three wavelengths were chosen, and they were 10, 20 and 50 cm.

Based on the expression for the maximum wavelengths that are trapped by ducts of height d , the following observation is made:

Table (4-1) - Trapped Wavelengths

Date	d (meters)	λ max (cm)
3rd Jan.	42	22.65
5th Apr.	85	65.20
4th Sept.	94	75.82
4th Dec.	75	54.04

- a. For 10 and 20 cm wavelengths the field is trapped for all the four cases.
- b. For 50 cm wavelengths the field is not trapped for Jan. 3rd case, however, it is trapped for the remaining three days.

4.3.1 The Zero-Crossing Technique For Trapped Modes

For the four days of M-profile data and for three wavelengths 10, 20 and 50 cm, the transcendental function $\phi(\xi)$ is plotted for various real values of ξ varying from -5 to +5. These plots are displayed in Figs. (4-5 to 4-16). The zero-crossing values of ξ , or equivalently ξ_{1d} , for which $\phi(\xi) = 0$ are the solutions of the transcendental equation. Consider now the January 3rd profile and $\lambda = 10$ cm case (Fig. 4-5). The zero-crossings take place for the following ξ_{1d} values:

$$\xi_{1d} = -1.25, 0.68, 2.8, 5.25$$

First observe that the zero-crossing at -1.67 is not a true crossing as is evident from the computations for finer spacings of the ξ_{1d} values. The $\phi(\xi)$ will continue to decrease approaching $-\infty$ for ξ_{1d} values in the vicinity of -1.65. Likewise for $\xi_{1d} \rightarrow -1.68$, the $\phi(\xi)$ will increase approach $+\infty$; hence no zero-crossing for $\xi_{1d} = -1.67$ is possible.

The first ξ_{1d} for which $\phi(\xi) = 0$ is -1.25 and this negative root needs to be interpreted. Consider the field E_y associated with this root and observe how it behaves as the height increases from $z=0$ to $z=d$ and $z \gg d$.

λ - 0.1
 a - 42.0
 p/a - 4.8

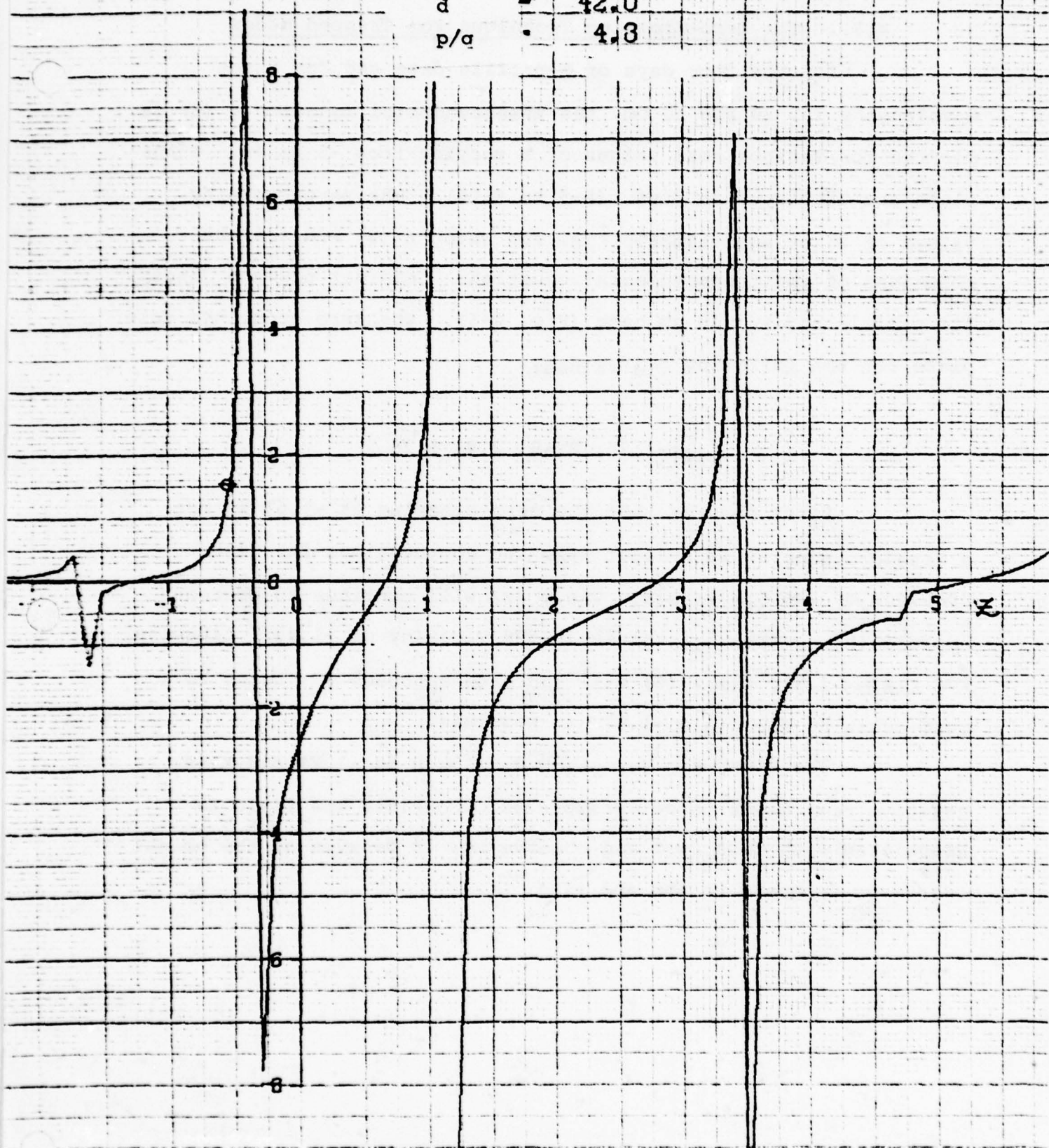


FIG. (4-5) PLOTS OF $\Phi(z)$ AS A FUNCTION OF z

λ	-	0.2
d	-	42.0
p/τ	-	4.8

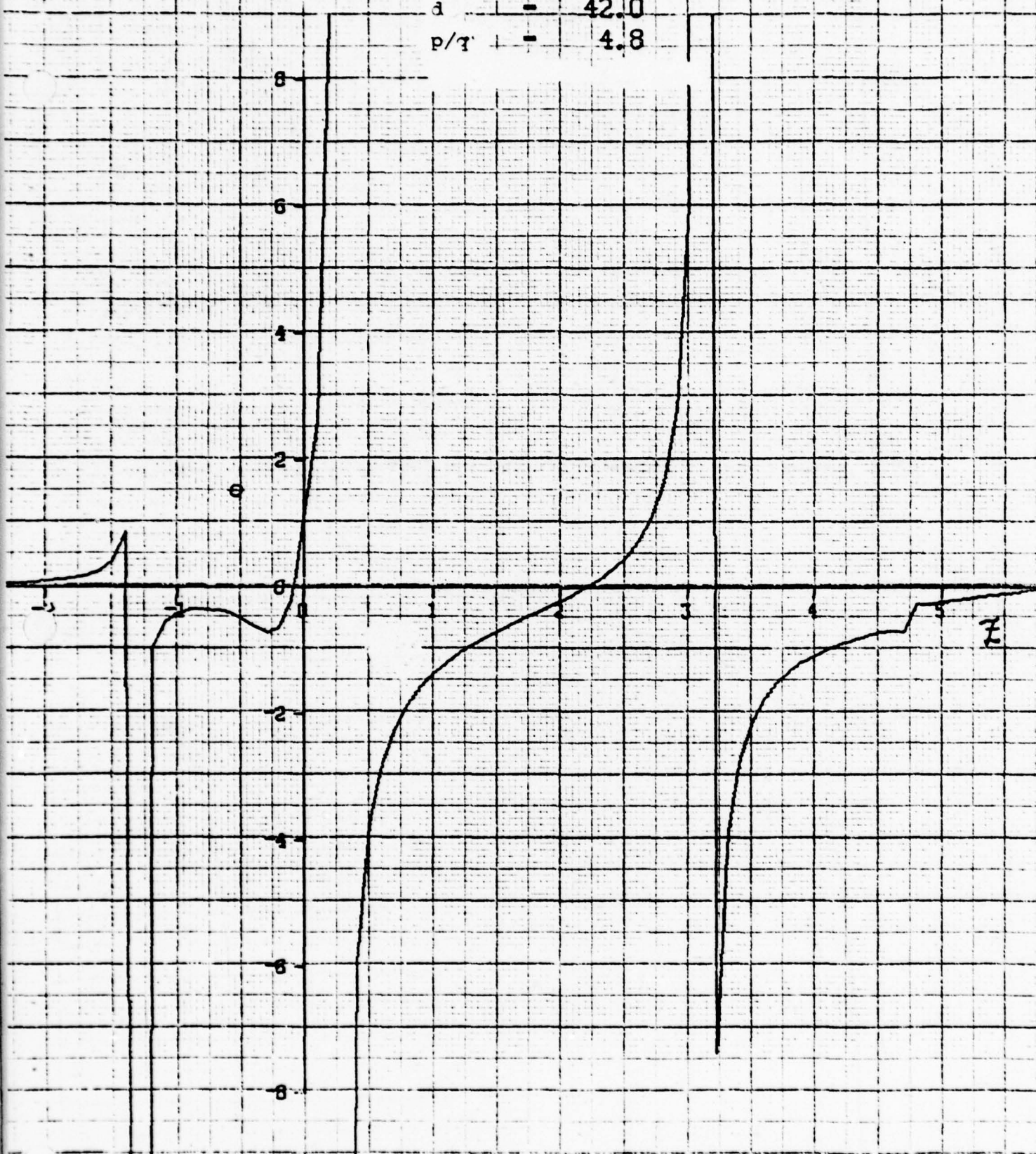


FIG. (11-6) PLOTS OF $\eta(z)$ AS A FUNCTION OF z

λ	-	0.5
d	-	42.0
p/q	-	4.8

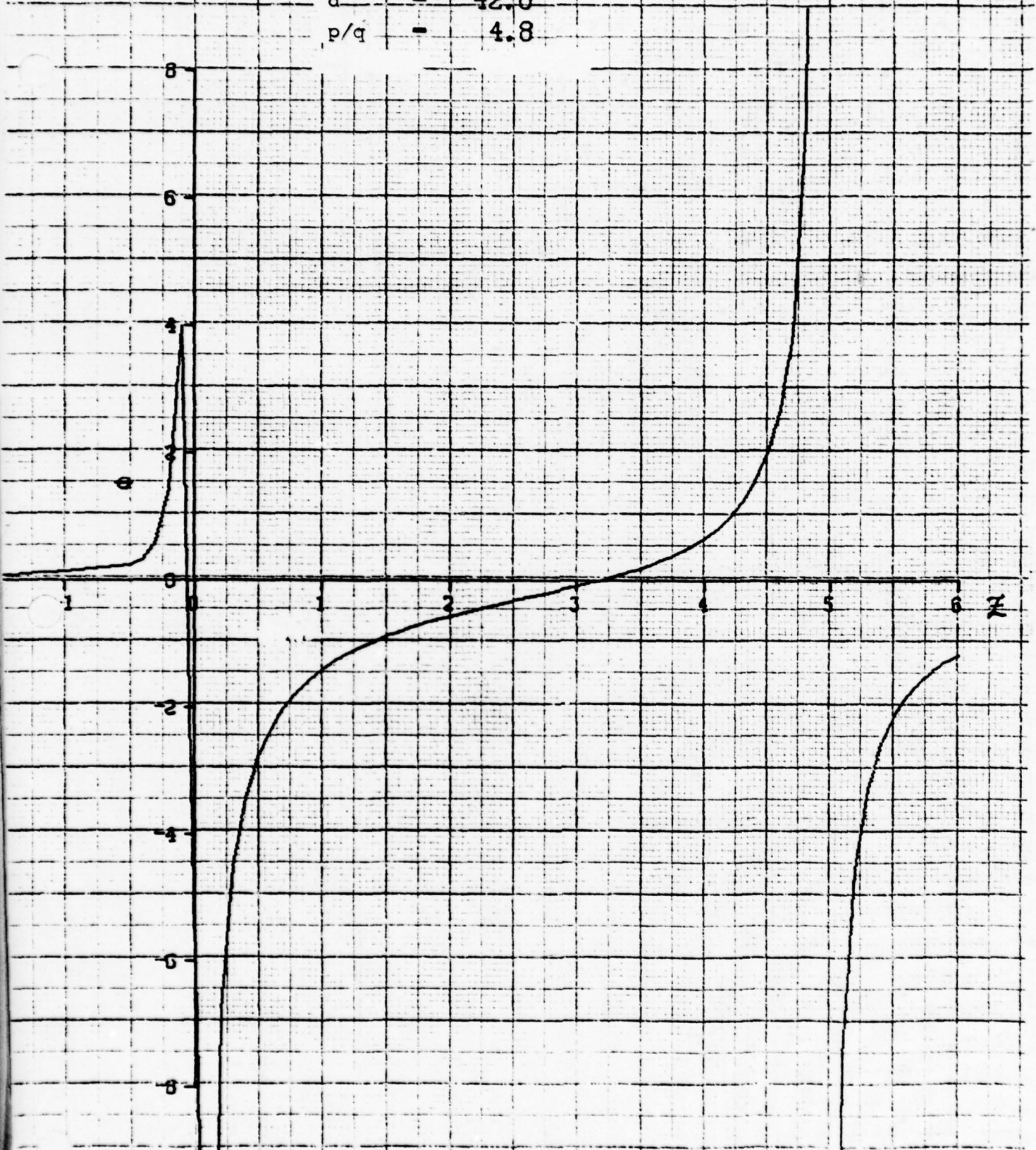


FIG. (4-7) PLOTS OF $y(z)$ AS A FUNCTION OF z

λ - 0.1
 d - 85.0
 p/α - 3.6

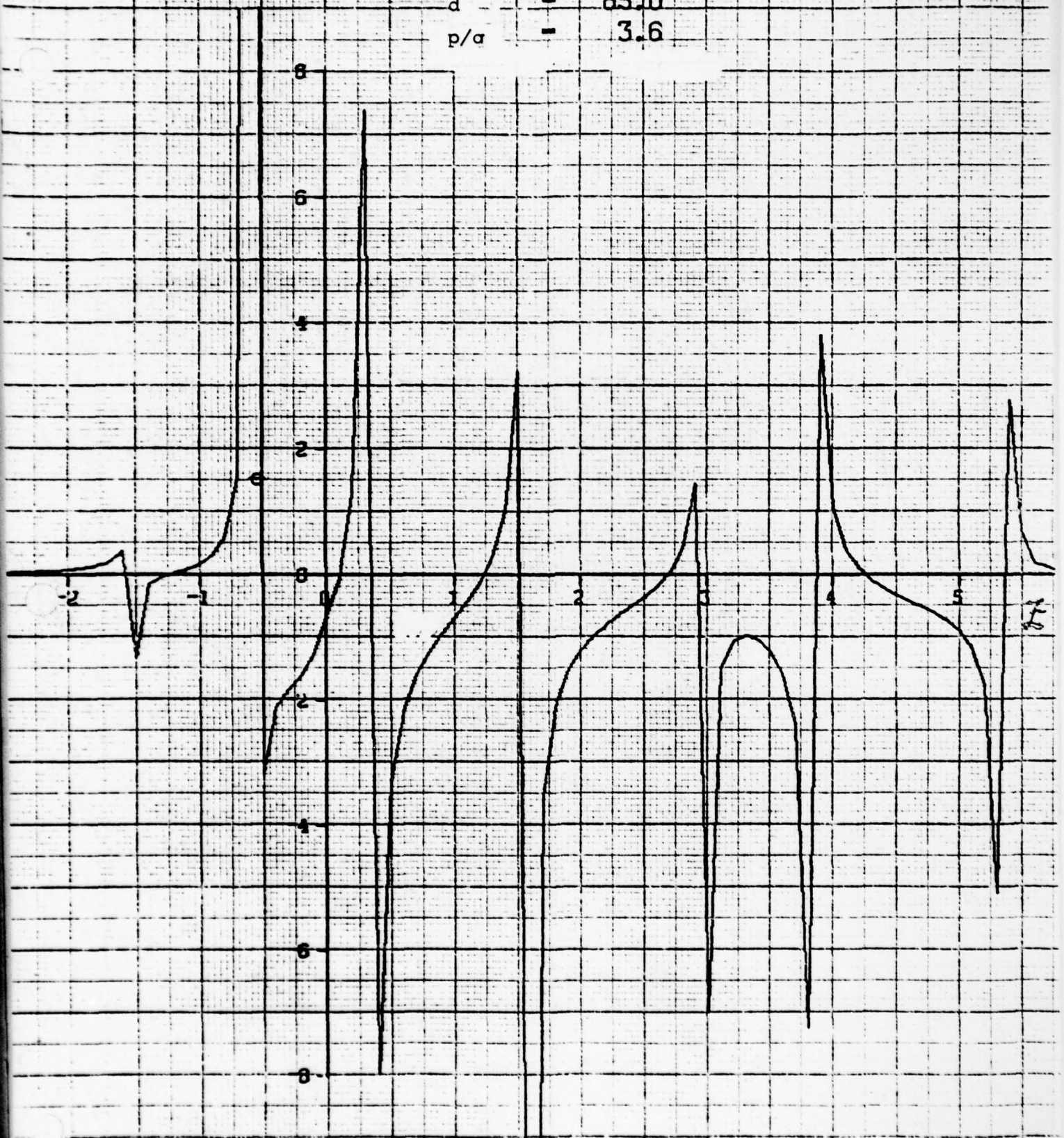
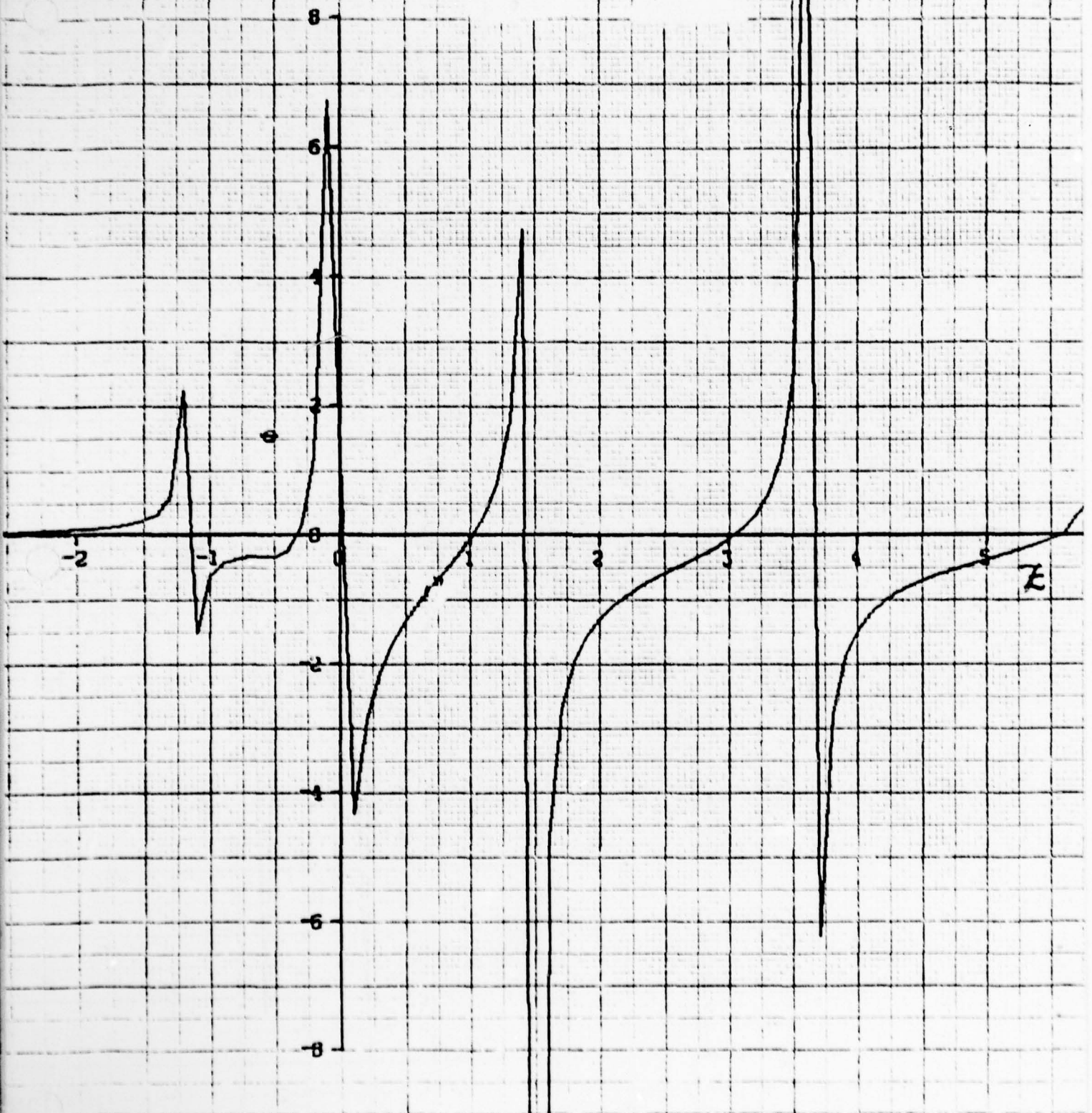


FIG. (4-8) PLOTS OF $g(z)$ AS A FUNCTION OF z

66

λ	-	0.2
d	-	85.0
p/q	-	3.6

FIG. (4-9) PLOTS OF $q(z)$ AS A FUNCTION OF z

67
 λ - 1.5
 d - 85.0
 p/q - 3.6

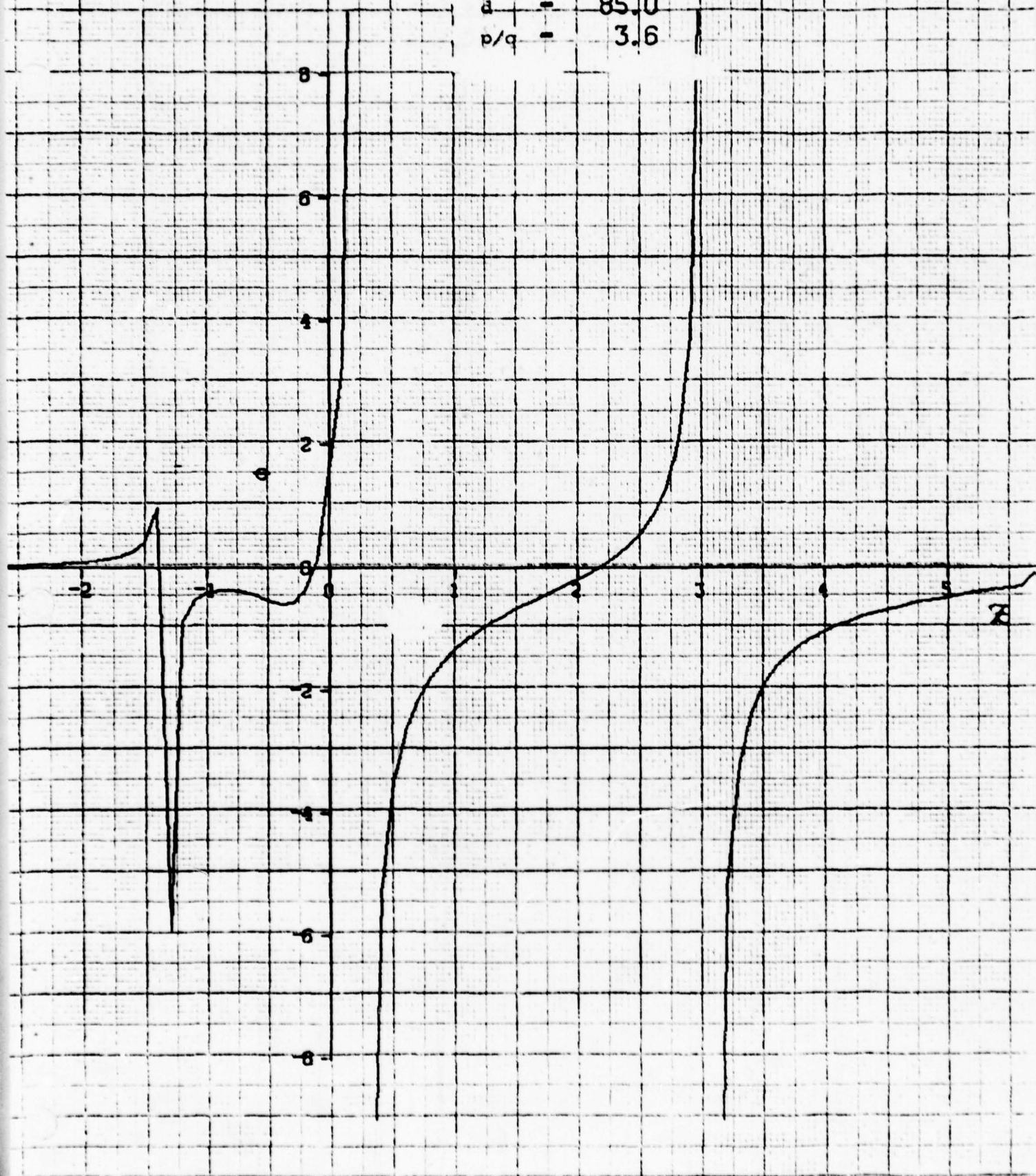


FIG. (4-10) PLOTS OF $f(z)$ AS A FUNCTION OF z

$\lambda = 0.1$
 $d = 94.0$
 $p/q = 0.6$

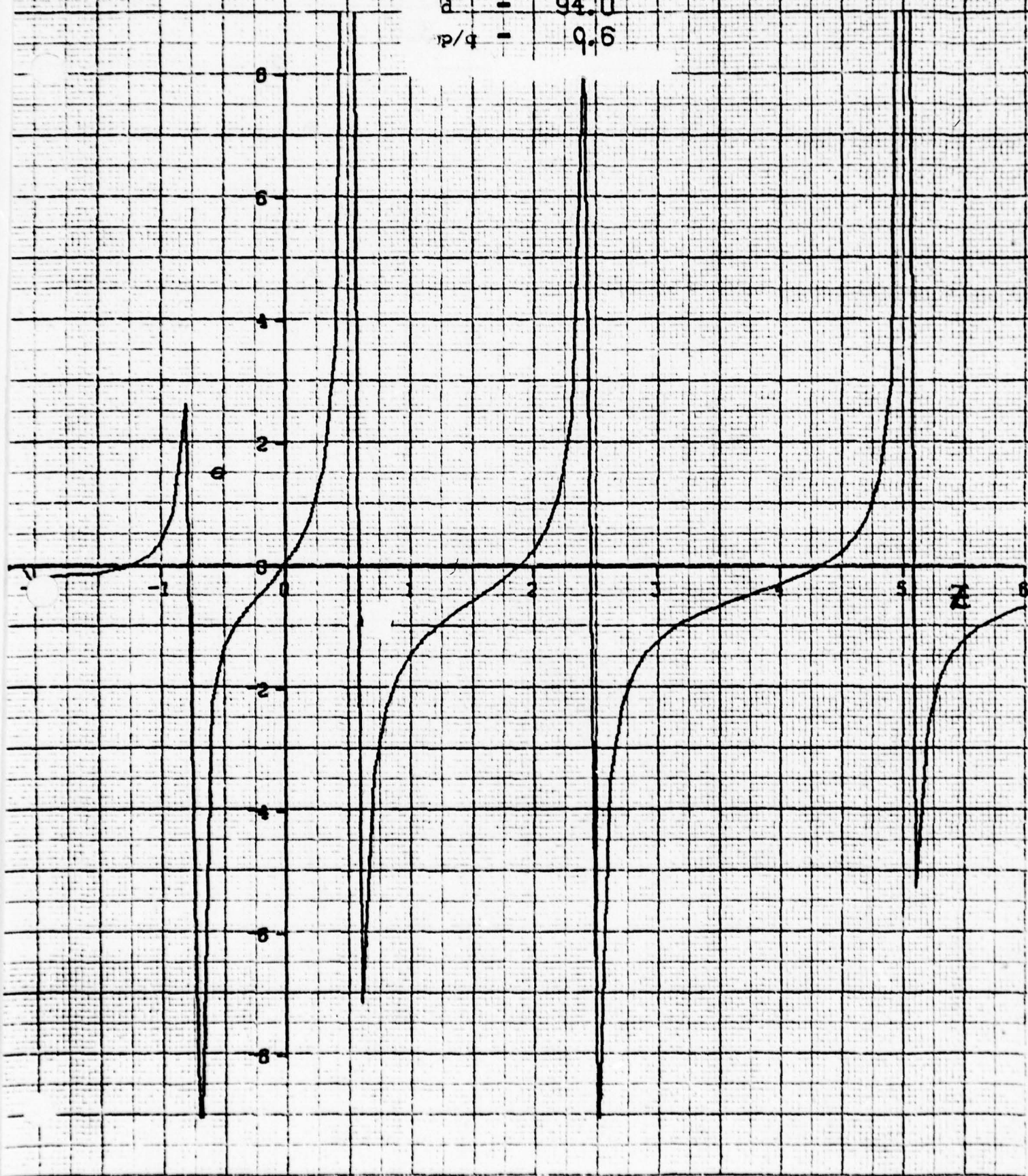


FIG. (4.11) PLOTS OF $\phi(z)$ AS A FUNCTION OF z

$\lambda = 0.2$
 $d = 94.0$
 $p/q = 0.6$



FIG. (4-12) PLOTS OF $\phi(z)$ AS A FUNCTION OF z

λ - 0.5
 a - 94.0
 p/q - 0.6

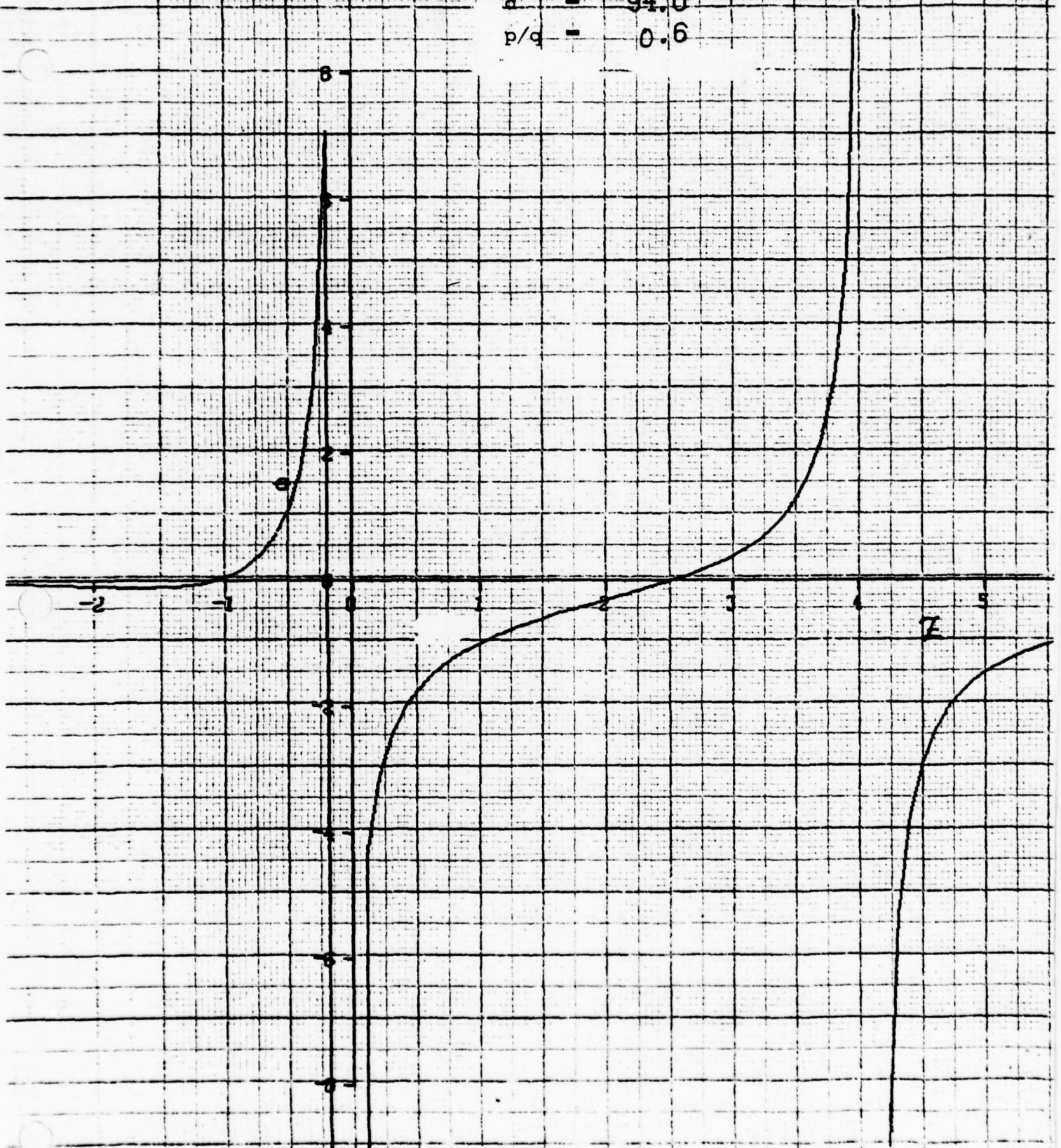


FIG. (4-13) PLOTS OF $D(z)$ AS A FUNCTION OF z

λ - 0.1
 d - 72.0
 p/q - 0.3

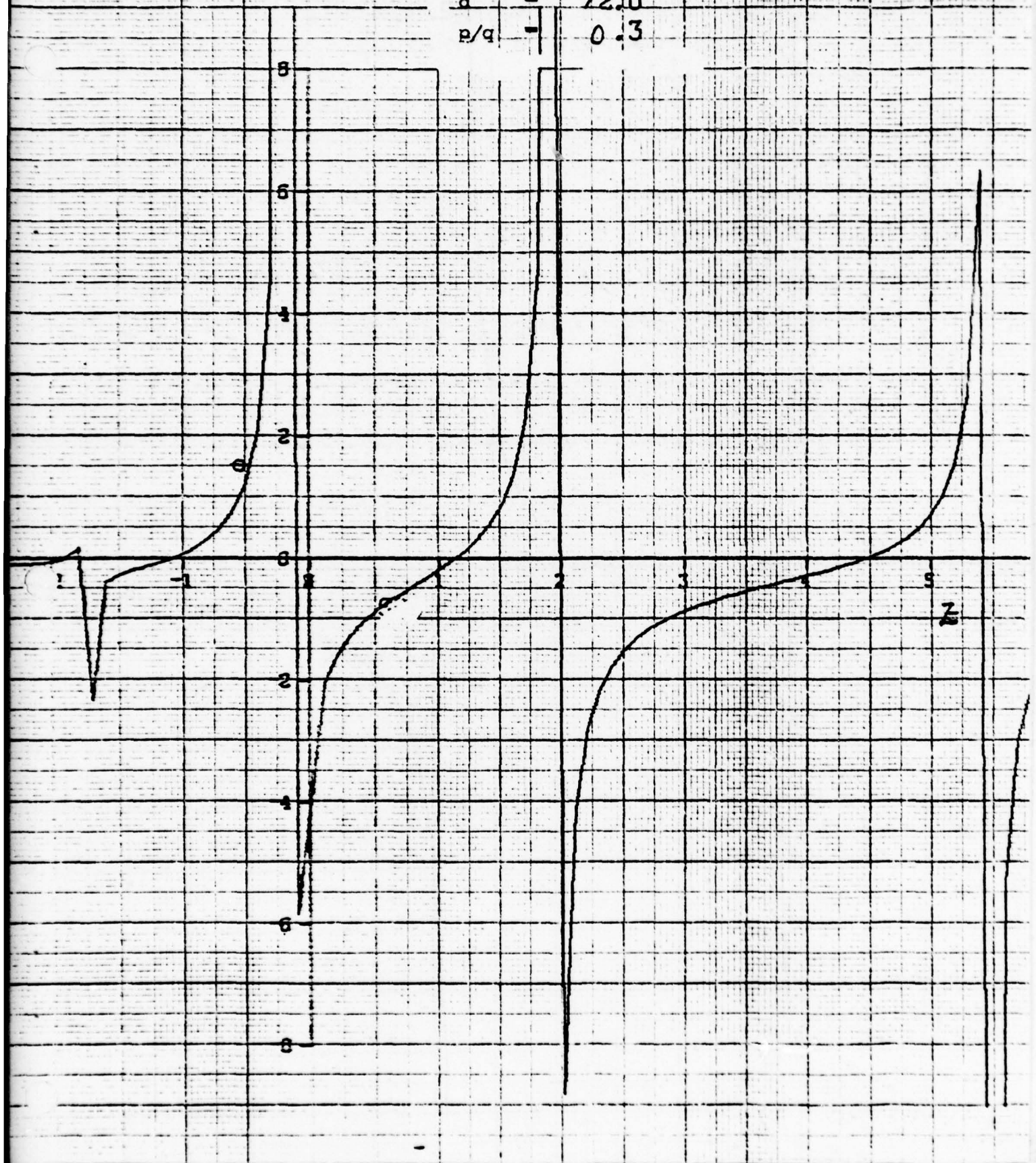


FIG. (4-14) PLOTS OF $\phi(z)$ AS A FUNCTION OF z

$\lambda = 0.2$
 $\sigma = 72.0$
 $p/q = 0.3$

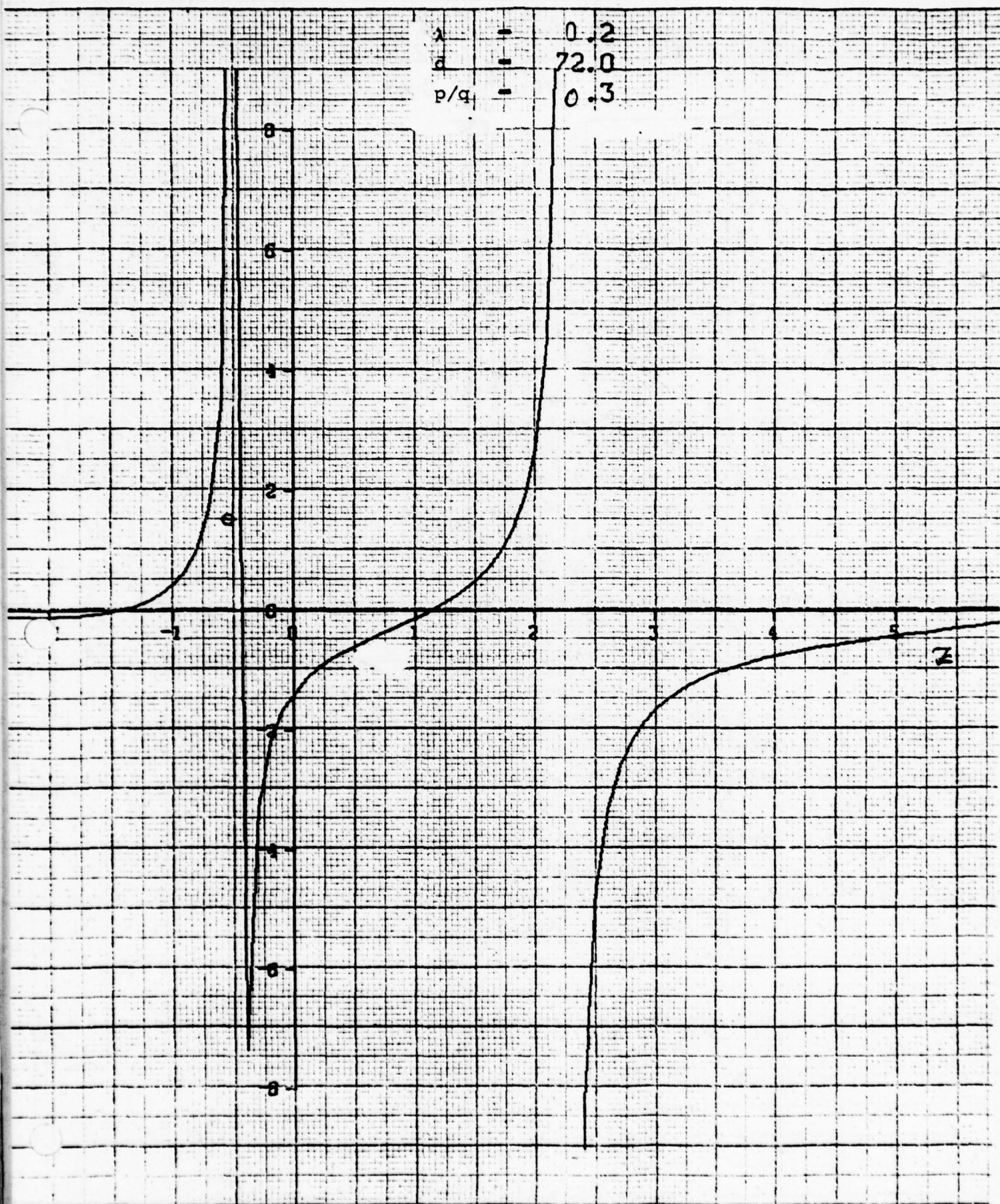


FIG. (4-15) PLOTS OF $\theta(z)$ AS A FUNCTION OF z

15

λ	-	0.5
d	-	72.0
p/σ	-	0.3
	-	

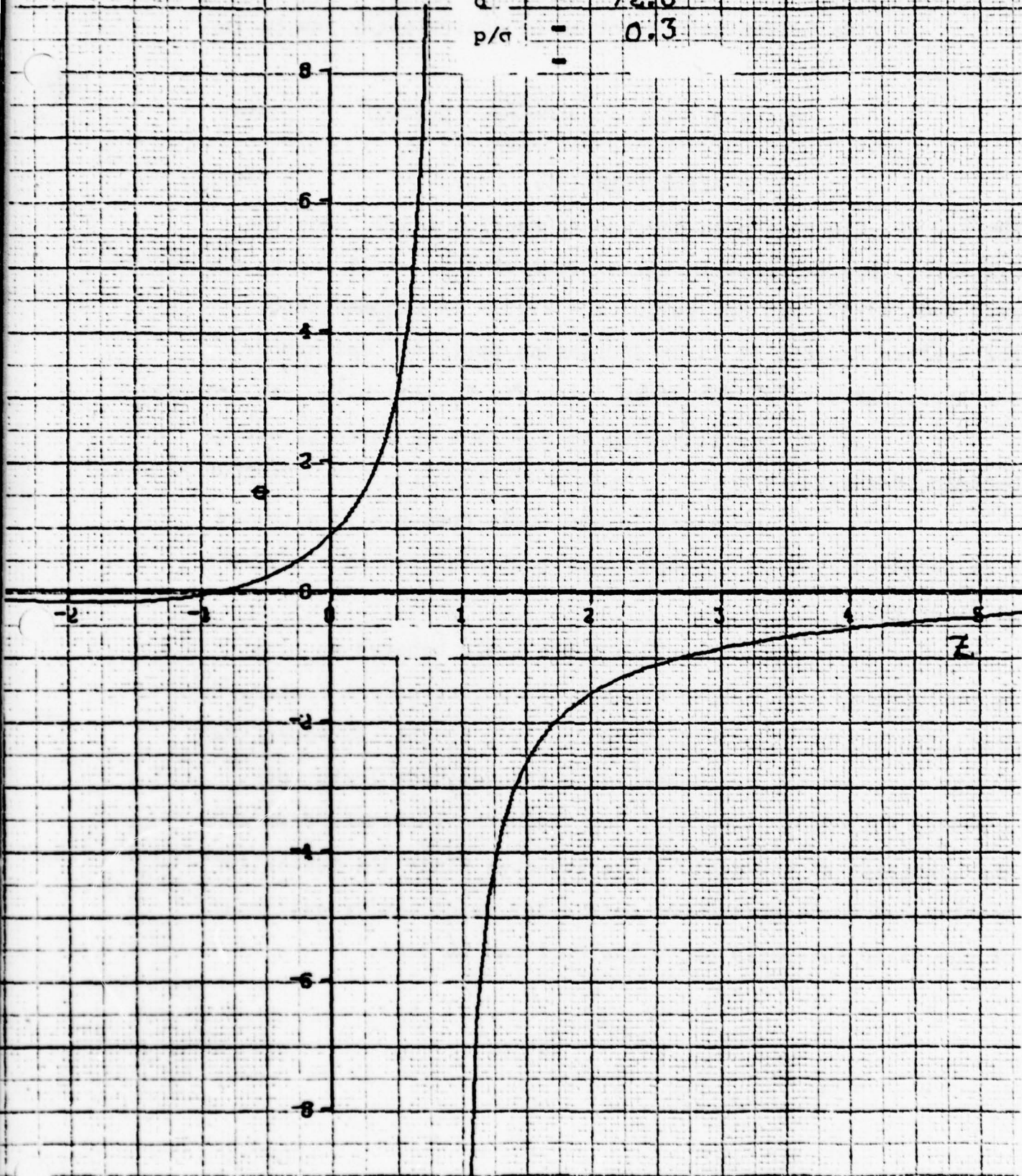


FIG. (4-16) PLOTS OF $\phi(z)$ AS A FUNCTION OF z

The height gain function or equivalently the E_y is given by

$$E_{y<} = A_i(-\xi_{<}) - \frac{A_i(-\xi_{10})}{B_i(-\xi_{10})} B_i(-\xi_{<}) \quad z < d$$

$$= A_i(-\xi_{>}) + j B_i(-\xi_{>}) \quad z > d$$

The $\xi_{<}$, $\xi_{>}$, ξ_{10} have been defined in Section 4.1.1. For the ξ_{1d} value, the $\xi_{<}$ range in values from +5.9 to -1.25 and $\xi_{>}$ approaches zero from -3.57; and for height $z = 77.8$ m it becomes zero.

For greater heights it is an increasing positive real number.

For these parameters, the field intensity E_y will behave as follows:

a. E_y oscillates up to $z = 35$ m at which $\xi_{<}$ starts becoming negative.

b. It increases in amplitude from $z = 35$ m to the duct height $z = 42$ m. It continues to increase up to $z = 77.8$ m at which $\xi_{>} \rightarrow 0$

c. Beyond $z = 77.8$ m the field behaves as if it is attenuating with height since $\xi_{>}$ is positive real number. The intensity of the field above the duct height is higher than in the duct and may be construed as the dominant leaky mode. However, this fact alone will not yield the information as to the intensity of the field above the duct since the excitation problem has to be worked out before any quantitative estimates of the field intensity above the duct can be made.

4.3.2 The Leaky Modes

Up until now we sought solutions of the transcendental equation which were positive or negative real numbers. The determination of the solutions of the transcendental equation for complex values is much more involved and time consuming, and the resources of this contract do not permit detailed analysis. Nonetheless, some already developed approximate expressions are used to determine the complex eigenvalues or solutions characterizing leaky modes.

The expression which is used to determine the leaky modes is given by (2)

$$A_m = \left\{ \xi_m + g + \frac{1}{12} S g^4 - \frac{1}{90} S \xi_m g^6 \right. \\ \left. + \frac{(13S^2 - 5S)}{1260} g^7 + \frac{1}{1260} S \xi_m^2 g^8 \right. \\ \left. + \dots \right\}$$

Here, $g = \frac{d}{H}$, $H = (k_0^2 q)^{-1/3}$, $S = 1 - s^3$, $s^3 = \frac{p}{q}$ and ξ_m are the zeros of the Hankel function of second kind and one third order and are given by

$$\begin{aligned} \xi_1 &= -1.169 + j2.025 \\ 2 \quad &-2.044 + j3.54 \\ 3 \quad &-2.76 + j4.78 \end{aligned}$$

The expression for the eigenvalue $A_m = \alpha_m + jB_m$ is valid for small values of g ($g \leq 1$). That is, the duct height is comparable to the scale height H and for these values of g the eigenvalues approach the zeroes of the Hankel function of the second kind and one third order.

Recognizing that for $\lambda=100$ cm the field will not be trapped by any of the ducts; $\lambda=100$ cm was chosen for calculations. Thus for $\lambda=100$ cm and for two days of duct profile, the complex eigenvalues are presented in the table as follows:

Table (4-2) Eigenvalues for Leaky Modes

$\lambda=100$ cm	Jan.	Dec.
	$g = 0.545$	$g = 0.6646$
A_1	$-0.574+j2.02$	$-0.48+j2.021$
2	$-1.448+j3.53$	$-1.354+j3.53$
3	$-2.163+j4.78$	$-2.07+j4.77$

Use of the same equation for $\lambda=50$ cm leads to results which do not appear to be valid. For $\lambda=50$ cm, $g = 1.378$ for Jan. 3rd duct and $g=1.476$ for Dec. 4th duct and thus the expression for $g > 1$ does not seem to hold.

4.4 The Height Gain Functions for the Trapped Modes

As discussed before, the variation of the field with height, also termed the height gain function, will reveal whether or not there exists field outside the duct. For this reason, height gain functions for individual modes have been computed and they are shown in Figs. (4-17 through 4-53).

The height gain functions are the plots of modal E field i.e., they are the plots of the following expressions:

$$E_{y<} = A_i(-\xi_{<}) - \frac{A_i(-\xi_{10})}{B_i(-\xi_{10})} \cdot B_i(-\xi_{<}) \quad z < d$$

$$E_{y>} = A_i(-\xi_{>}) + jB_i(-\xi_{>}) \quad z > d$$

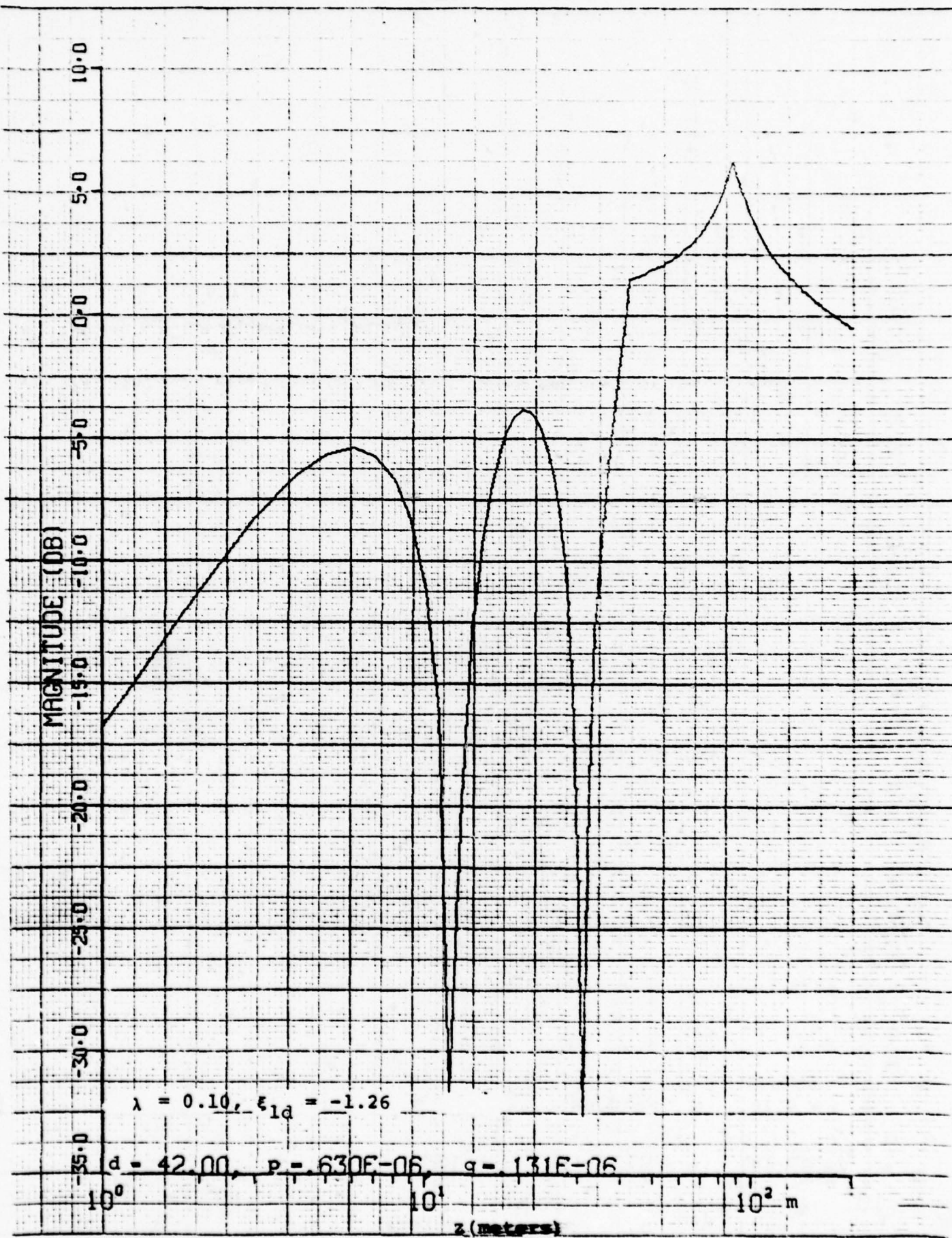


Fig. (4-17) Height-Gain Functions - January

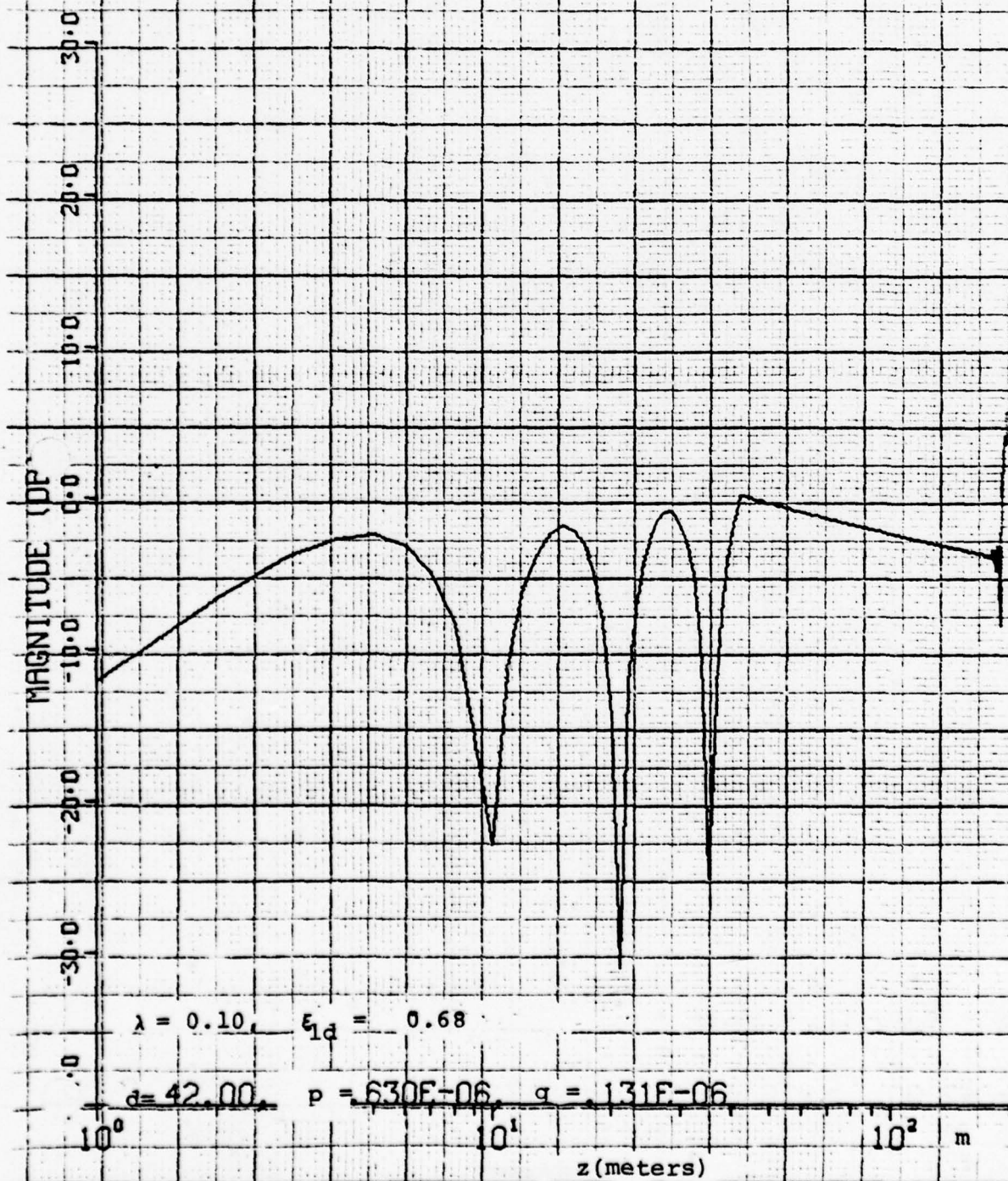


Fig. (4-18) Height-Gain Functions - January

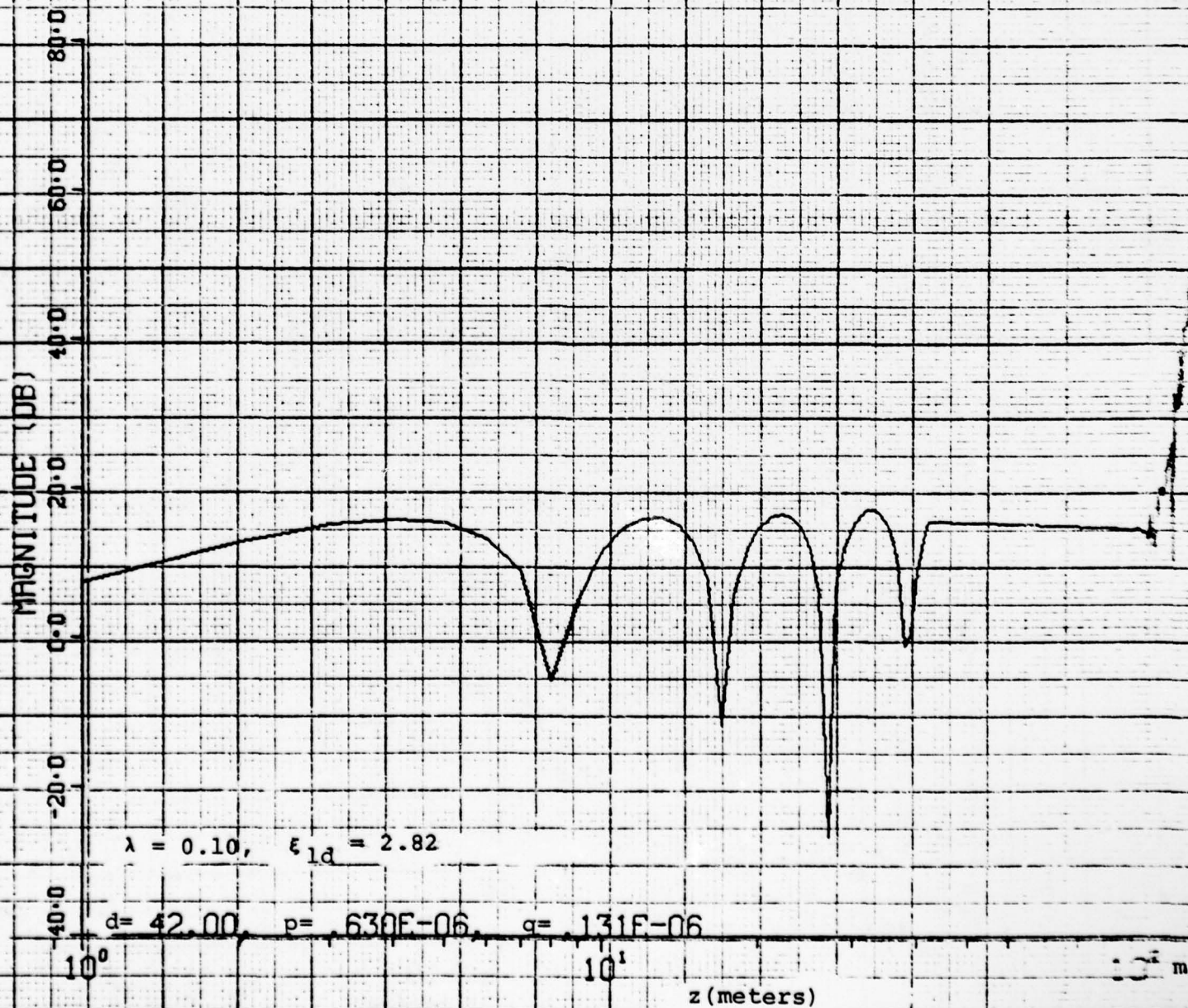


Fig. (4-19) Height-Gain Functions - January

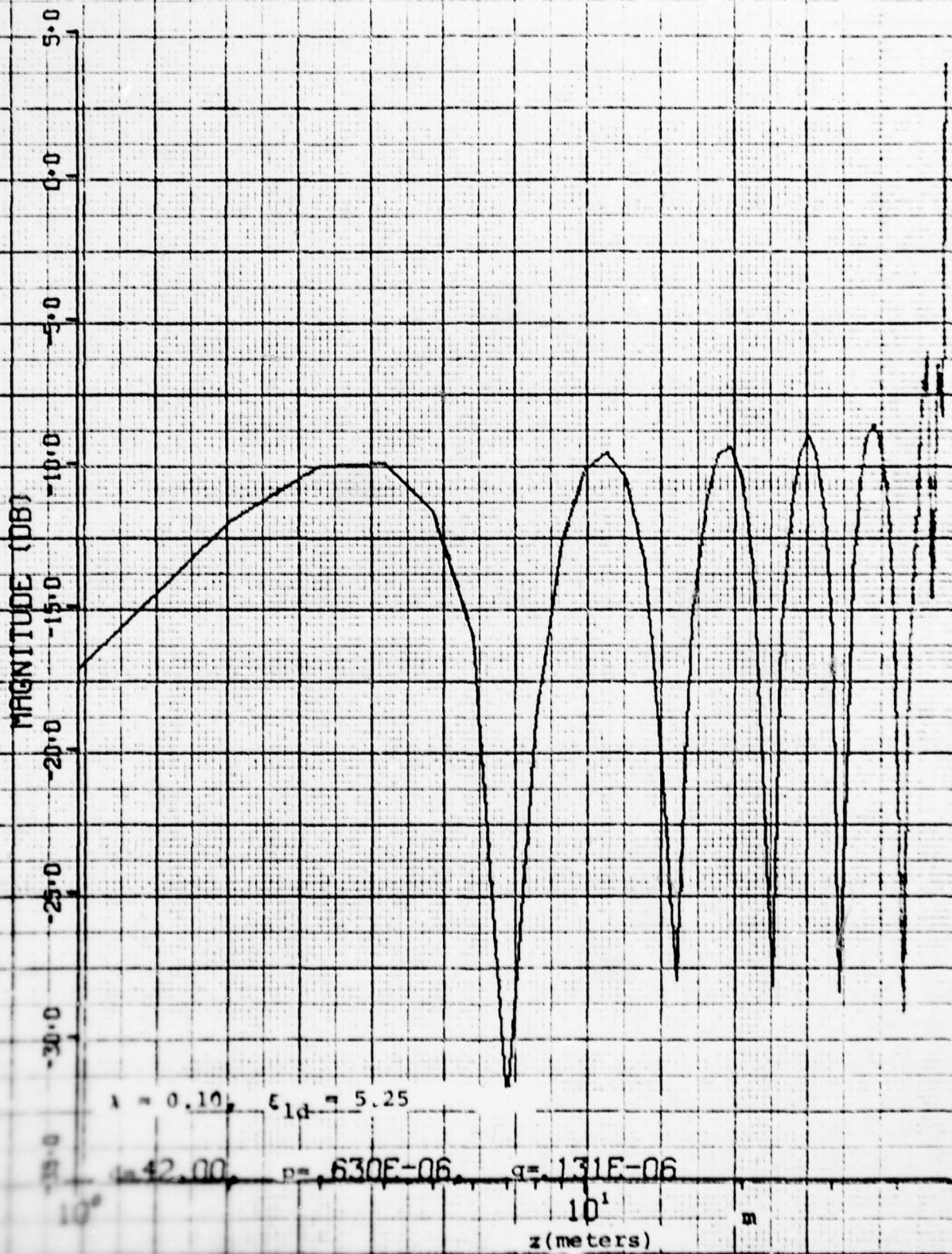


Fig. (4-20) Height-Gain Functions - January

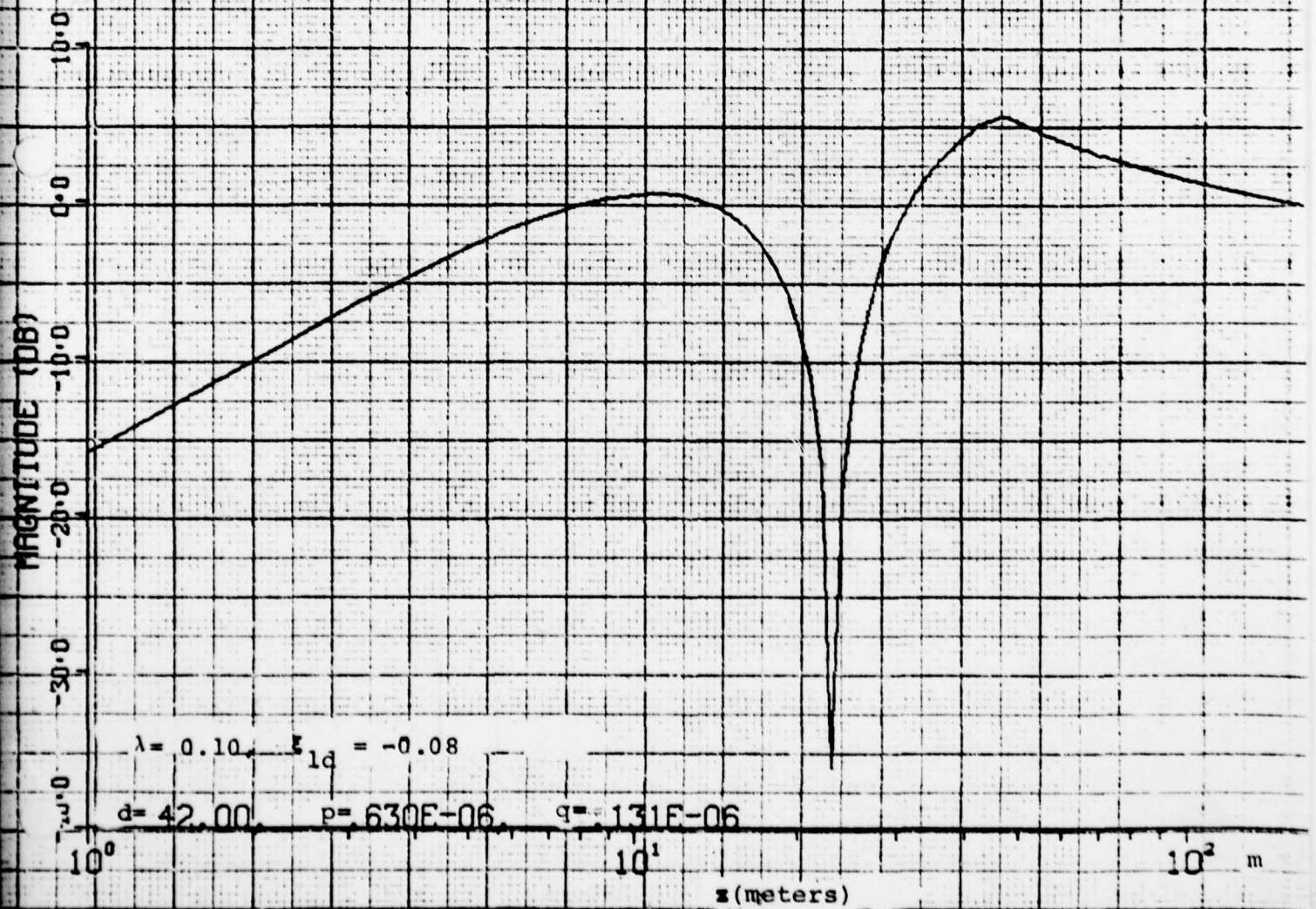


Fig. (4-21) Height-Gain Functions - January

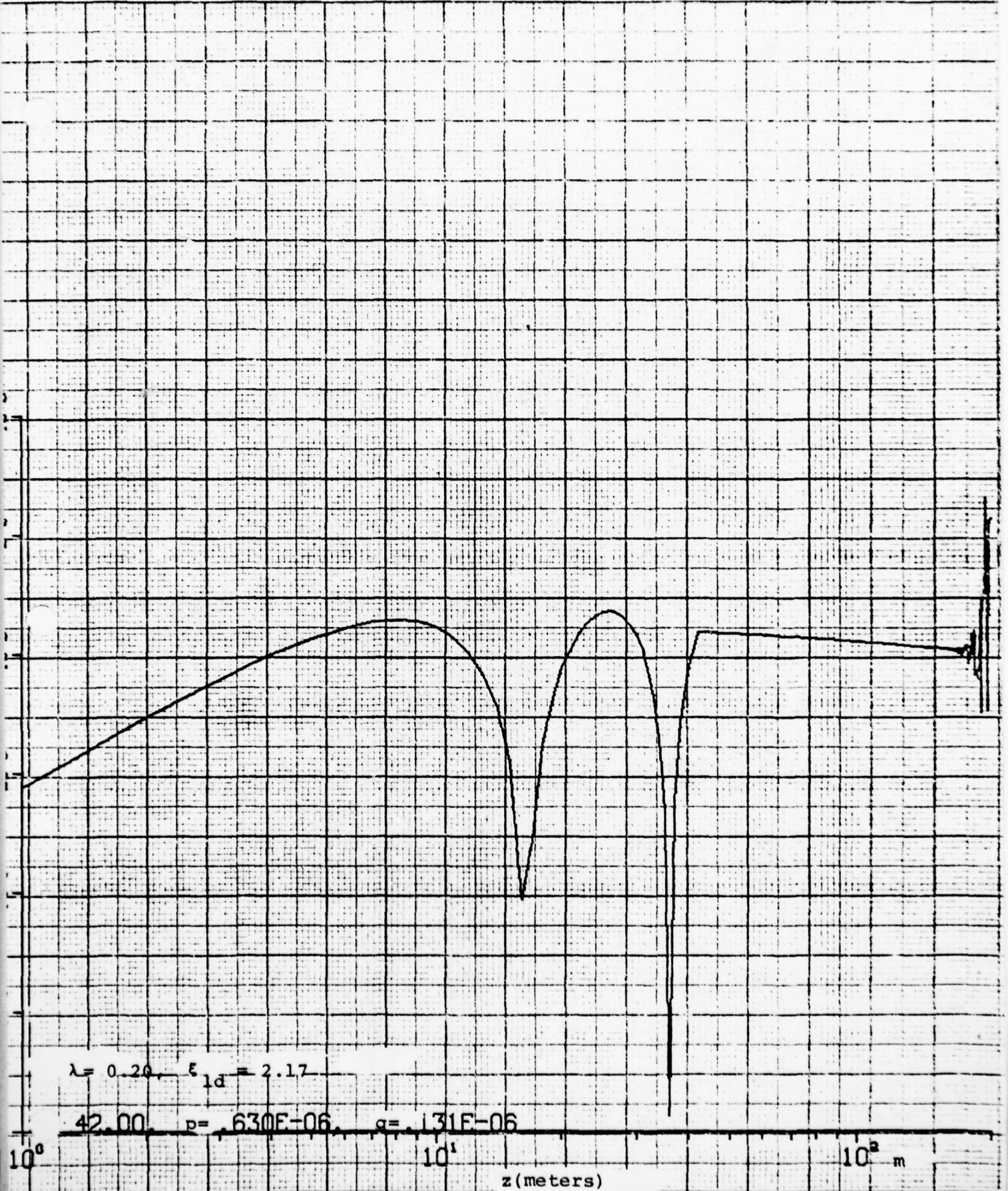


Fig. (4-22) Height-Gain Functions - January

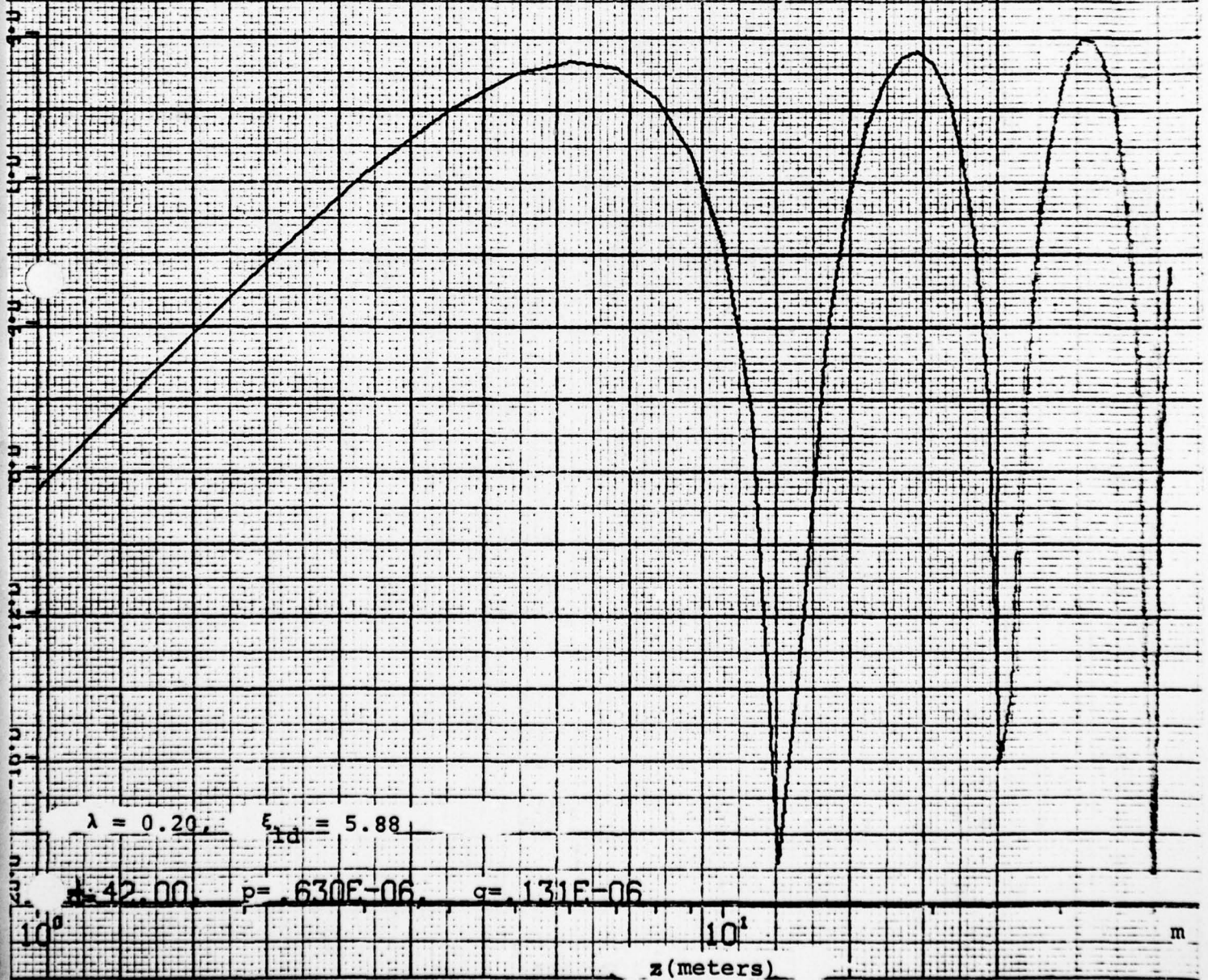


Fig. (4-23) Height-Gain Functions - January

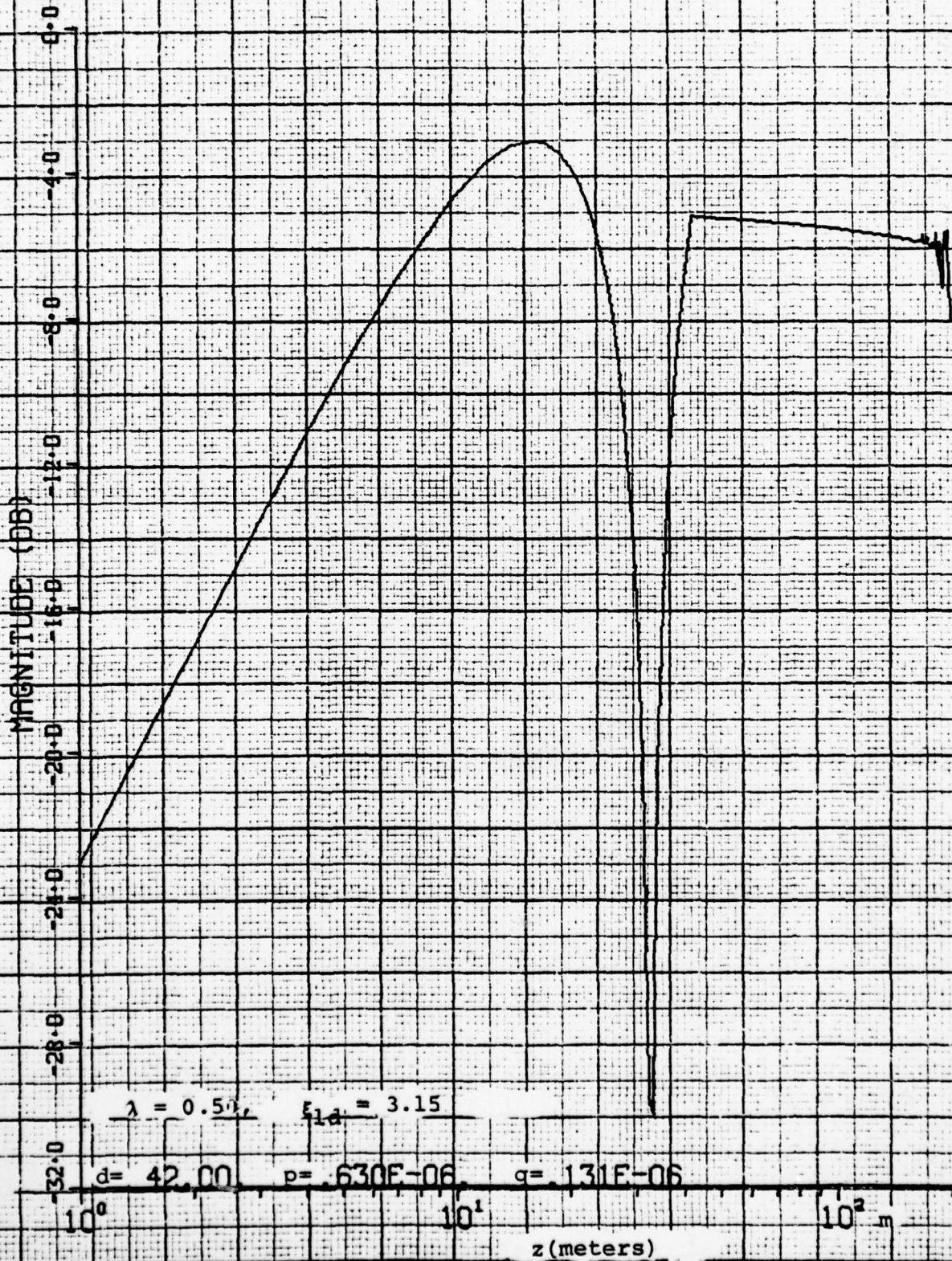


Fig. (4-24) Height-Gain Functions - January

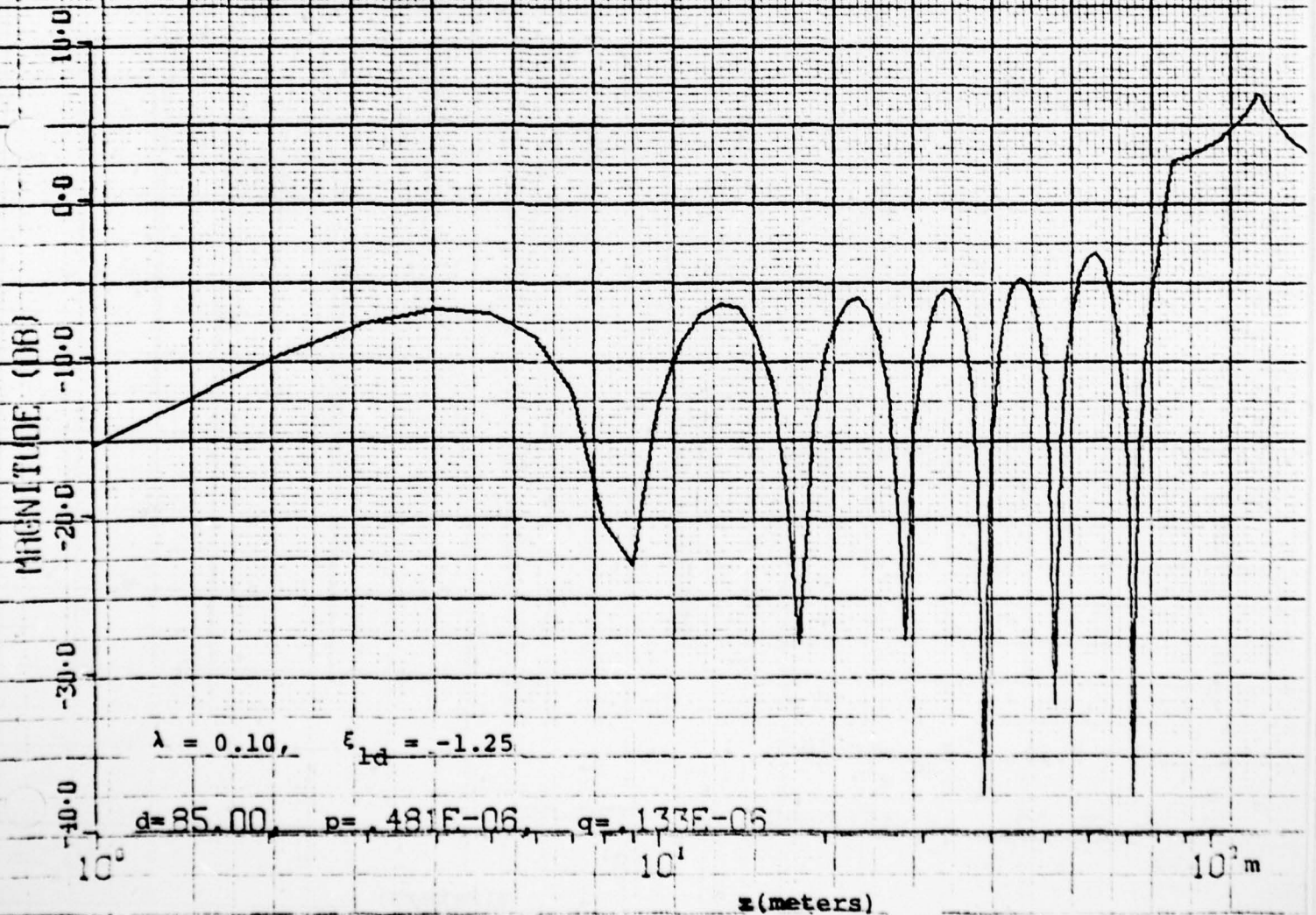


Fig. (4-25) Height-Gain Functions - April

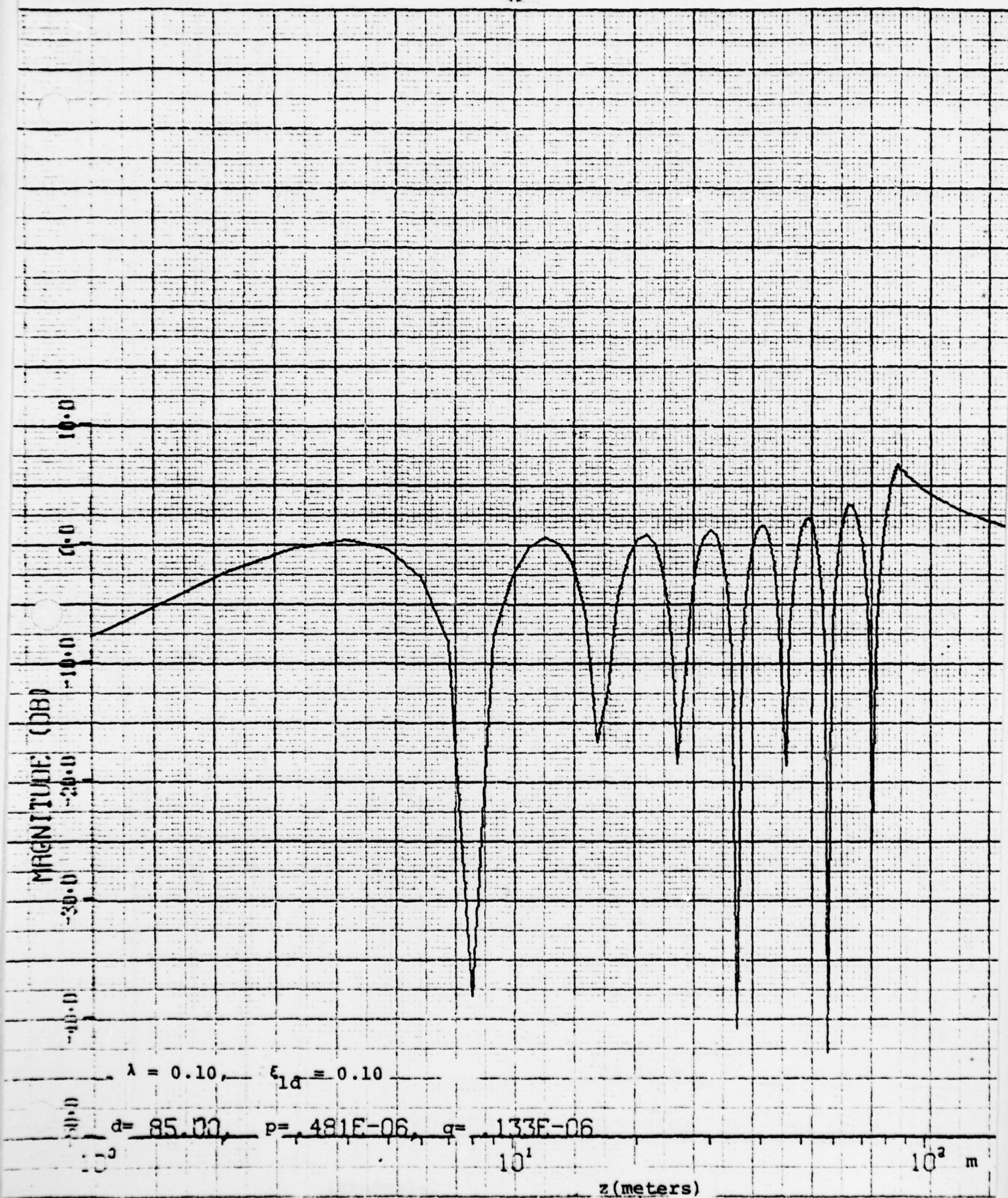


Fig. (4-26) Height-Gain Functions - April

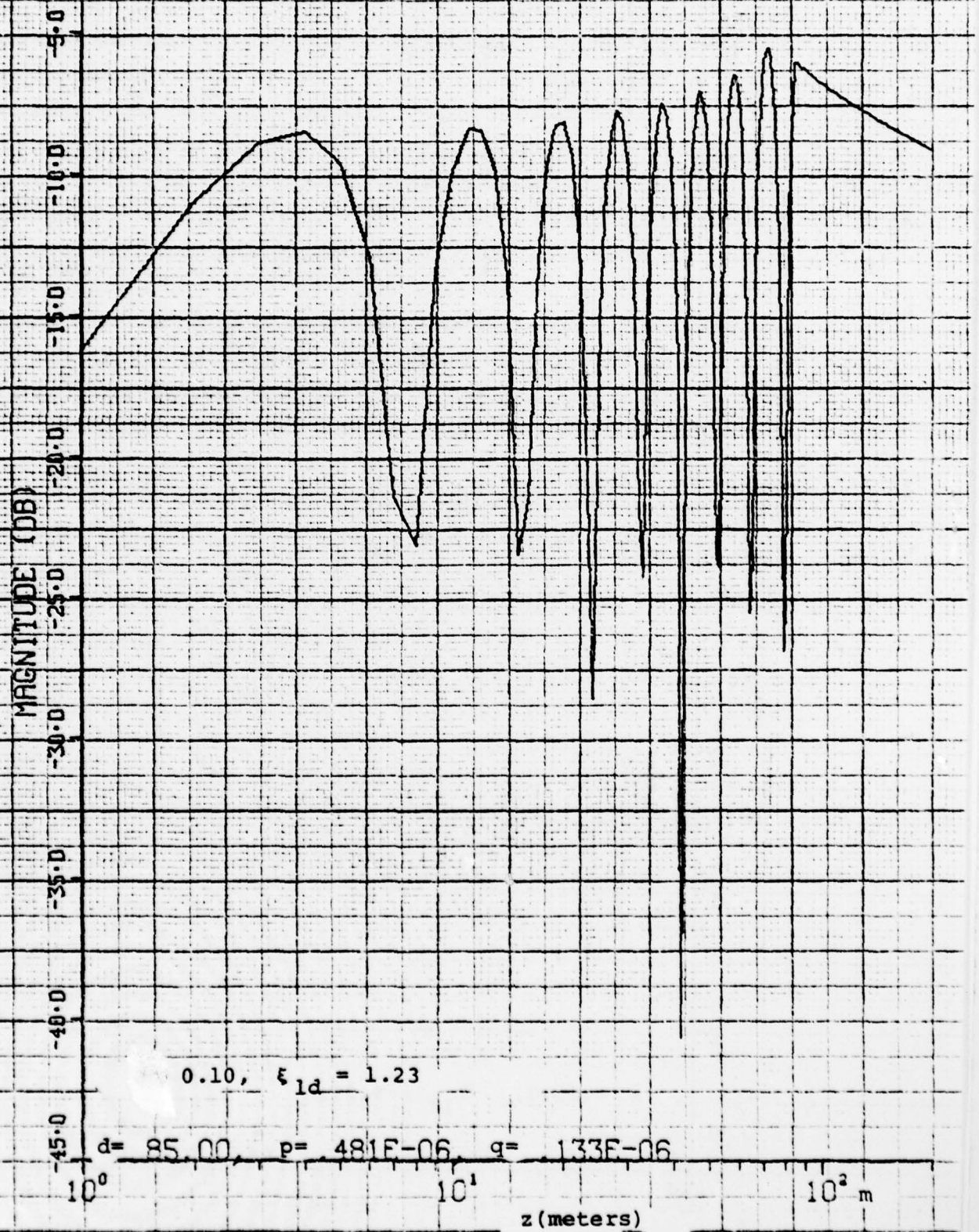


Fig. (4-27) Height-Gain Functions - April

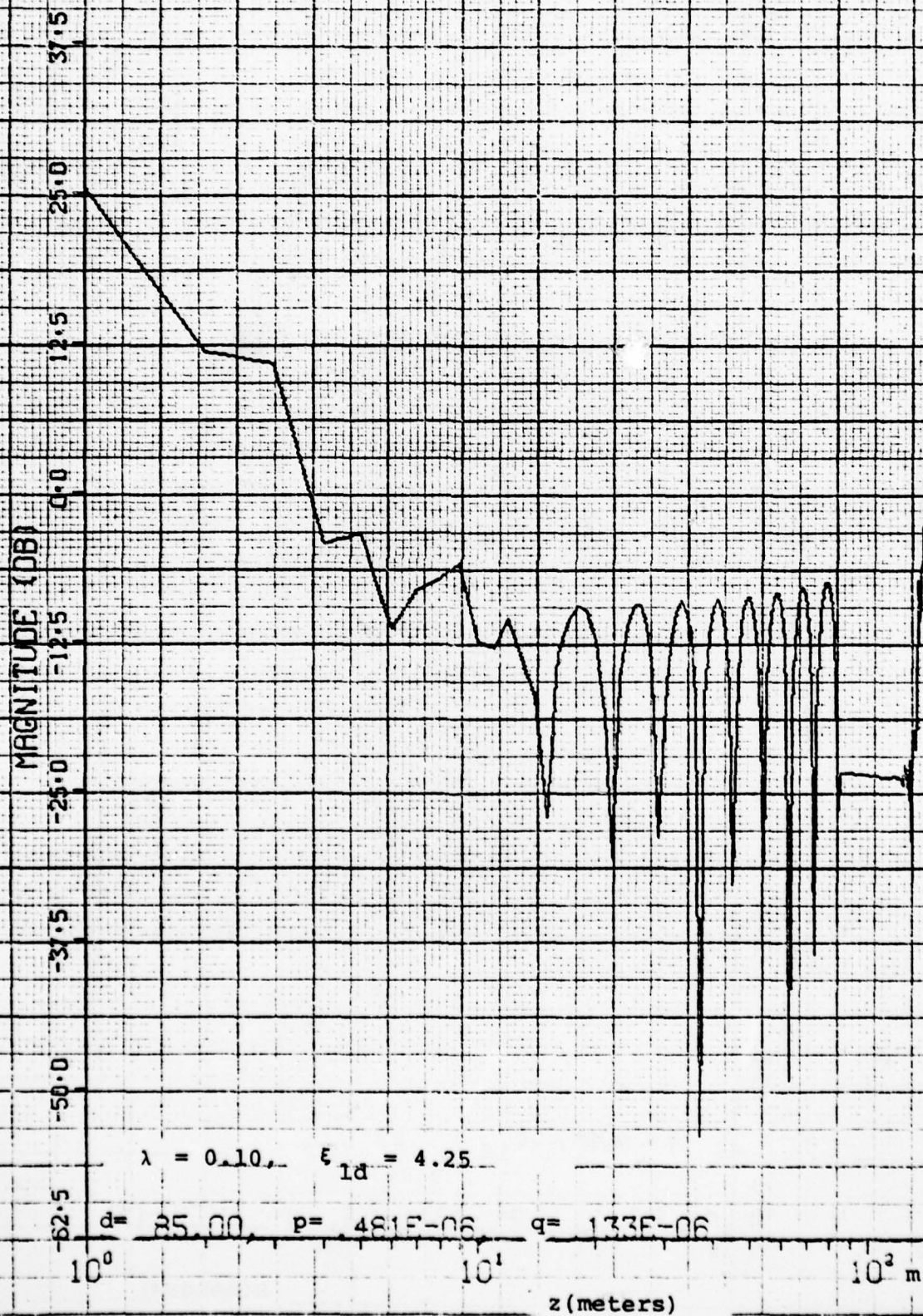


Fig. (4-28) Height-Gain Functions - April

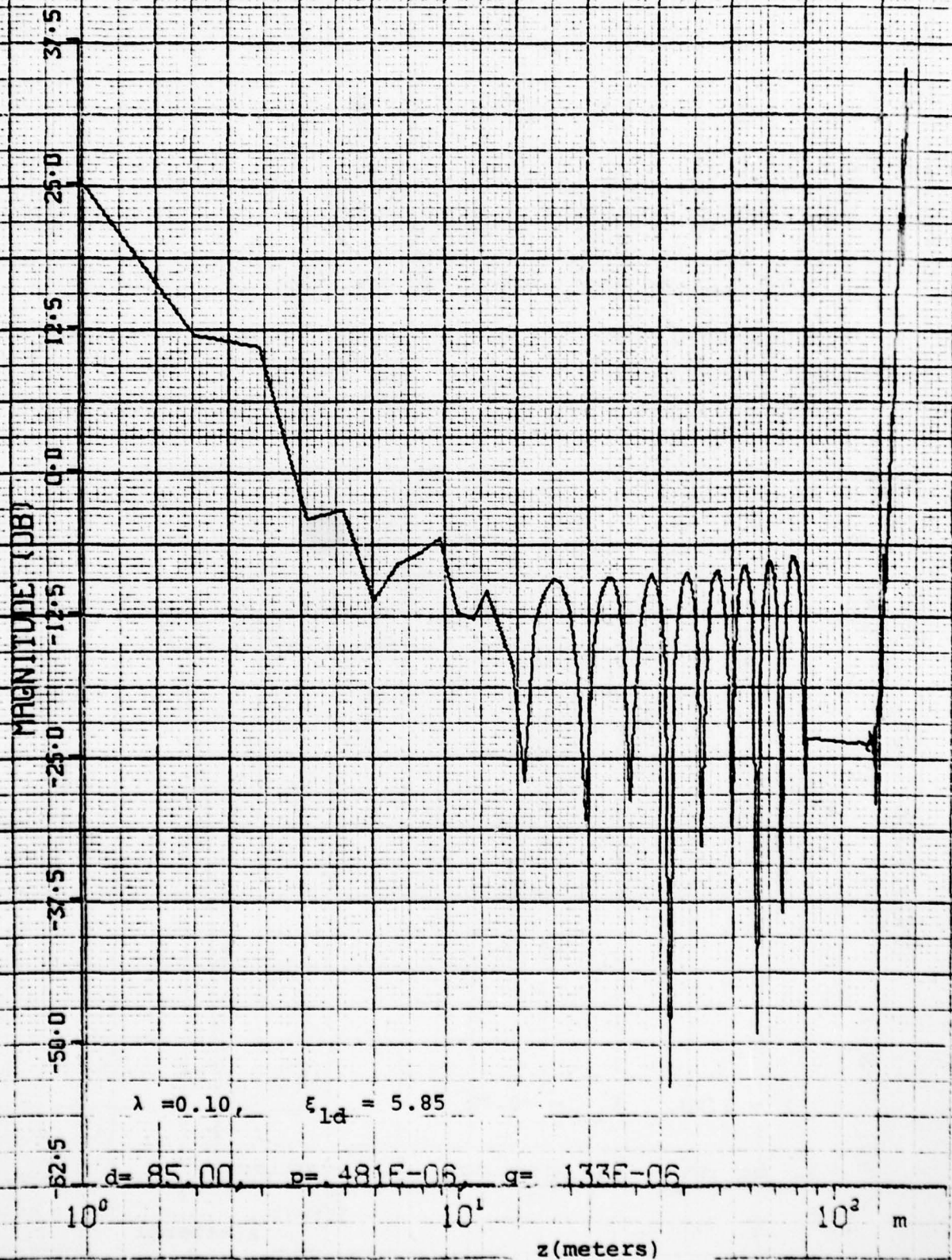


Fig. (4-29) Height-Gain Functions - April

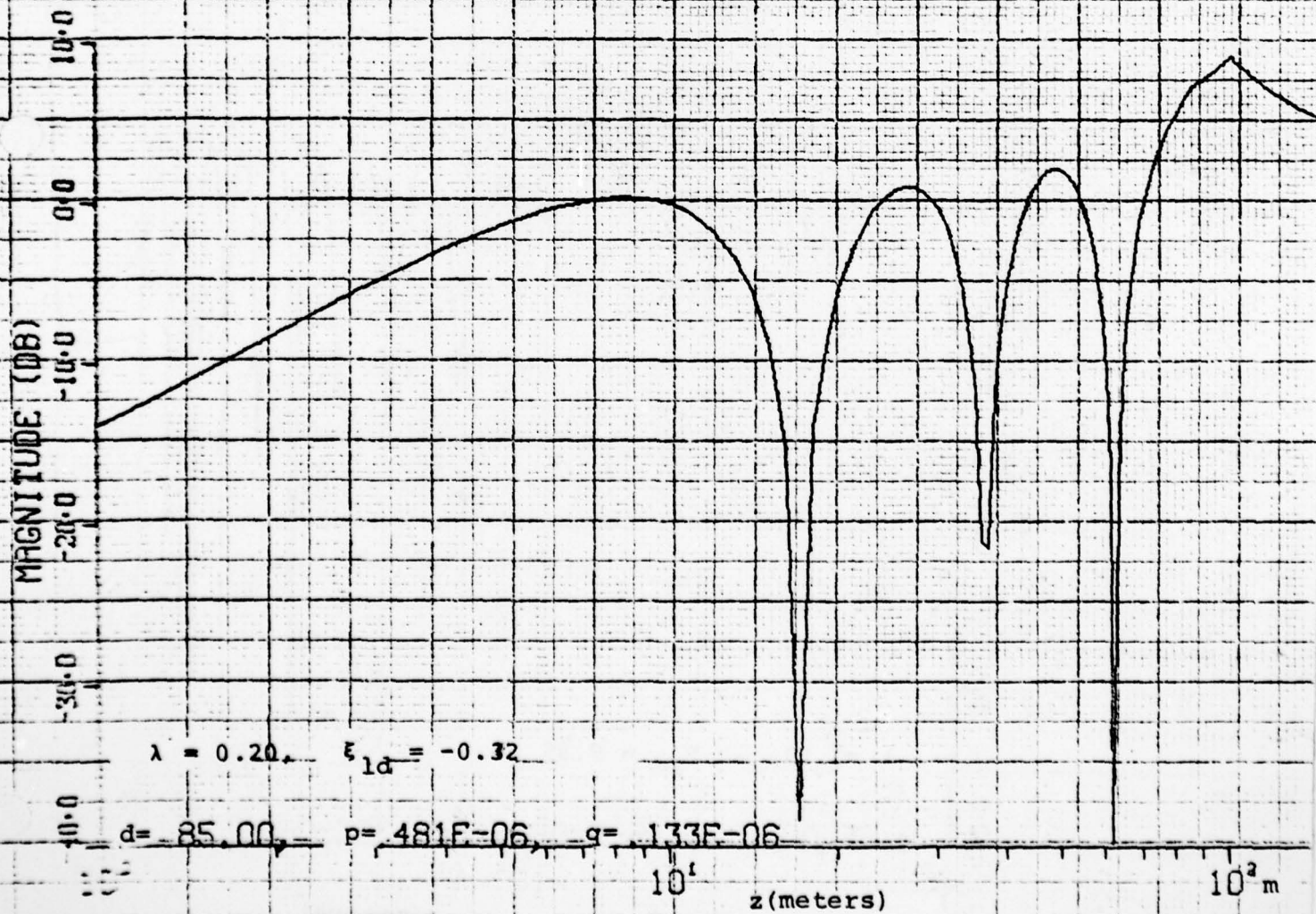


Fig. (4-30) Height-Gain Functions - April

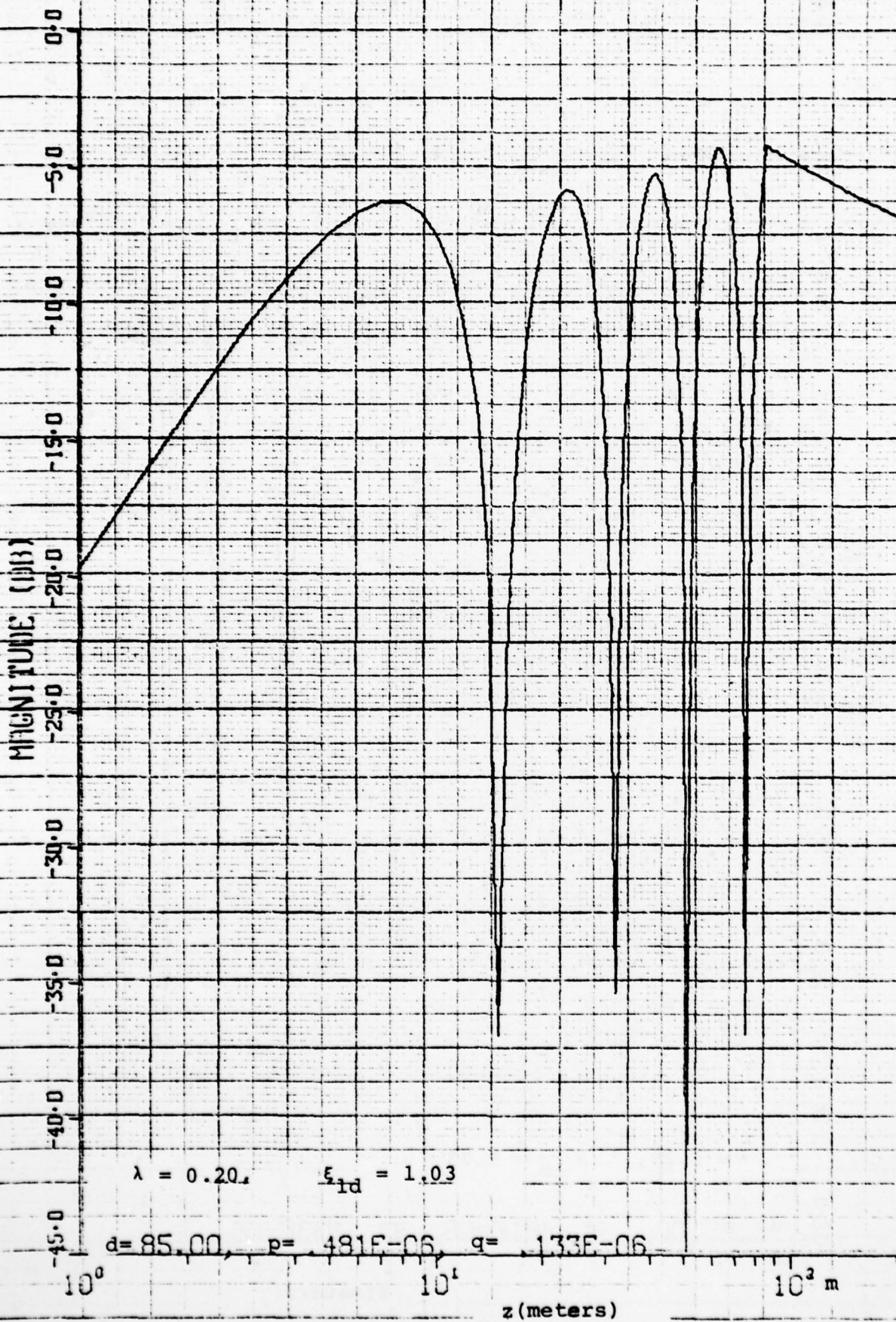


Fig. (4-31) Height-Gain Functions - April

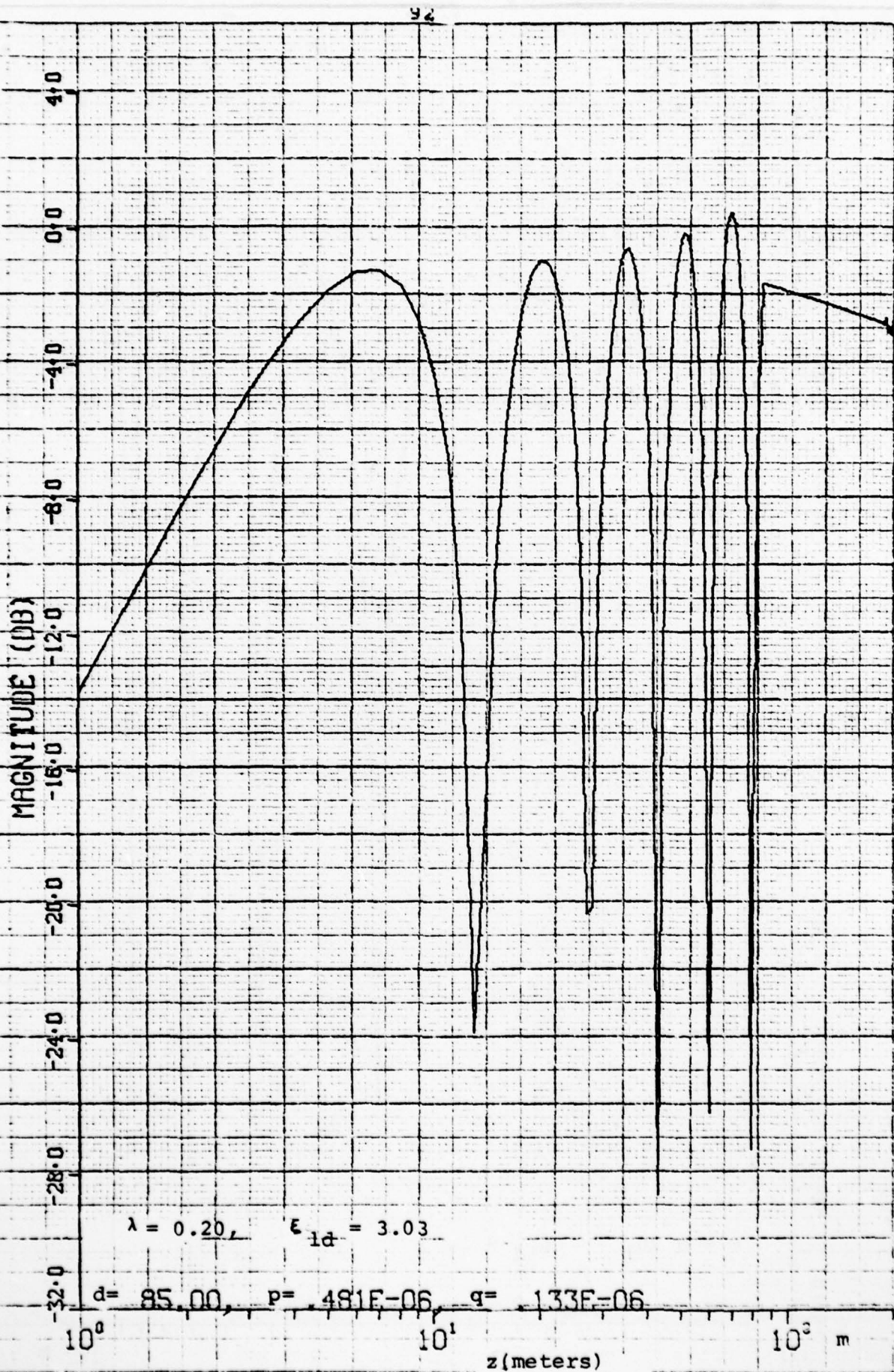


Fig. (4-32) Height-Gain Functions - April

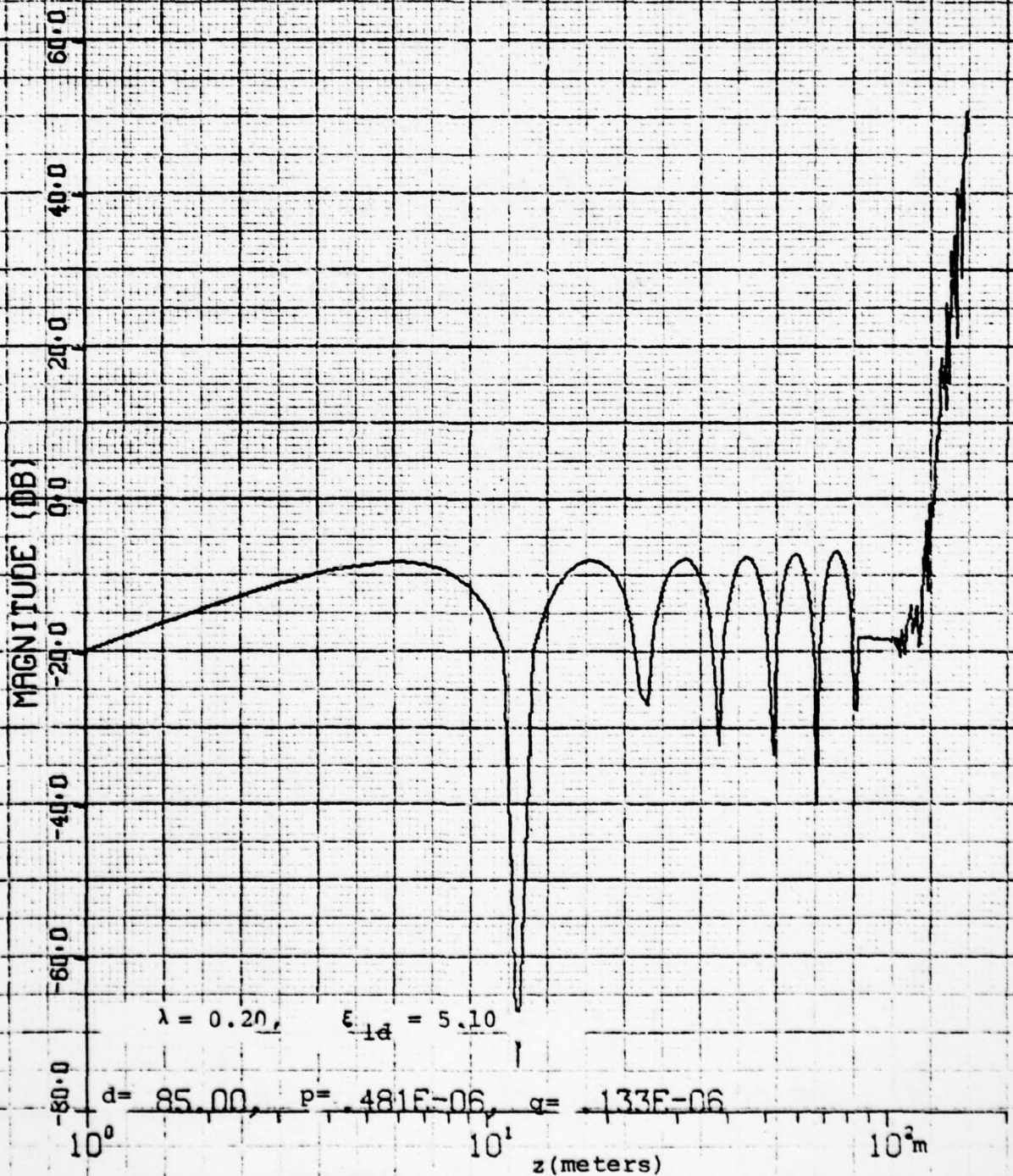


Fig. (4-33) Height-Gain Functions - April

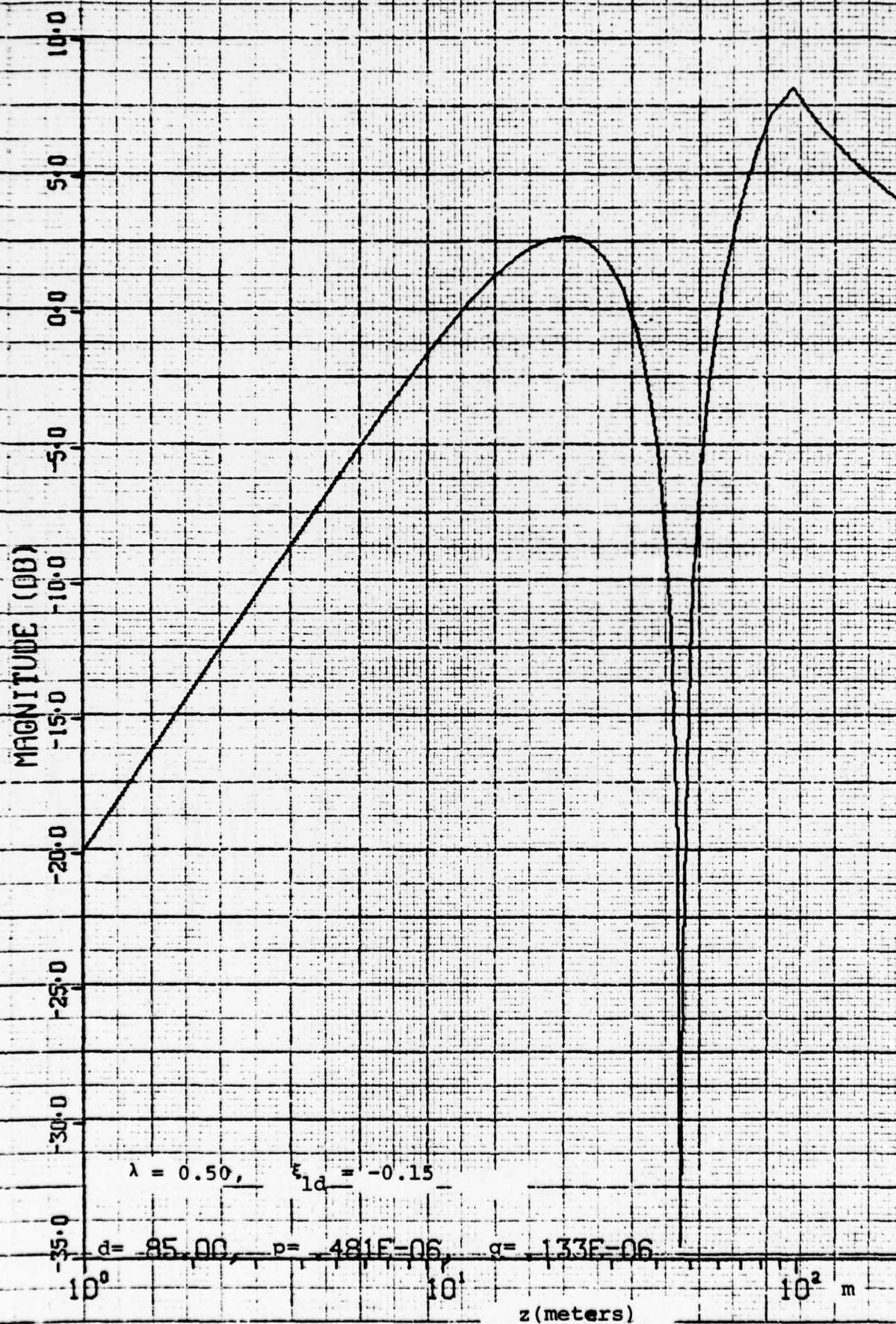


Fig. (4-34) Height-Gain Functions - April

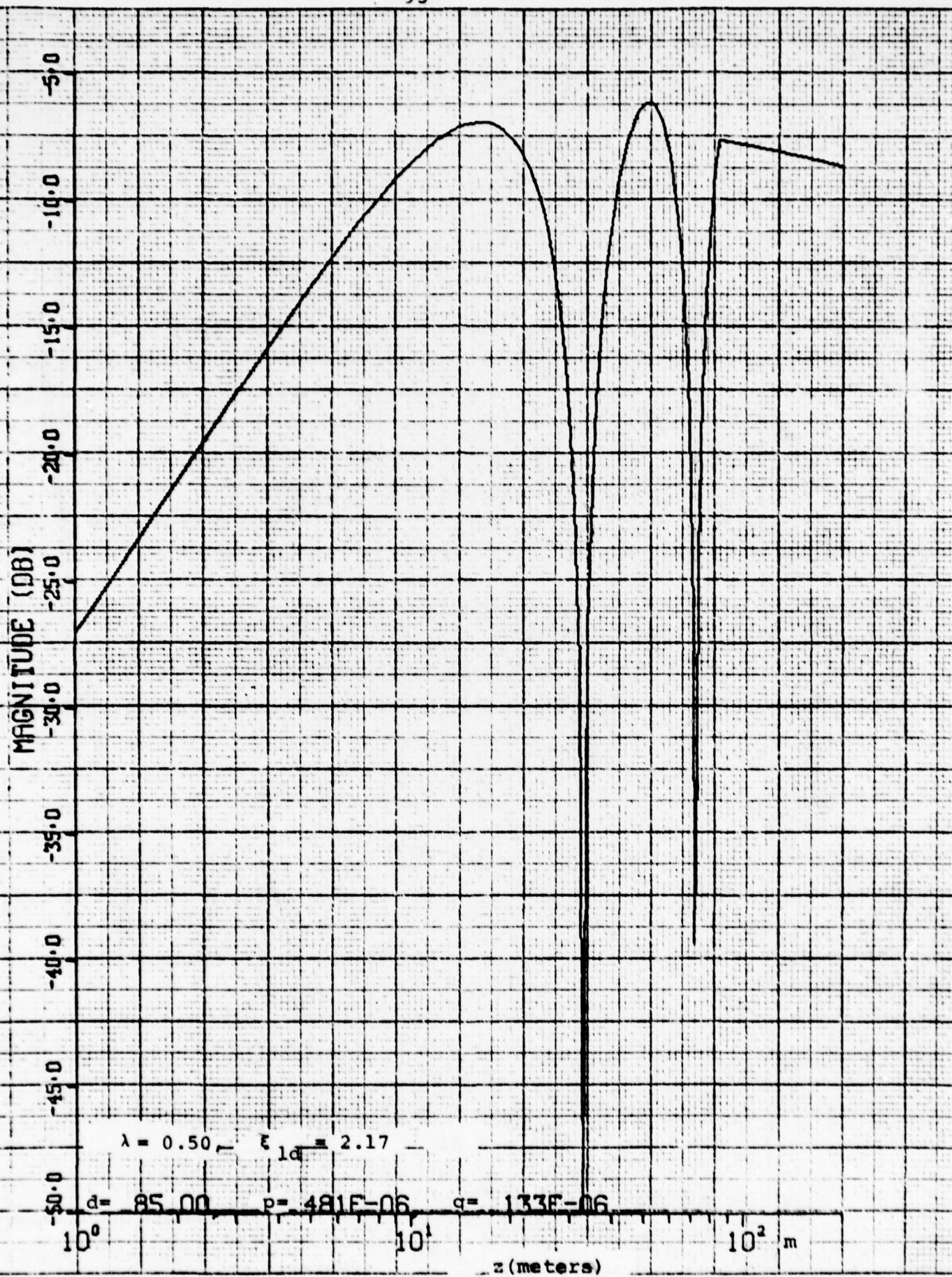


Fig. (4-35) Height-Gain Functions - April

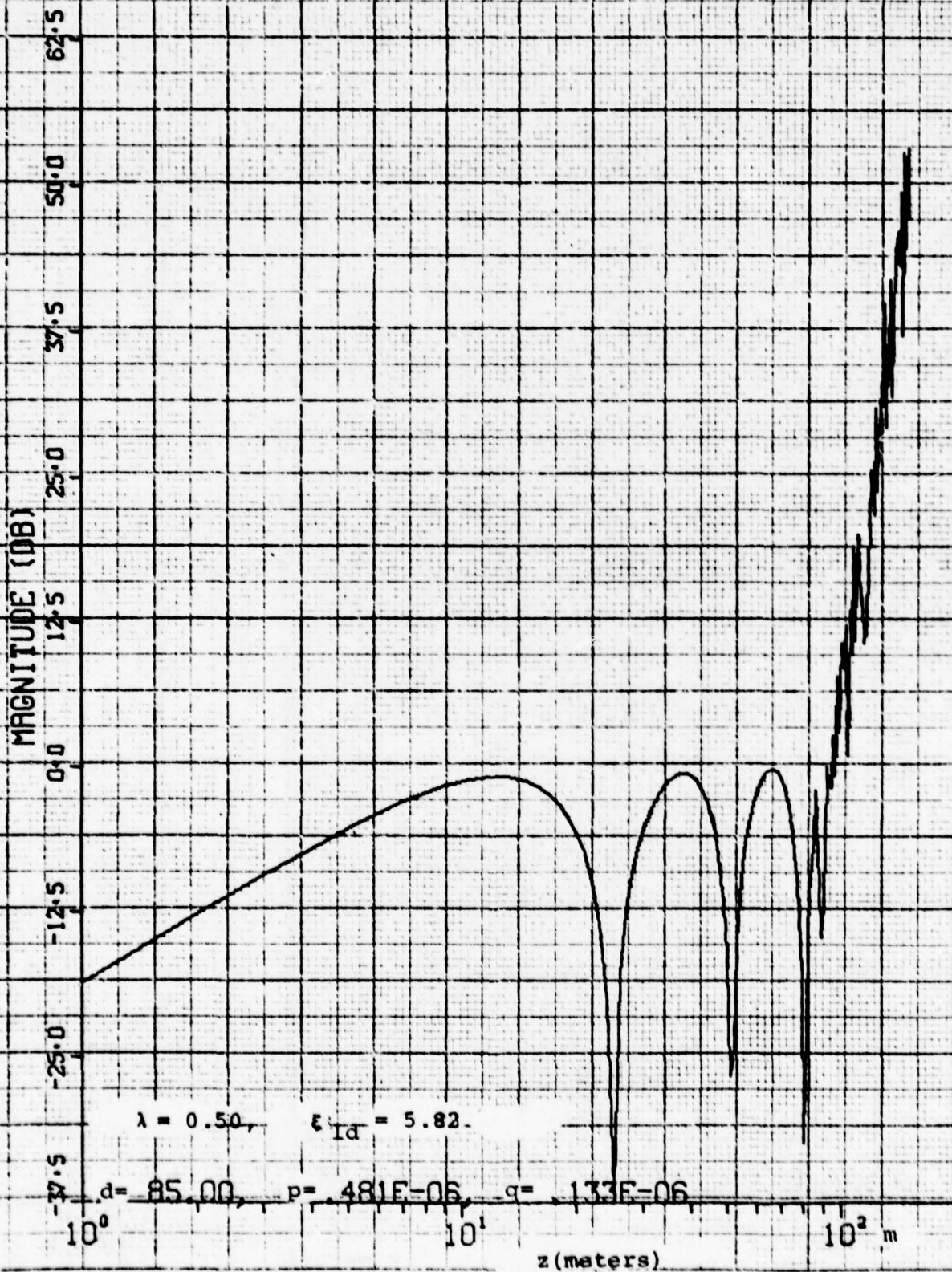


Fig. (4-36) Height-Gain Functions - April

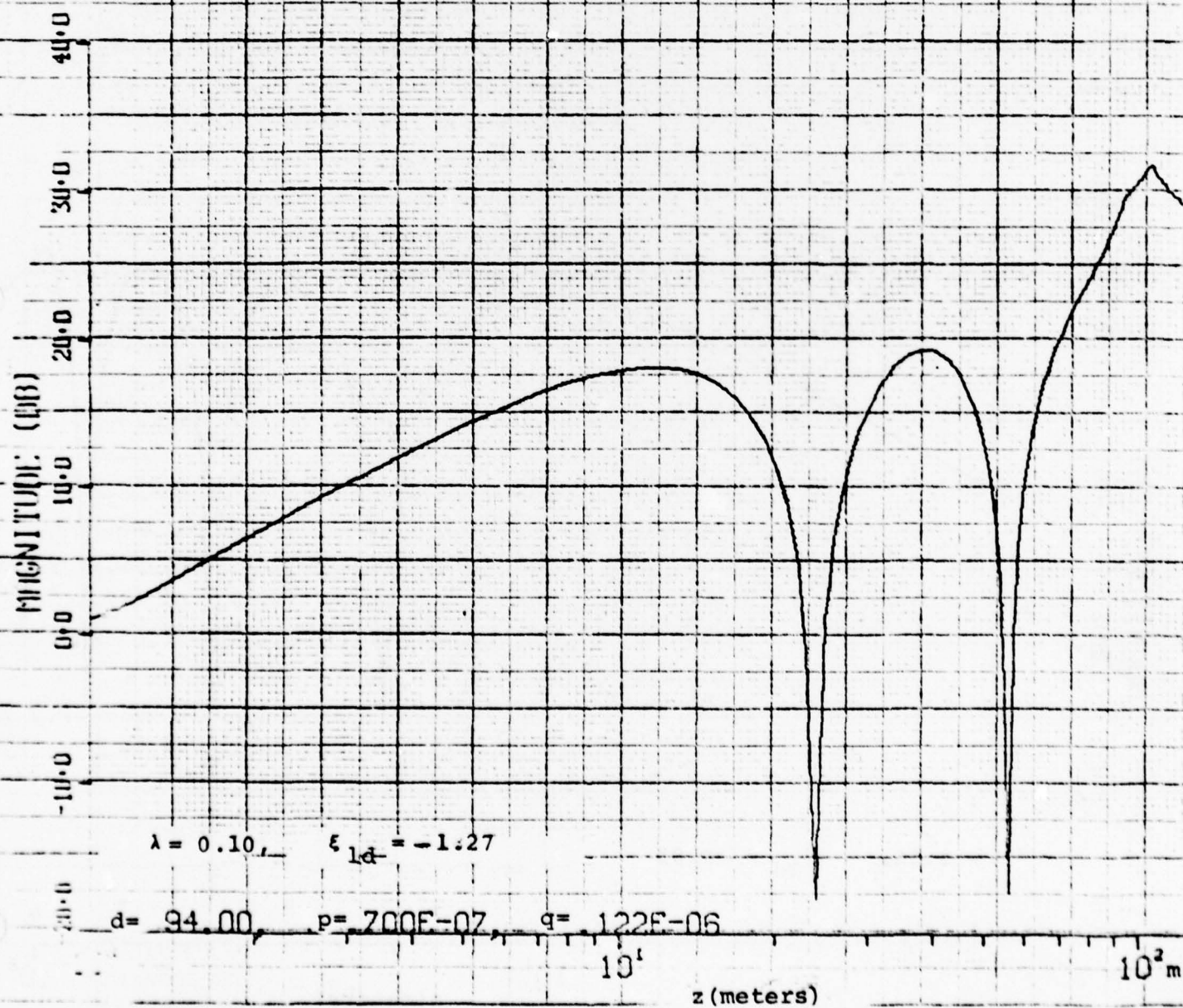


Fig. (4-37) Height-Gain Functions - September

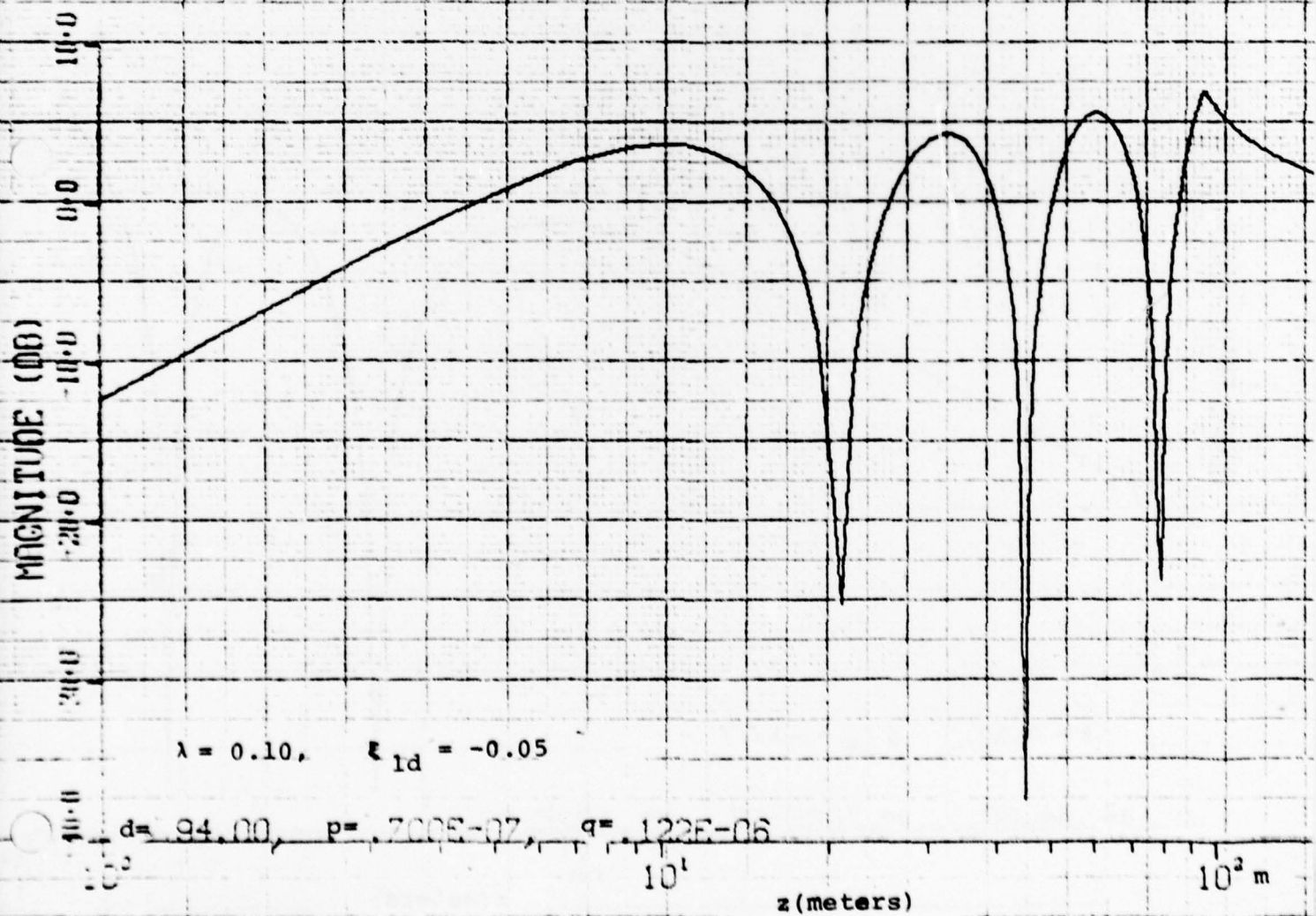


Fig. (4-38) Height-Gain Functions - September

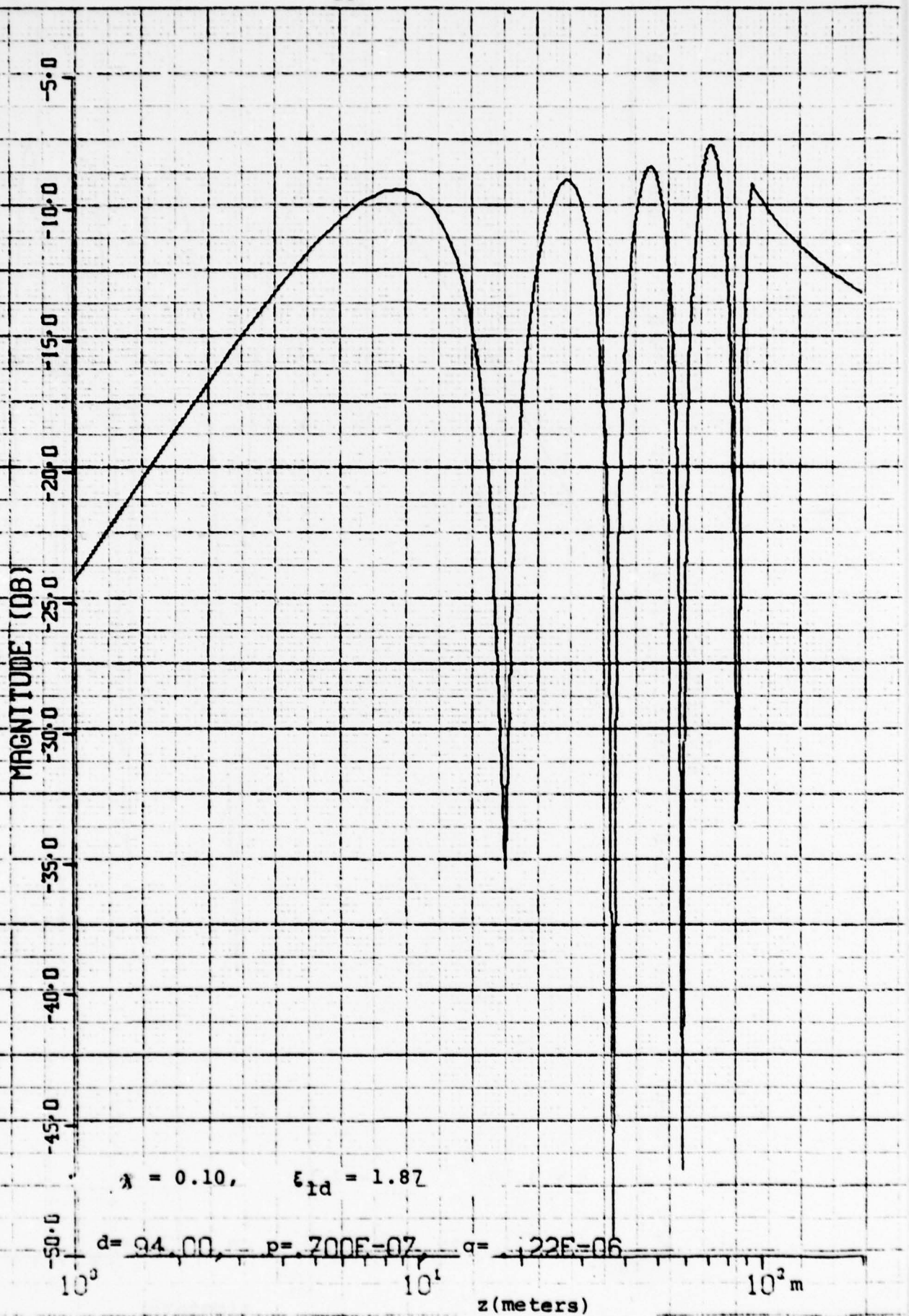


Fig. (4-39) Height-Gain Functions - September

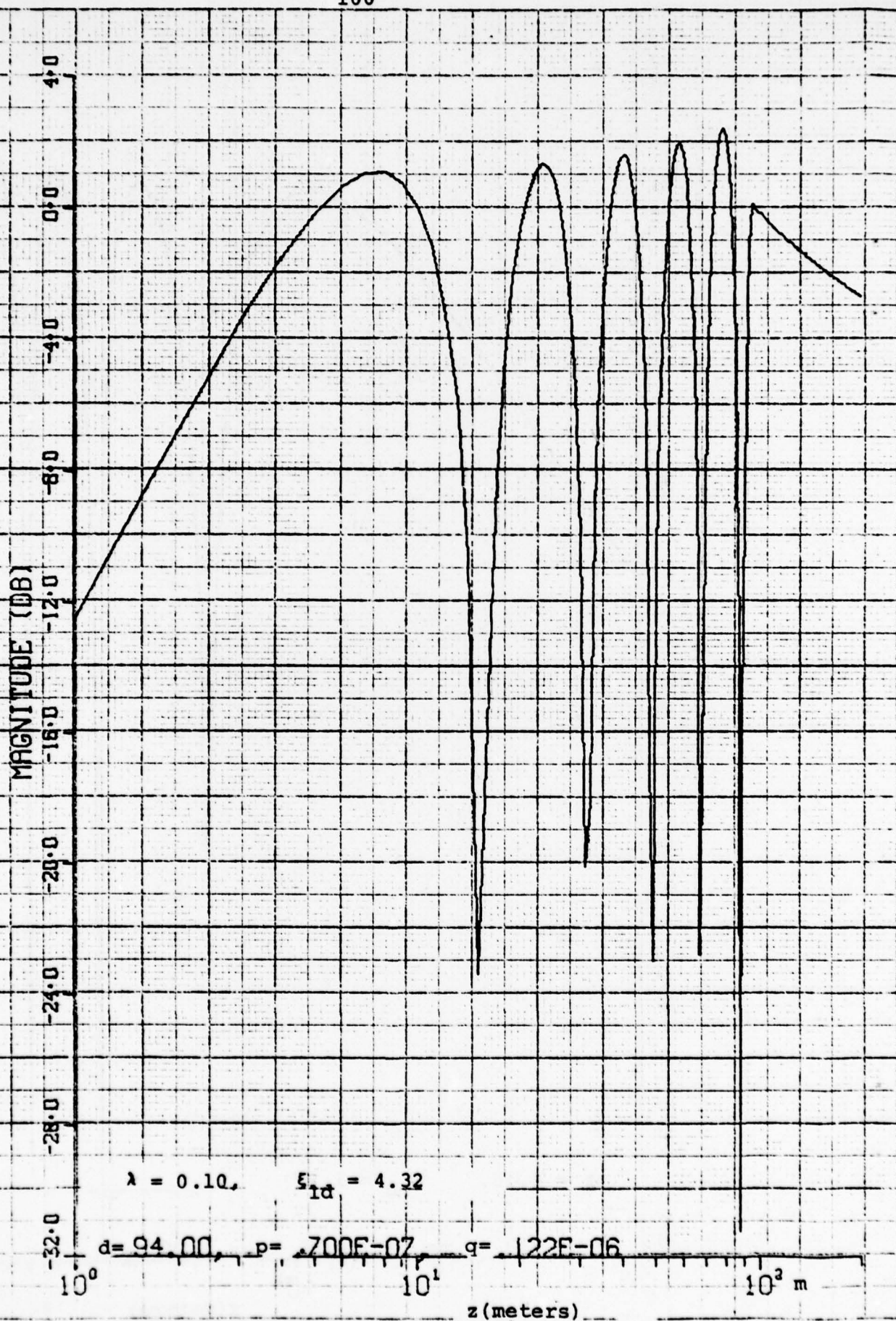


Fig. (4-40) Height-Gain Functions - September

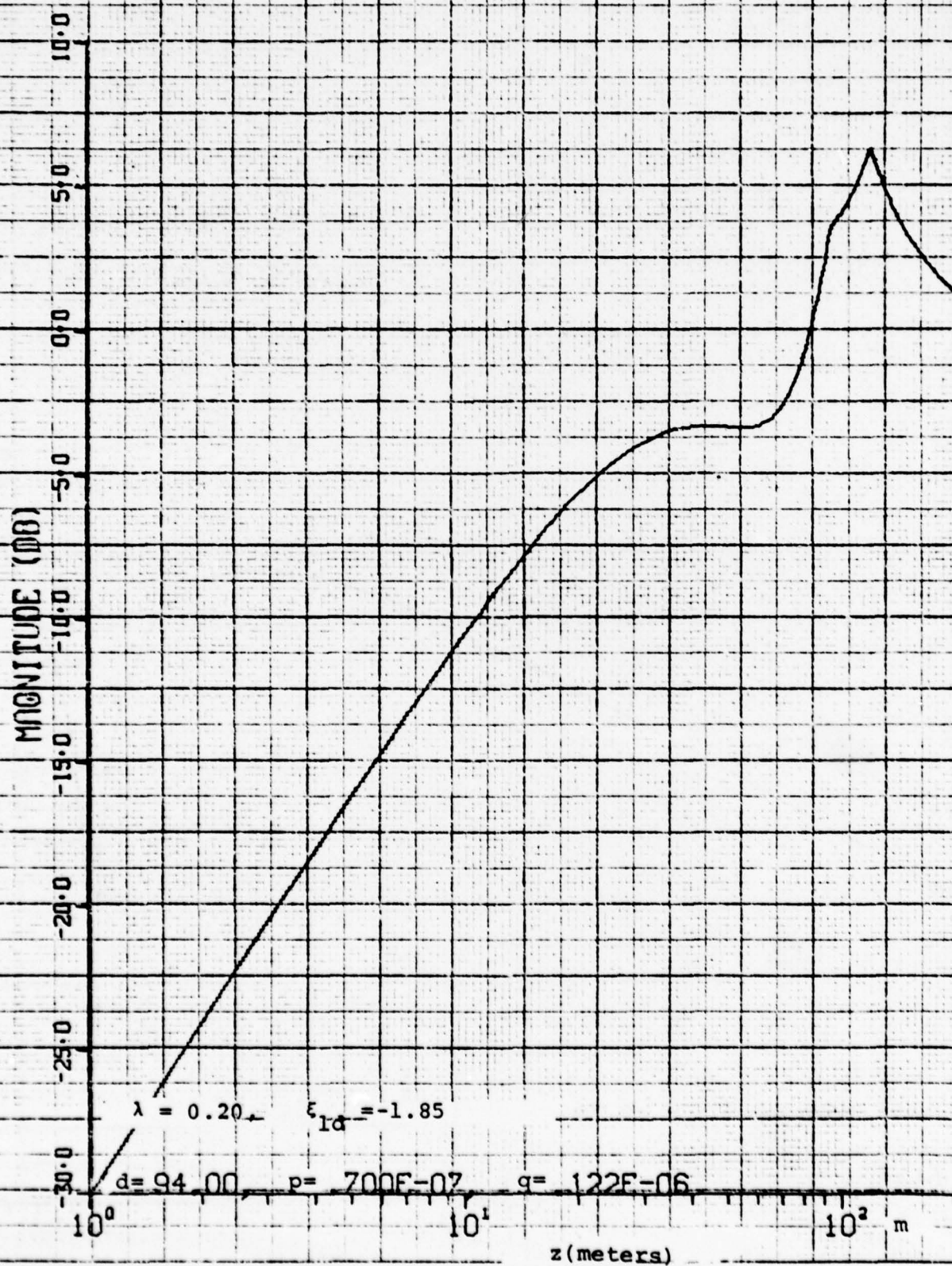


Fig. (4-41) Height-Gain Functions - September

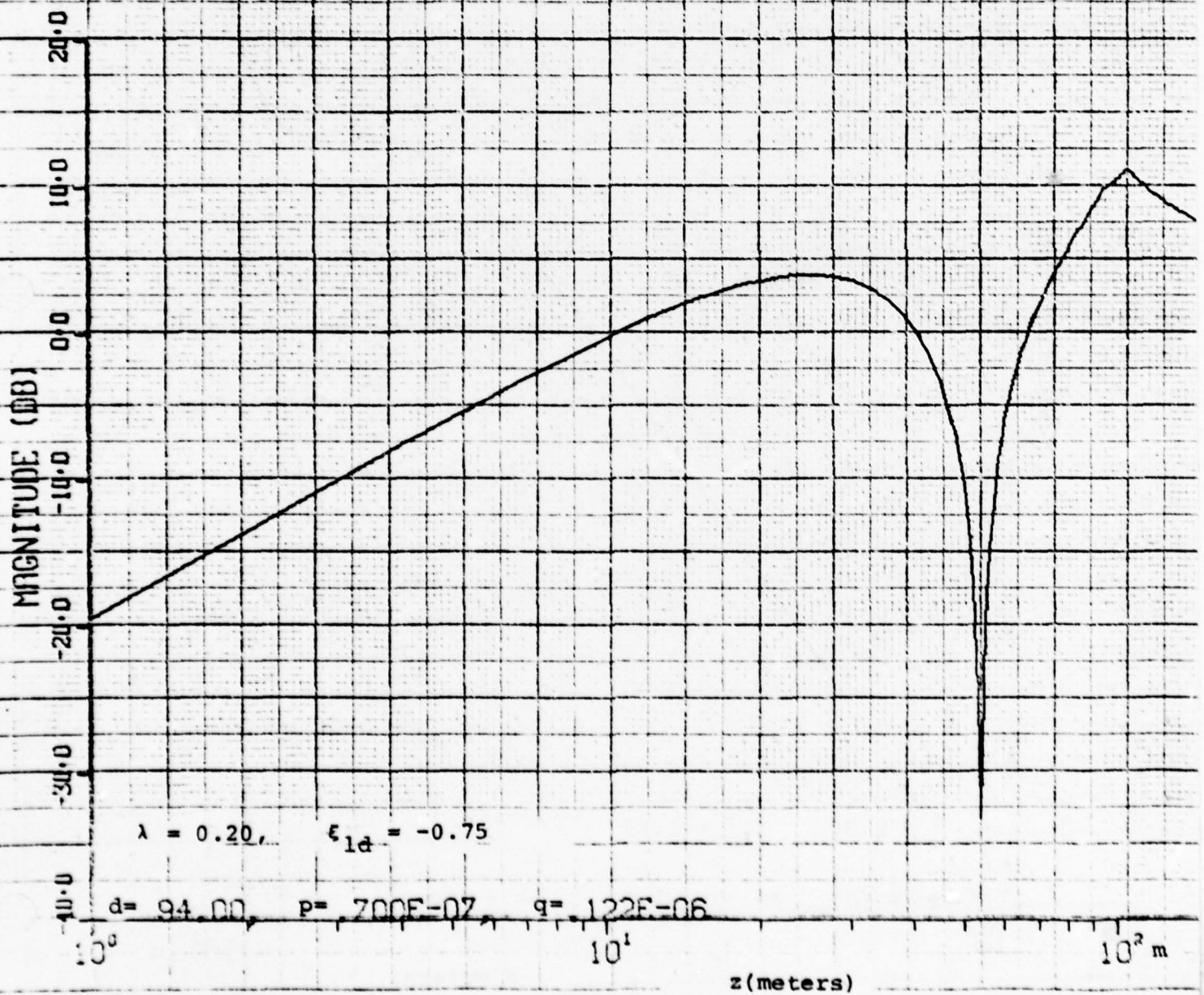


Fig. (4-42) Height-Gain Functions - September

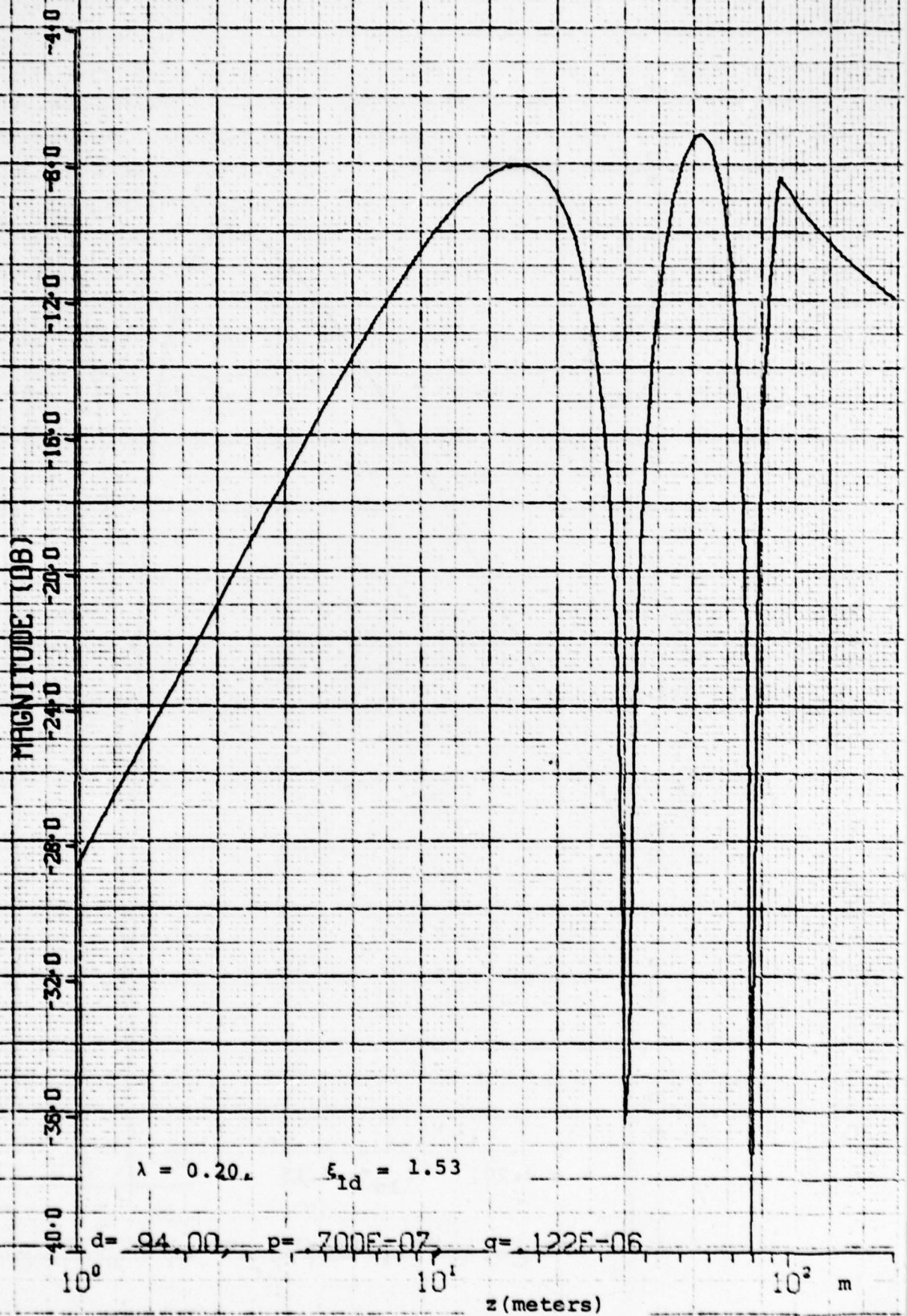


Fig. (4-43) Height-Gain Functions - September

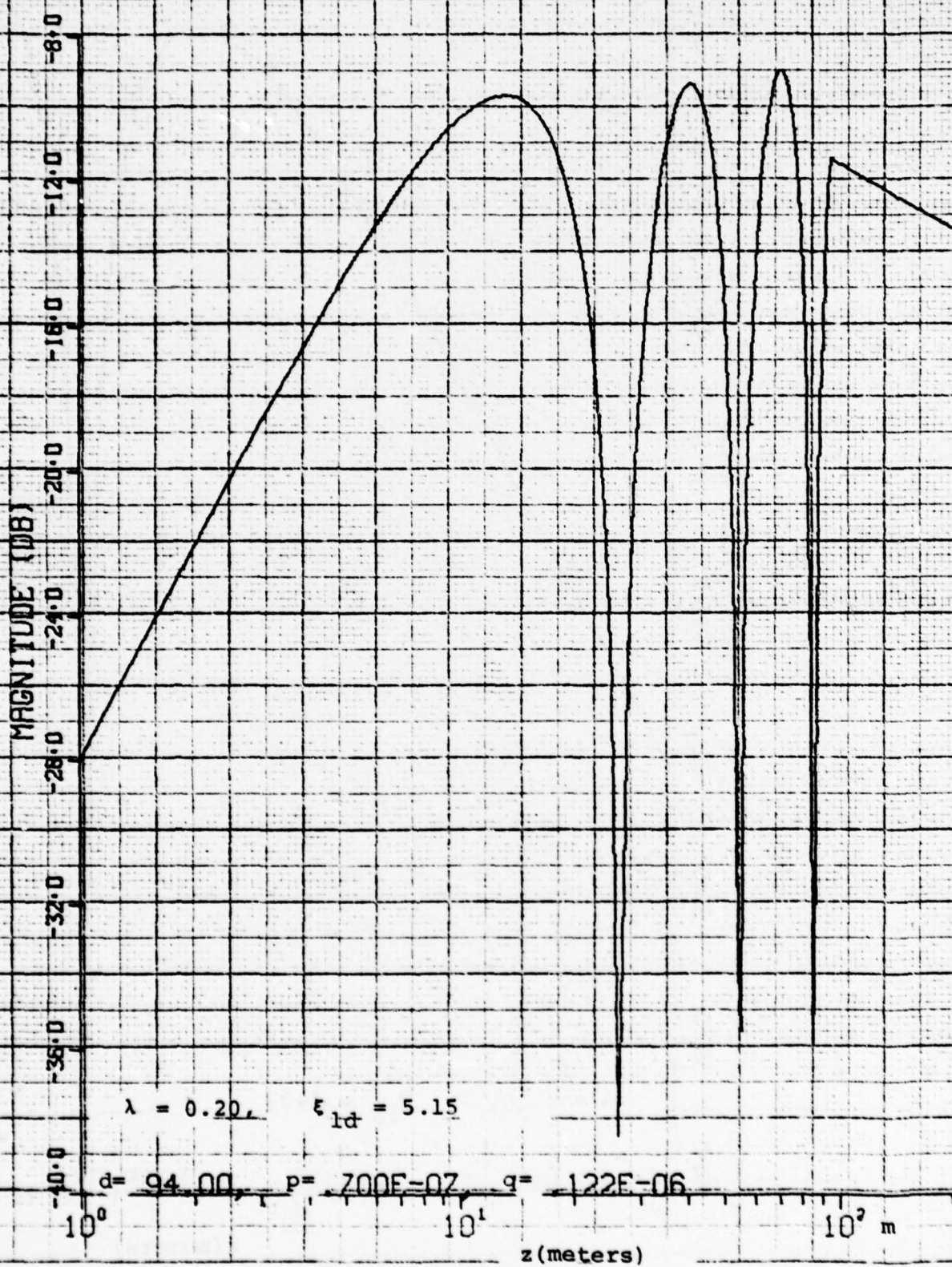


Fig. (4-44) Height-Gain Functions - September

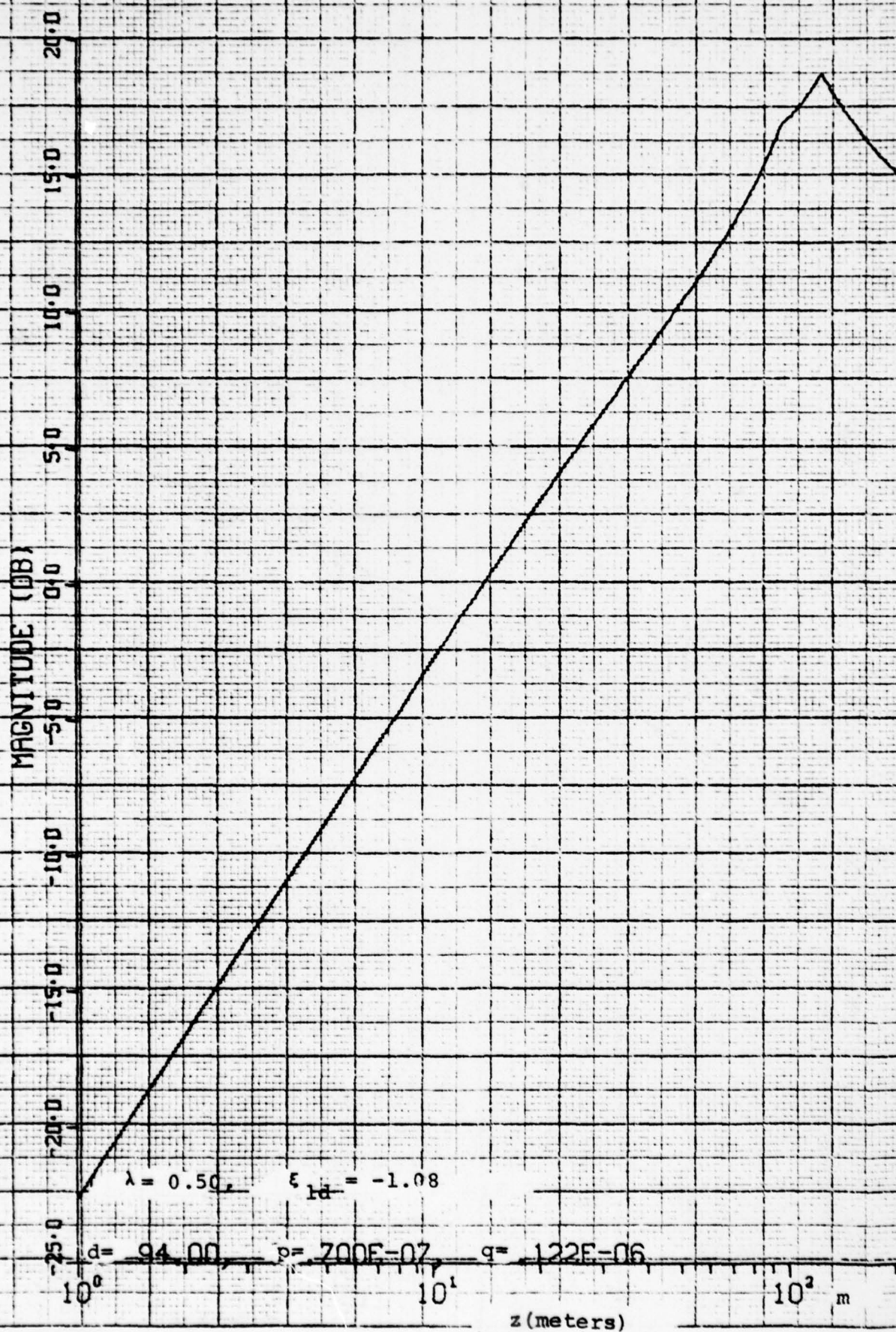


Fig. (4-45) Height-Gain Functions - September

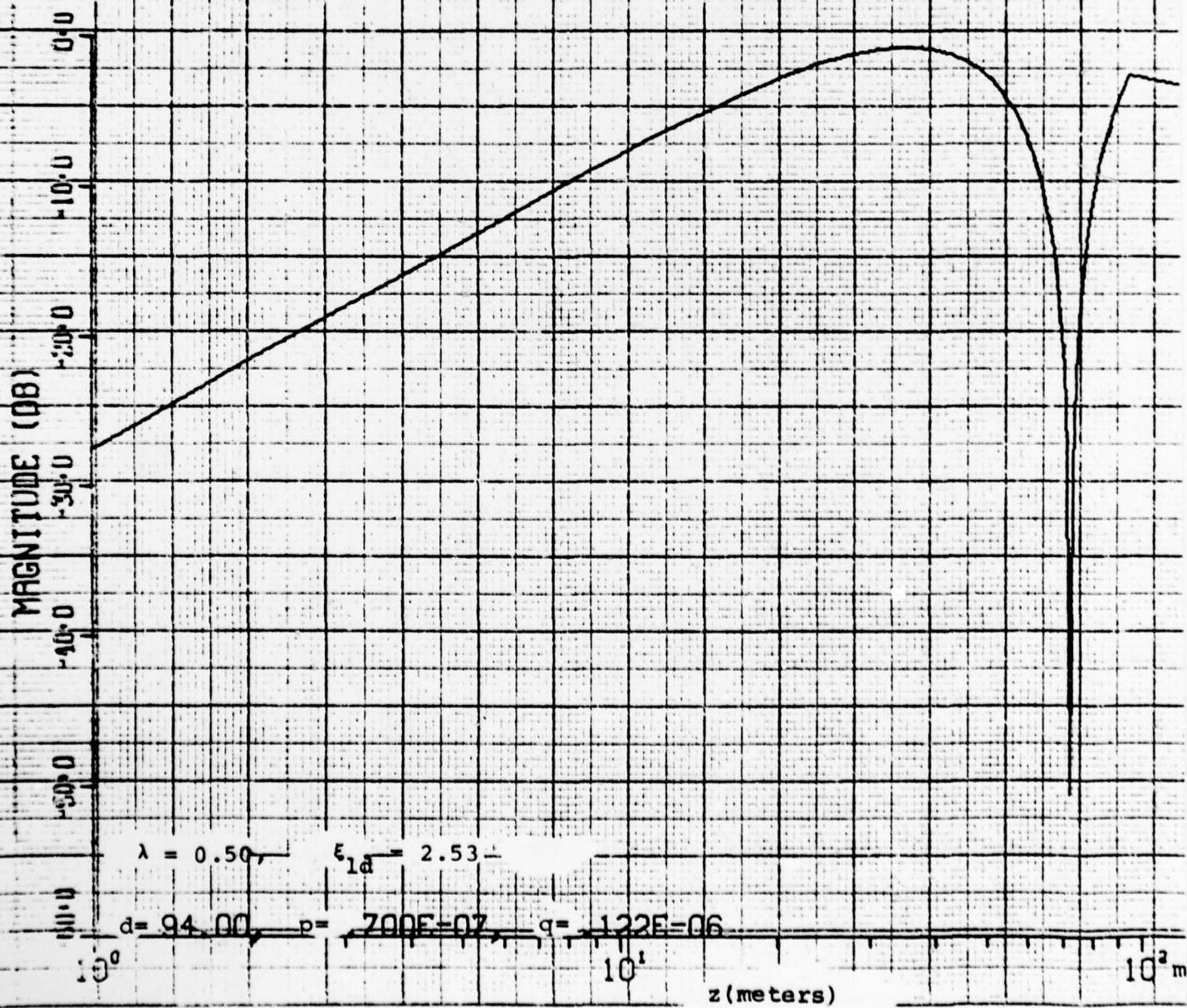


Fig. (4-46) Height-Gain Functions - September

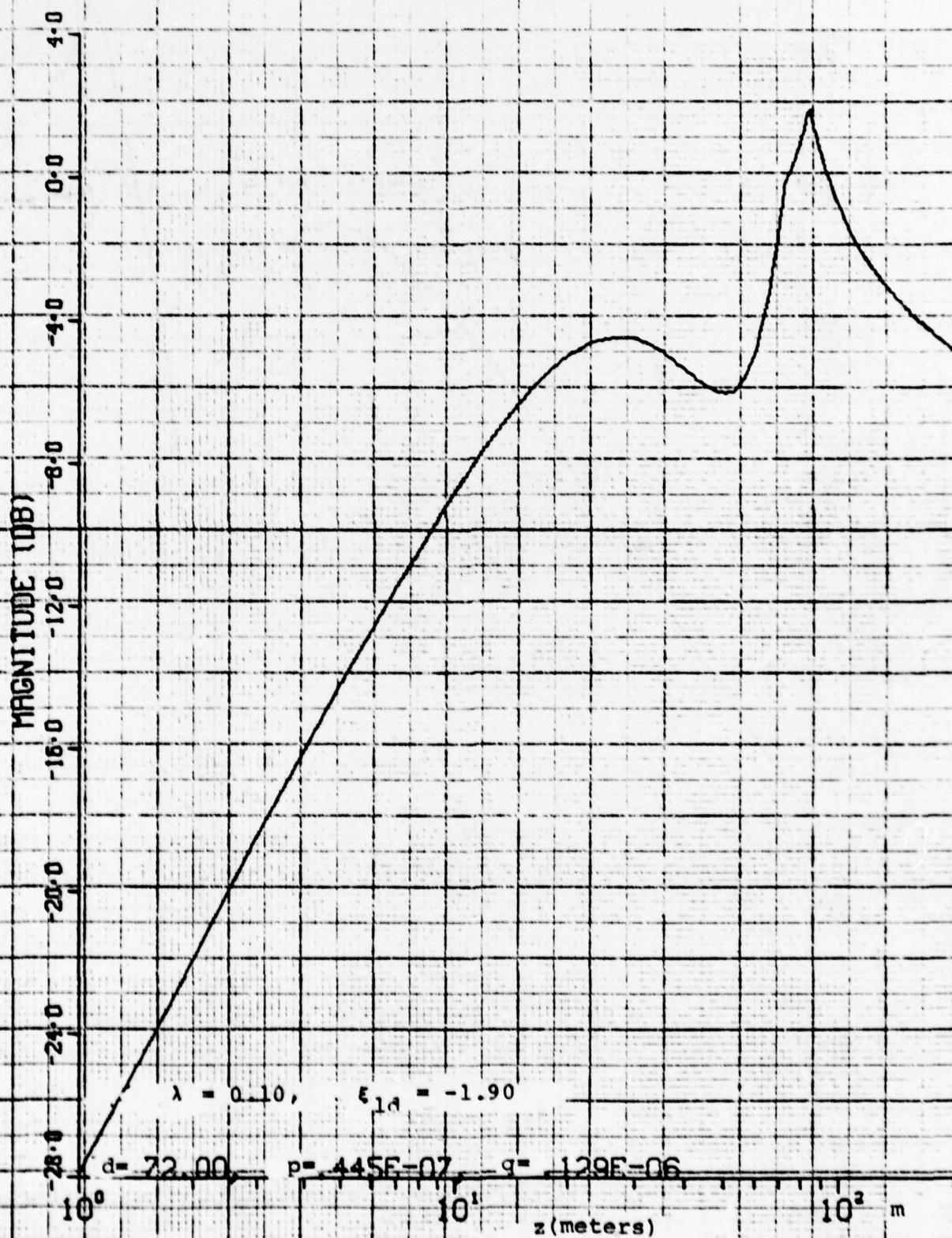


Fig. (4-47) Height-Gain Functions - December

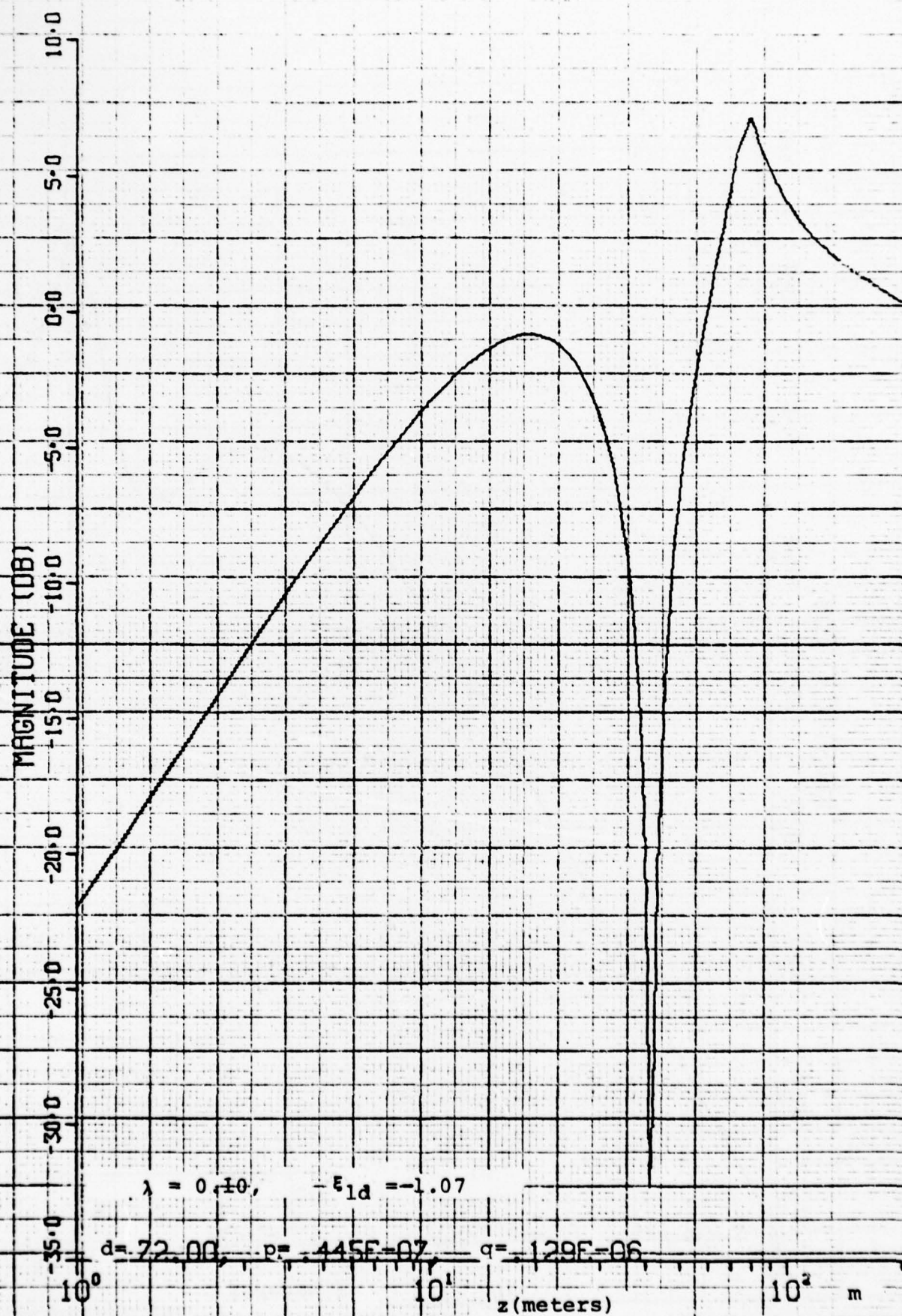


Fig. (4-48) Height-Gain Functions - December

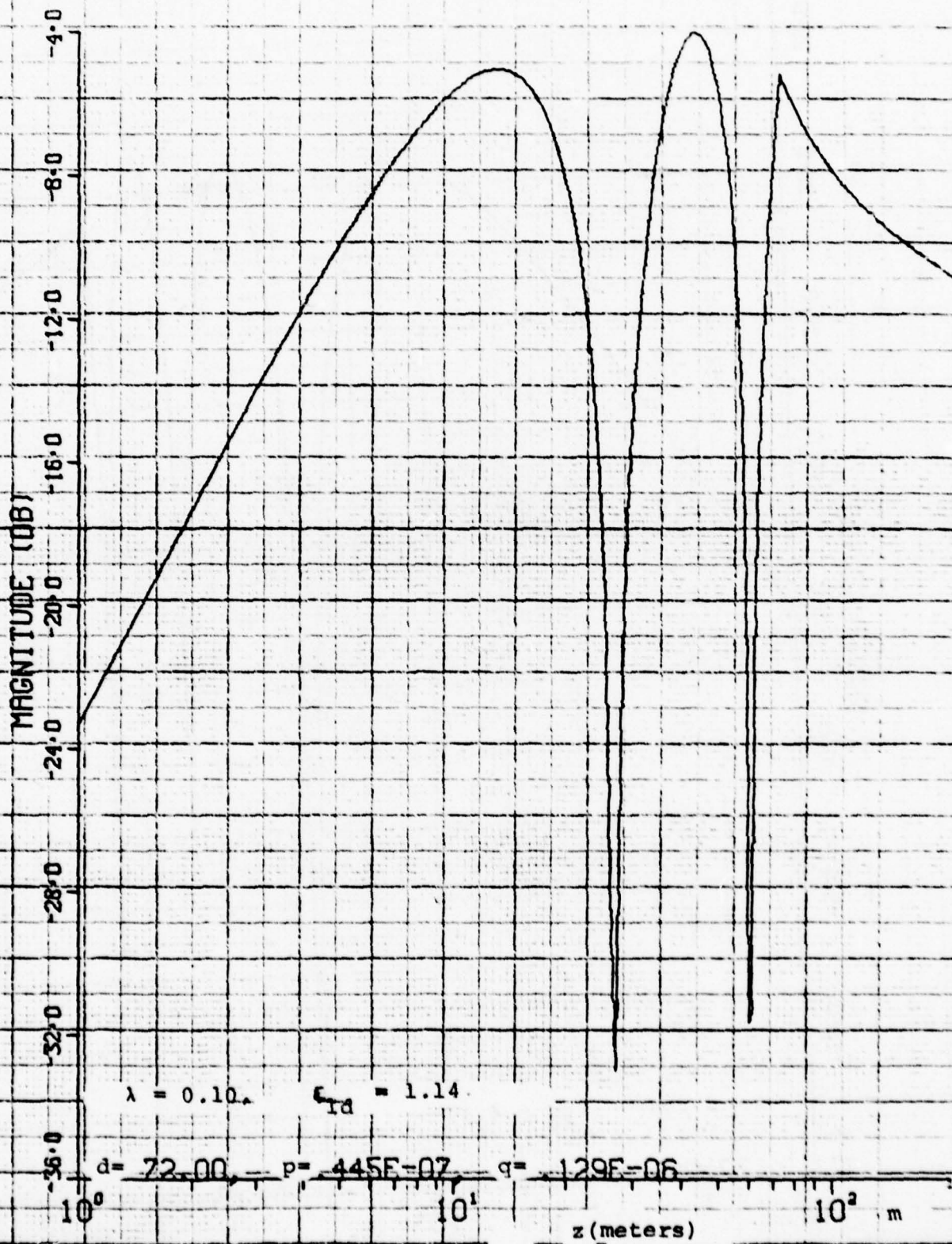


Fig. (4-49) Height-Gain Functions - December

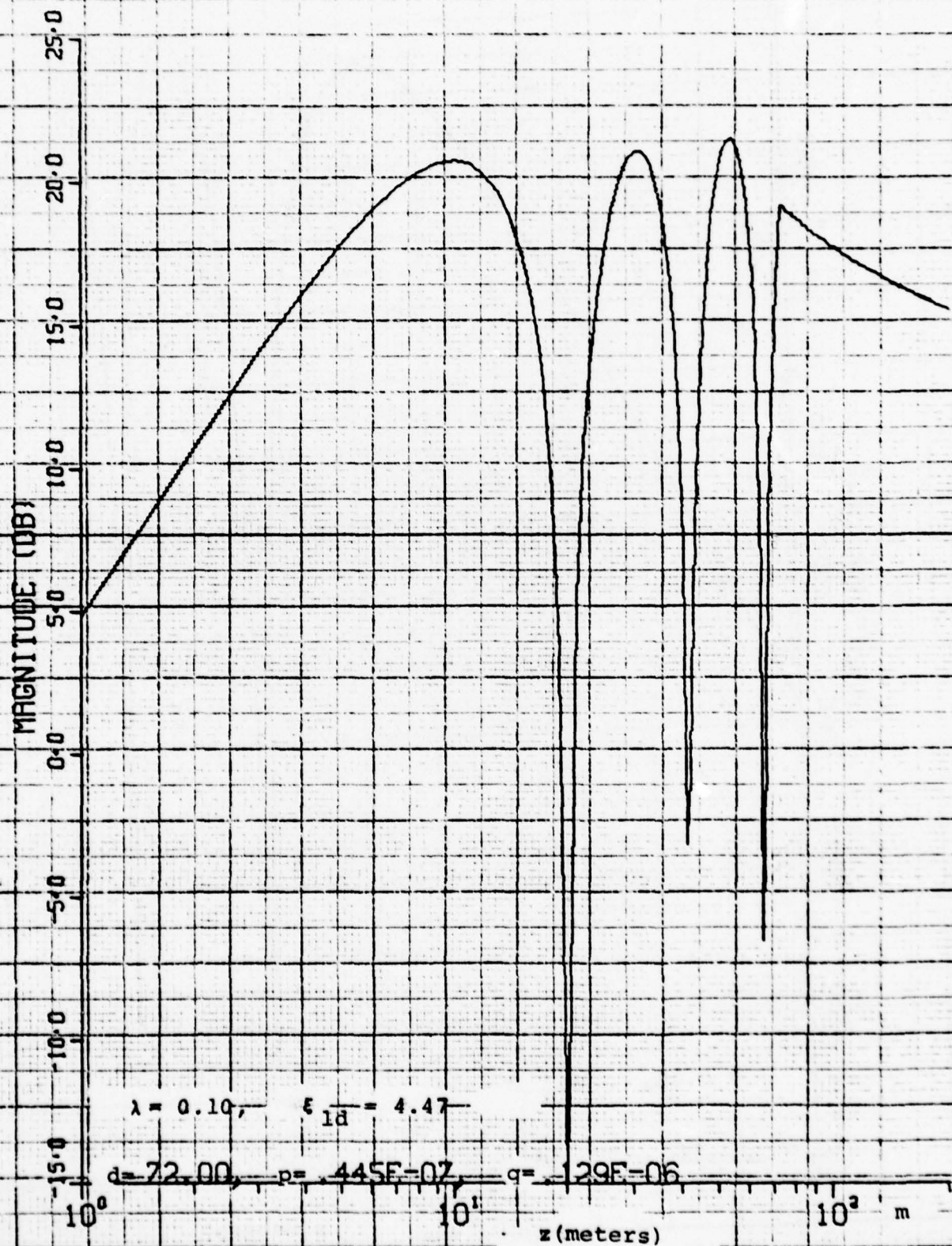


Fig. (4-50) Height-Gain Functions - December

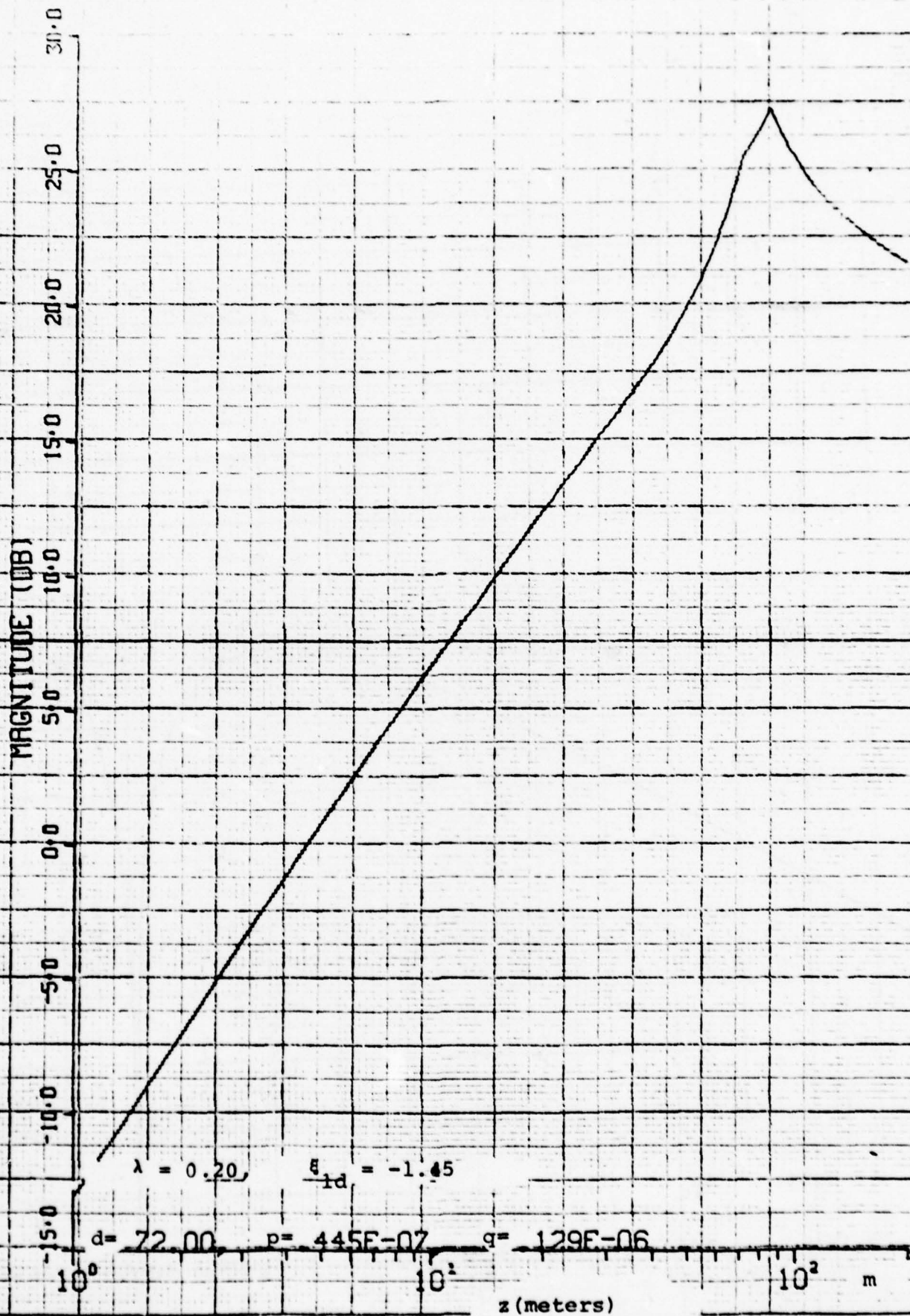


Fig. (4-51) Height-Gain Functions - December

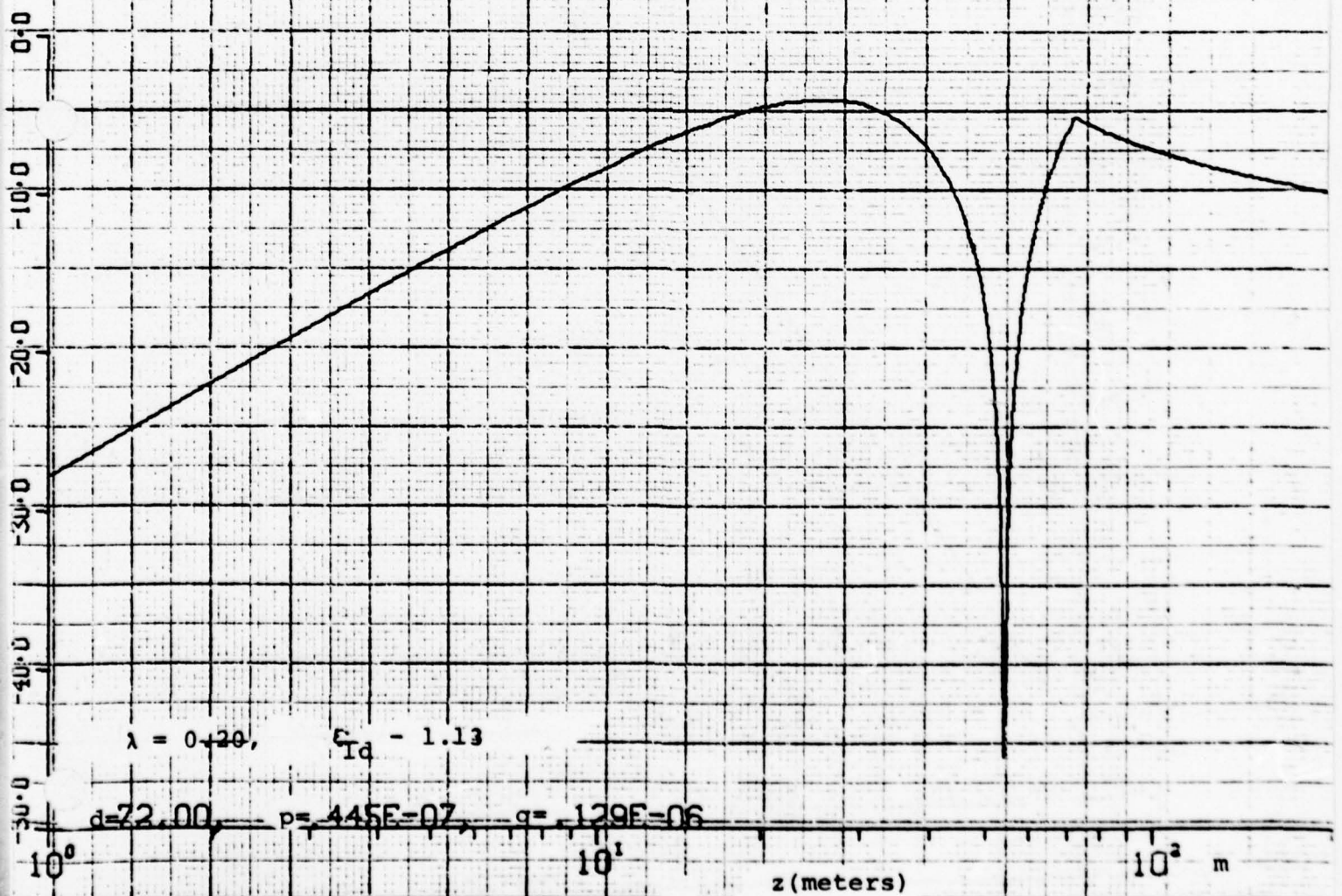


Fig. (4-52) Height-Gain Functions - December

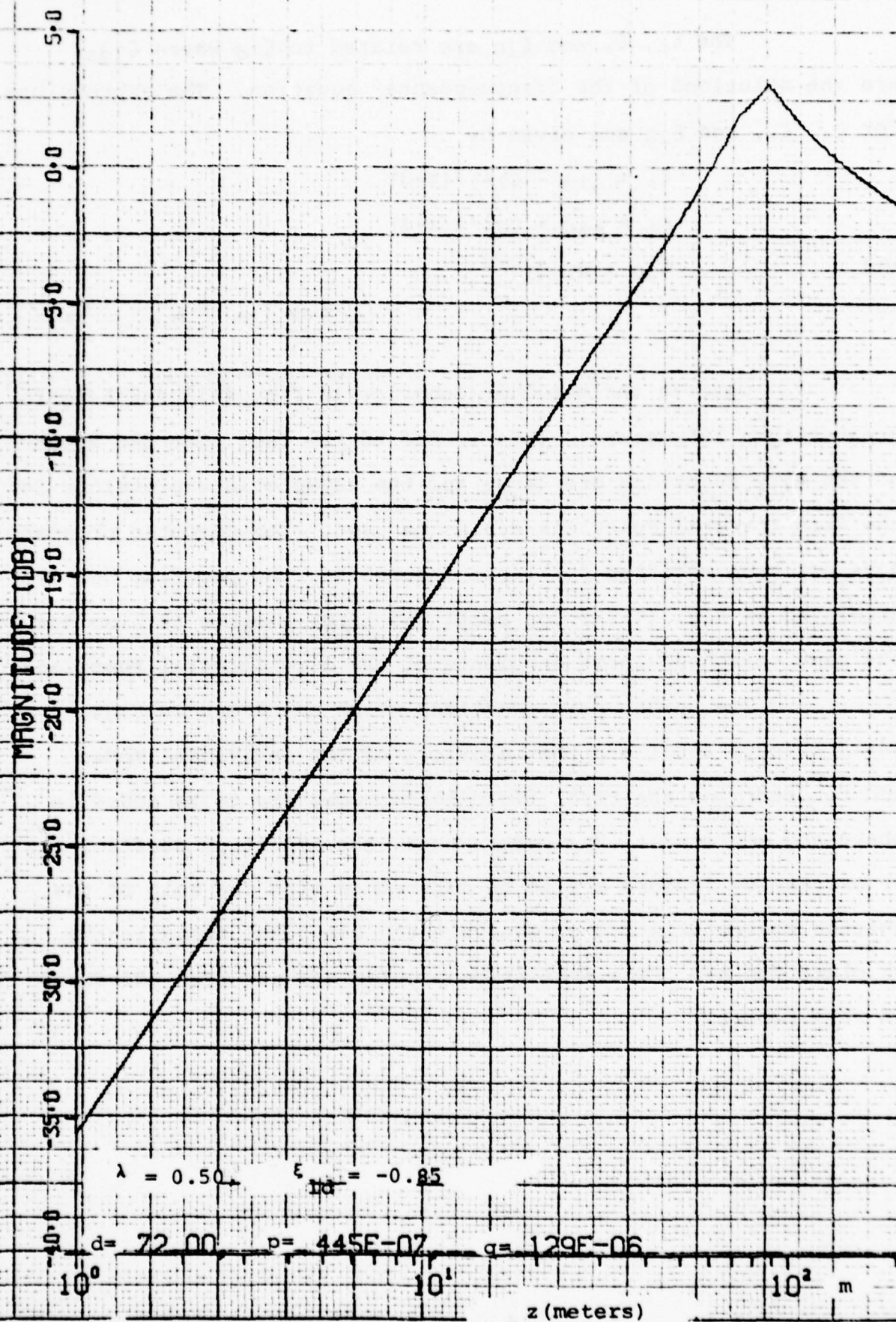


Fig. (4-53) Height-Gain Functions - December

The $\xi_<$, $\xi_>$ and ξ_{10} are related to ξ_{1d} where ξ_{1d} s are the solutions of the transcendental equation. The expressions for $\xi_<$, $\xi_>$, and ξ_{10} are given by

$$\xi_< = \xi_{1d} - C_1^{1/3}(z-d)$$

$$\xi_> = \xi_{1d} + C_2^{1/3}(z-d)$$

and
$$\xi_{10} = B_1/C_1^{2/3}$$

Observe the peculiar behavior in Fig. 4-18 for heights greater than 100 meters. This is due to the fact that the arguments of the Airy Functions are large and the asymptotic expressions for the Airy Integral Functions are to be used. The computer programs have not been modified for large arguments. The peculiar behavior displayed in Fig. (4-28) for small and large heights is also due to the same reason of large arguments of the Airy Integral Functions.

The height gain functions which are shown in Figs. (4-17 through 4-53) are the behaviors of the individual modes and to determine the total field these modes are to be added in phase and amplitude. But before that, the amplitude coefficients or excitation factors are to be determined with the help of the antenna characteristics or equivalently the total field in the yz plane for $x=0$. The excitation problem has not been addressed in this report.

5. SUMMARY / RECOMMENDATIONS

5.1 Summary

In this phase of the program, the electromagnetic propagation through a medium, which was characteristic of meteorological conditions around Canton Island, was considered in depth. The meteorological conditions around Canton Island were represented by bilinear and trilinear refractive index profiles.

For the propagation analysis, both the geometrical optics or ray trajectory approach and the physical optics or the guided wave approach were considered. The relative merits of these approaches were highlighted. The ray trajectories for four different days of meteorological data were also generated.

The guided mode approach was pursued to determine the propagation behavior for both the bilinear and trilinear refractive index profiles.

The numerical analysis to determine the modal solutions and the corresponding height-gain functions was carried out only for the bilinear profile. The modal solutions were obtained by iterative numerical analysis of the transcendental equation for the trapped modes only.

For the leaky modes, a previously developed approximate expression was used. The validity of the expression for duct heights smaller than the frequency dependent scale height was established.

Although leaky modes are indicative of the field above the duct height, for quantitative assessment of the field intensity in the shadow zone, the excitation problem has to be solved. This has not been addressed in this phase of the program.

5.2 Recommendations

The usefulness of the guided wave propagation analysis hinges on the ability to generate radar coverage diagrams. The radar coverage diagrams in the presence of different kinds of meteorological ducts would enable one to evaluate the performance degradation of ESD sponsored surveillance radar systems.

For the generation of radar coverage diagrams, the following tasks need to be completed.

1. An effective analytical technique to determine the complex eigenvalues representing leaky modes.
2. Determining the amplitude coefficients of the trapped and leaky modes by addressing the excitation problems or by specifying the antenna characteristics.
3. Applying these techniques to different meteorological conditions and different radar systems parameters.

These tasks can constitute the second phase of the program.

6. REFERENCES

1. B.R. Bean and E.J. Dutton - Radio Meteorology, Dover Publication, 1968
2. D.E. Kerr - Propagation of Short Radio Waves, Radiation Laboratory Series Vol. 13, McGraw-Hill, 1951
3. A. Zanca - (Editor) - Modern Topics in Microwave Propagation and Air-Sea Interaction, Proceedings of the NATO Advanced Study Institute, Sorento, Italy, June 5-14, 1973 - D. Reidel Publishing Company
4. J.R. Wait - Electromagnetic Waves in Stratified Media, Macmillan Company, 1962
5. P. Beckman and A. Spizzichino - The Scattering of Waves from Rough Surfaces, Macmillan Company, 1963
6. D. Barton - Radars Vol. 5 - Radar Clutter ARTECH House, 1975
7. M. Abramowitz and L.A. Stegun (Edited by) Handbook of Mathematical Functions National Bureau of Standards - Applied Mathematics Series - 55, June 1964
8. K.G. Budden - The Wave Guide Mode Theory of Wave Propagation Prentice Hall, 1961
9. J.H. Richter and H.V. Hitney - The Effect of the Evaporation Duct on Microwave Propagation, NELC Report TR-1949, April 1975
10. H.V. Hitney - Propagation Modeling in the Evaporation Duct, NELC Report - TR-1947, April 1975
11. H. Jeske and K. Brooks - Comparison of Experimental on Duct Propagation above the Sea with the Mode Theory of Booker and Walkinshaw, Radio Science Vol. 1, August 1966
12. H.W. Fruchtenicht - Notes on Duct Influences on Line-of-Sight Propagation, IEEE Transactions on Antennas and Propagation Vol. AP-22, No. 2 - March 1974
13. J.K. DeRosa - Refractive Multipath in Low Angle Radar Tracking, IEEE International Radar Conference, 1975
14. G.H. Joshi - Propagation Modeling in the Presence of Meteorological Ducts, Raytheon Technical Memo No. GHJ:76:09, August 1976
15. L.M. Brekhovshikh - Waves in Layered Media, Academic Press, 1960

REFERENCES (CONT)

16. Tables of the Modified Hankel Functions of Order One-Third and of Their Derivatives, The Annals of the Computation Laboratory of Harvard University, Vol. II, Harvard University Press, 1945
17. J.C.P. Miller - The Airy Integral - Mathematical Tables, University Press Cambridge, 1946
18. G.N. Watson - The Diffraction of Electric Waves by the Earth, Proc. Roy. Soc. A, 95, 83, 1919
19. G.N. Watson - The Transmission of Electric Waves Round the Earth, Proc. Roy. Soc. A, 95, 546, 1919

APPENDIX I

Computer program to determine the roots
of the transcendental equation.


```
1 C 09-22-77 /JOST/
  PRIGRAM JOST(INPUT,OUTPUT,TAPE2,PLFILEM65)
5 C
  COMMON /XFACT/XFACT(150),FT(43),CT(43),FTP(43),CTP(43),
    * FMULT,GMULT,JMOL(2),XPI(120),YPI(120),IMOL(100)
7 C
  COMPLEX 820,820Y1,820Y2
9 C
  DOUBLE PRECISION C1,FMULT,FT,FTP,GMULT,CT,CTP
  DOUBLE PRECISION PA3,800,8000,811,1000,XFACT,XK0,XNUM
  DOUBLE PRECISION 80001,80002,XNUM1,XNUM2,XDEB1,XDEB2
11 C
  DIMENSION D(4),P(4),PA(4),XL(3)
13 C
  DATA D/42.05,09.0,72./
  DATA P/.630E-6,081E-6,07E-6,0045E-6/
  DATA PA/4.0,3.61,0.579,0.344/
  DATA XL/.1,0.2,0.5/
  DATA JMOL/10HAPPROX 10HEXACT /
17 C
  CALL NGAMMA(2,0,3,0,FMULT,IER1)
  CALL NGAMMA(4,0,3,0,GMULT,IER2)
  FMULT=(2.00(1,0,3))/FMULT
  GMULT=(2.00(1,0,3))/(GMULT*5.00(2,0,3))
19 C
  PT=0.9ATAN(1.)
  CALL CFAC
  CALL CUMPS
  CALL MORRIS
  CALL INTXS
  CALL PAGE(15,0,10,75)
  CALL PHYSOR(1.5,1.5)
  CALL VAXANG(0.)
  CALL CROSS
  CALL MIXALF(0STANDARD,1M9)
  CALL MIX2ALF(0L/CGREEN,1M1)
21 C
  PRINT (2,90)
  FORMAT(1H1,///,
23 *B LAMBOA 820m//,
25 *B -----
27 *B -----)
29 C
  DO 300 IXL=1,1
  DO 300 IDEB=1,1
31 C
  DO 300 ILOOP=1,1
  820=2.33919EXP(CMPLX(0,2.0PI/3.3))
  PRINT 95,IXL,IXL,DEB(ILOOP),P(ILOOP),PA(ILOOP),820
  FORMAT(1H1,///,
33 *B LAMBOA
35 *B D
37 *B P
39 *B P/A
41 *B 820
43 *B 820
```

120

Appendix I
I-1THIS PAGE IS BEST QUALITY PRACTICABLE
FROM COPY FURNISHED TO DDG

```
00 PA30PA(11000100(1.23.)
01 XN02.0P1/11(11L)
02 C1P(110001)XK0002
03 000CAB0(020)/PA3002
04 PRINT 96,JHOL(100)
05 FORMAT(//,21,A10,/,
06 PRINT 97 1 020 0.13X.0 0000 01100
07 FORMAT(, - - - 0.13X.0 - - -
08 DO 200 101.1
09 ICNTP0
10 DO 120 J01.121
11 000-6.+(J-11)1.1
12 IF(100.00.0100 TO 120
13 IF(1001(000.020.0000.P1,PA3,0(1000),C1,XNUM,1000)
14 .ME.0100 TO 300
15 PRINT 121,000.XNUM
16 FORMAT(, 00000.015.0.0 XNUM0.013.0)
17 ICNTP0+1
18 VP1(1000)XNUM
19 VP1(1000)XNUM
20 CONTINUE
21 IF(100.00.0100 TO 150
22 GO TO 300
23 IF(1001(, 00000.000.0201,00001.P1,PA3,0(1000),C1,XNUM,1000)
24 .ME.0100 TO 300
25 IF(1001(1.00001.0000.0202,00002.P1,PA3,0(1000),C1,XNUM,1000)
26 .ME.0100 TO 300
27 IF(100.00.11011.000-XNUM/(XNUM0-XNUM)/(, 00002.0000)
28 IF(100.00.21011.000-XNUM/XNUM/1000
29 PRINT 111,1.000.0000.011
30 FORMAT(
31 10.1M(, 2615.0.1M), 2015.0)
32 DO 300 0011
33 PRINT (2,250)X1(11L),0(1000),P(1000),PA(1000),011,000,
34 JHOL(100)
35 FORMAT(2612.0.1M(, 2612.0.1M), 21.010)
36 CALL 10000PL
37 PRINT(2,511)
38 FORMAT(111)
39 ENDPFILE 2
40 END
```

121
Appendix I
I-2

THIS PAGE IS BEST QUALITY PRACTICABLE
FROM COPY FURNISHED TO DDC

CARD NO. SEVERITY DETAILS DIAGNOSIS OF PROBLEM

45 1 LOWER LIMIT .GE. UPPER LIMIT, ONE TRIP LOOP.
47 1 LOWER LIMIT .GE. UPPER LIMIT, ONE TRIP LOOP.
49 1 LOWER LIMIT .GE. UPPER LIMIT, ONE TRIP LOOP.
51 1 LOWER LIMIT .GE. UPPER LIMIT, ONE TRIP LOOP.
53 1 THERE IS NO PATH TO THIS STATEMENT.

DECLARATION

THIS PAGE IS BEST QUALITY PRACTICABLE
FROM COPY FURNISHED TO DDC

82128

PAGE 9

77/09/22, 13.59.33

PTM 0.64052

73/74 DPT01 TRACE

PROGRAM J087

STATISTICS

PROGRAM LENGTH

SUFFIX LENGTH

CH LABELED COMMON LENGTH

32000 CH USED

7345 070

33618 1777

17345 990

124

Appendix I
I-9

THIS PAGE IS BEST QUALITY PRACTICABLE
FROM COPY FURNISHED TO DDG

```

100  FUNCTION-IABJ(ARG,AI,BI,AIP,BIP)
101  COMMON /XFACT/XFACT(30),PT(43),GT(43),FT(43),STP(43),
102  * PMULT,MULT,JMUL(2),ZPI(120),VPI(120),IMUL(100)
103  DOUBLE PRECISION A,AI,AIP,ARG,B,BIP,BIP,P,MULT
104  DOUBLE PRECISION FP,FT,PT,PMULT,OP,OT,OTP,XFACT
105  DATA C1,C2,C3,C4,C5,C6,C7,C8,C9,C10,C11,C12,C13,C14,C15,
106  * PRINT 9,0 ARG,ARG
107  IABJ=1
108  A=1.
109  B=1.
110  C=1.
111  D=1.
112  E=1.
113  F=1.
114  G=1.
115  H=1.
116  I=1.
117  J=1.
118  K=1.
119  L=1.
120  M=1.
121  N=1.
122  O=1.
123  P=1.
124  Q=1.
125  R=1.
126  S=1.
127  T=1.
128  U=1.
129  V=1.
130  W=1.
131  X=1.
132  Y=1.
133  Z=1.
134  AA=1.
135  AB=1.
136  AC=1.
137  AD=1.
138  AE=1.
139  AF=1.
140  AG=1.
141  AH=1.
142  AI=1.
143  AJ=1.
144  AK=1.
145  AL=1.
146  AM=1.
147  AN=1.
148  AO=1.
149  AP=1.
150  AQ=1.
151  AR=1.
152  AS=1.
153  AT=1.
154  AU=1.
155  AV=1.
156  AW=1.
157  AX=1.
158  AY=1.
159  AZ=1.
160  BA=1.
161  BB=1.
162  BC=1.
163  BD=1.
164  BE=1.
165  BF=1.
166  BG=1.
167  BH=1.
168  BI=1.
169  BJ=1.
170  BK=1.
171  BL=1.
172  BM=1.
173  BN=1.
174  BO=1.
175  BP=1.
176  BQ=1.
177  BR=1.
178  BS=1.
179  BT=1.
180  BU=1.
181  BV=1.
182  BW=1.
183  BX=1.
184  BY=1.
185  BZ=1.
186  CA=1.
187  CB=1.
188  CC=1.
189  CD=1.
190  CE=1.
191  CF=1.
192  CG=1.
193  CH=1.
194  CI=1.
195  CJ=1.
196  CK=1.
197  CL=1.
198  CM=1.
199  CN=1.
200  CO=1.
201  CP=1.
202  CQ=1.
203  CR=1.
204  CS=1.
205  CT=1.
206  CU=1.
207  CV=1.
208  CW=1.
209  CX=1.
210  CY=1.
211  CZ=1.
212  DA=1.
213  DB=1.
214  DC=1.
215  DD=1.
216  DE=1.
217  DF=1.
218  DG=1.
219  DH=1.
220  DI=1.
221  DJ=1.
222  DK=1.
223  DL=1.
224  DM=1.
225  DN=1.
226  DO=1.
227  DP=1.
228  DQ=1.
229  DR=1.
230  DS=1.
231  DT=1.
232  DU=1.
233  DV=1.
234  DW=1.
235  DX=1.
236  DY=1.
237  DZ=1.
238  EA=1.
239  EB=1.
240  EC=1.
241  ED=1.
242  EE=1.
243  EF=1.
244  EG=1.
245  EH=1.
246  EI=1.
247  EJ=1.
248  EK=1.
249  EL=1.
250  EM=1.
251  EN=1.
252  EO=1.
253  EP=1.
254  EQ=1.
255  ER=1.
256  ES=1.
257  ET=1.
258  EU=1.
259  EV=1.
260  EW=1.
261  EX=1.
262  EY=1.
263  EZ=1.
264  FA=1.
265  FB=1.
266  FC=1.
267  FD=1.
268  FE=1.
269  FF=1.
270  FG=1.
271  FH=1.
272  FI=1.
273  FJ=1.
274  FK=1.
275  FL=1.
276  FM=1.
277  FN=1.
278  FO=1.
279  FP=1.
280  FQ=1.
281  FR=1.
282  FS=1.
283  FT=1.
284  FU=1.
285  FV=1.
286  FW=1.
287  FX=1.
288  FY=1.
289  FZ=1.
290  GA=1.
291  GB=1.
292  GC=1.
293  GD=1.
294  GE=1.
295  GF=1.
296  GG=1.
297  GH=1.
298  GI=1.
299  GJ=1.
300  GK=1.
301  GL=1.
302  GM=1.
303  GN=1.
304  GO=1.
305  GP=1.
306  GQ=1.
307  GR=1.
308  GS=1.
309  GT=1.
310  GU=1.
311  GV=1.
312  GW=1.
313  GX=1.
314  GY=1.
315  GZ=1.
316  HA=1.
317  HB=1.
318  HC=1.
319  HD=1.
320  HE=1.
321  HF=1.
322  HG=1.
323  HH=1.
324  HI=1.
325  HJ=1.
326  HK=1.
327  HL=1.
328  HM=1.
329  HN=1.
330  HO=1.
331  HP=1.
332  HQ=1.
333  HR=1.
334  HS=1.
335  HT=1.
336  HU=1.
337  HV=1.
338  HW=1.
339  HX=1.
340  HY=1.
341  HZ=1.
342  IA=1.
343  IB=1.
344  IC=1.
345  ID=1.
346  IE=1.
347  IF=1.
348  IG=1.
349  IH=1.
350  II=1.
351  IJ=1.
352  IK=1.
353  IL=1.
354  IM=1.
355  IN=1.
356  IO=1.
357  IP=1.
358  IQ=1.
359  IR=1.
360  IS=1.
361  IT=1.
362  IU=1.
363  IV=1.
364  IW=1.
365  IX=1.
366  IY=1.
367  IZ=1.
368  JA=1.
369  JB=1.
370  JC=1.
371  JD=1.
372  JE=1.
373  JF=1.
374  JG=1.
375  JH=1.
376  JI=1.
377  JJ=1.
378  JK=1.
379  JL=1.
380  JM=1.
381  JN=1.
382  JO=1.
383  JP=1.
384  JQ=1.
385  JR=1.
386  JS=1.
387  JT=1.
388  JU=1.
389  JV=1.
390  JW=1.
391  JX=1.
392  JY=1.
393  JZ=1.
394  KA=1.
395  KB=1.
396  KC=1.
397  KD=1.
398  KE=1.
399  KF=1.
400  KG=1.
401  KH=1.
402  KI=1.
403  KJ=1.
404  KK=1.
405  KL=1.
406  KM=1.
407  KN=1.
408  KO=1.
409  KP=1.
410  KQ=1.
411  KR=1.
412  KS=1.
413  KT=1.
414  KU=1.
415  KV=1.
416  KW=1.
417  KX=1.
418  KY=1.
419  KZ=1.
420  LA=1.
421  LB=1.
422  LC=1.
423  LD=1.
424  LE=1.
425  LF=1.
426  LG=1.
427  LH=1.
428  LI=1.
429  LJ=1.
430  LK=1.
431  LL=1.
432  LM=1.
433  LN=1.
434  LO=1.
435  LP=1.
436  LQ=1.
437  LR=1.
438  LS=1.
439  LT=1.
440  LU=1.
441  LV=1.
442  LW=1.
443  LX=1.
444  LY=1.
445  LZ=1.
446  MA=1.
447  MB=1.
448  MC=1.
449  MD=1.
450  ME=1.
451  MF=1.
452  MG=1.
453  MH=1.
454  MI=1.
455  MJ=1.
456  MK=1.
457  ML=1.
458  MM=1.
459  MN=1.
460  MO=1.
461  MP=1.
462  MQ=1.
463  MR=1.
464  MS=1.
465  MT=1.
466  MU=1.
467  MV=1.
468  MW=1.
469  MX=1.
470  MY=1.
471  MZ=1.
472  NA=1.
473  NB=1.
474  NC=1.
475  ND=1.
476  NE=1.
477  NF=1.
478  NG=1.
479  NH=1.
480  NI=1.
481  NJ=1.
482  NK=1.
483  NL=1.
484  NM=1.
485  NN=1.
486  NO=1.
487  NP=1.
488  NQ=1.
489  NR=1.
490  NS=1.
491  NT=1.
492  NU=1.
493  NV=1.
494  NW=1.
495  NX=1.
496  NY=1.
497  NZ=1.
498  OA=1.
499  OB=1.
500  OC=1.
501  OD=1.
502  OE=1.
503  OF=1.
504  OG=1.
505  OH=1.
506  OI=1.
507  OJ=1.
508  OK=1.
509  OL=1.
510  OM=1.
511  ON=1.
512  OO=1.
513  OP=1.
514  OQ=1.
515  OR=1.
516  OS=1.
517  OT=1.
518  OU=1.
519  OV=1.
520  OW=1.
521  OX=1.
522  OY=1.
523  OZ=1.
524  PA=1.
525  PB=1.
526  PC=1.
527  PD=1.
528  PE=1.
529  PF=1.
530  PG=1.
531  PH=1.
532  PI=1.
533  PJ=1.
534  PK=1.
535  PL=1.
536  PM=1.
537  PN=1.
538  PO=1.
539  PP=1.
540  PQ=1.
541  PR=1.
542  PS=1.
543  PT=1.
544  PU=1.
545  PV=1.
546  PW=1.
547  PX=1.
548  PY=1.
549  PZ=1.
550  QA=1.
551  QB=1.
552  QC=1.
553  QD=1.
554  QE=1.
555  QF=1.
556  QG=1.
557  QH=1.
558  QI=1.
559  QJ=1.
560  QK=1.
561  QL=1.
562  QM=1.
563  QN=1.
564  QO=1.
565  QP=1.
566  QQ=1.
567  QR=1.
568  QS=1.
569  QT=1.
570  QU=1.
571  QV=1.
572  QW=1.
573  QX=1.
574  QY=1.
575  QZ=1.
576  RA=1.
577  RB=1.
578  RC=1.
579  RD=1.
580  RE=1.
581  RF=1.
582  RG=1.
583  RH=1.
584  RI=1.
585  RJ=1.
586  RK=1.
587  RL=1.
588  RM=1.
589  RN=1.
590  RO=1.
591  RP=1.
592  RQ=1.
593  RR=1.
594  RS=1.
595  RT=1.
596  RU=1.
597  RV=1.
598  RW=1.
599  RX=1.
600  RY=1.
601  RZ=1.
602  SA=1.
603  SB=1.
604  SC=1.
605  SD=1.
606  SE=1.
607  SF=1.
608  SG=1.
609  SH=1.
610  SI=1.
611  SJ=1.
612  SK=1.
613  SL=1.
614  SM=1.
615  SN=1.
616  SO=1.
617  SP=1.
618  SQ=1.
619  SR=1.
620  SS=1.
621  ST=1.
622  SU=1.
623  SV=1.
624  SW=1.
625  SX=1.
626  SY=1.
627  SZ=1.
628  TA=1.
629  TB=1.
630  TC=1.
631  TD=1.
632  TE=1.
633  TF=1.
634  TG=1.
635  TH=1.
636  TI=1.
637  TJ=1.
638  TK=1.
639  TL=1.
640  TM=1.
641  TN=1.
642  TO=1.
643  TP=1.
644  TQ=1.
645  TR=1.
646  TS=1.
647  TT=1.
648  TU=1.
649  TV=1.
650  TW=1.
651  TX=1.
652  TY=1.
653  TZ=1.
654  UA=1.
655  UB=1.
656  UC=1.
657  UD=1.
658  UE=1.
659  UF=1.
660  UG=1.
661  UH=1.
662  UI=1.
663  UJ=1.
664  UK=1.
665  UL=1.
666  UM=1.
667  UN=1.
668  UO=1.
669  UP=1.
670  UQ=1.
671  UR=1.
672  US=1.
673  UT=1.
674  UY=1.
675  UZ=1.
676  VA=1.
677  VB=1.
678  VC=1.
679  VD=1.
680  VE=1.
681  VF=1.
682  VG=1.
683  VH=1.
684  VI=1.
685  VJ=1.
686  VK=1.
687  VL=1.
688  VM=1.
689  VN=1.
690  VO=1.
691  VP=1.
692  VQ=1.
693  VR=1.
694  VS=1.
695  VT=1.
696  VU=1.
697  VV=1.
698  VW=1.
699  VX=1.
700  VY=1.
701  VZ=1.
702  WA=1.
703  WB=1.
704  WC=1.
705  WD=1.
706  WE=1.
707  WF=1.
708  WG=1.
709  WH=1.
710  WI=1.
711  WJ=1.
712  WK=1.
713  WL=1.
714  WM=1.
715  WN=1.
716  WO=1.
717  WP=1.
718  WQ=1.
719  WR=1.
720  WS=1.
721  WT=1.
722  WU=1.
723  WV=1.
724  WW=1.
725  WX=1.
726  WY=1.
727  WZ=1.
728  XA=1.
729  XB=1.
730  XC=1.
731  XD=1.
732  XE=1.
733  XF=1.
734  XG=1.
735  XH=1.
736  XI=1.
737  XJ=1.
738  XK=1.
739  XL=1.
740  XM=1.
741  XN=1.
742  XO=1.
743  XP=1.
744  XQ=1.
745  XR=1.
746  XS=1.
747  XT=1.
748  XU=1.
749  XV=1.
750  XW=1.
751  XX=1.
752  XY=1.
753  XZ=1.
754  YA=1.
755  YB=1.
756  YC=1.
757  YD=1.
758  YE=1.
759  YF=1.
760  YG=1.
761  YH=1.
762  YI=1.
763  YJ=1.
764  YK=1.
765  YL=1.
766  YM=1.
767  YN=1.
768  YO=1.
769  YP=1.
770  YQ=1.
771  YR=1.
772  YS=1.
773  YT=1.
774  YU=1.
775  YV=1.
776  YW=1.
777  YX=1.
778  YY=1.
779  YZ=1.
780  ZA=1.
781  ZB=1.
782  ZC=1.
783  ZD=1.
784  ZE=1.
785  ZF=1.
786  ZG=1.
787  ZH=1.
788  ZI=1.
789  ZJ=1.
790  ZK=1.
791  ZL=1.
792  ZM=1.
793  ZN=1.
794  ZO=1.
795  ZP=1.
796  ZQ=1.
797  ZR=1.
798  ZS=1.
799  ZT=1.
800  ZU=1.
801  ZV=1.
802  ZW=1.
803  ZX=1.
804  ZY=1.
805  ZZ=1.
806  AA=1.
807  AB=1.
808  AC=1.
809  AD=1.
810  AE=1.
811  AF=1.
812  AG=1.
813  AH=1.
814  AI=1.
815  AJ=1.
816  AK=1.
817  AL=1.
818  AM=1.
819  AN=1.
820  AO=1.
821  AP=1.
822  AQ=1.
823  AR=1.
824  AS=1.
825  AT=1.
826  AU=1.
827  AV=1.
828  AW=1.
829  AX=1.
830  AY=1.
831  AZ=1.
832  BA=1.
833  BB=1.
834  BC=1.
835  BD=1.
836  BE=1.
837  BF=1.
838  BG=1.
839  BH=1.
840  BI=1.
841  BJ=1.
842  BK=1.
843  BL=1.
844  BM=1.
845  BN=1.
846  BO=1.
847  BP=1.
848  BQ=1.
849  BR=1.
850  BS=1.
851  BT=1.
852  BU=1.
853  BV=1.
854  BW=1.
855  BX=1.
856  BY=1.
857  BZ=1.
858  CA=1.
859  CB=1.
860  CC=1.
861  CD=1.
862  CE=1.
863  CF=1.
864  CG=1.
865  CH=1.
866  CI=1.
867  CJ=1.
868  CK=1.
869  CL=1.
870  CM=1.
871  CN=1.
872  CO=1.
873  CP=1.
874  CQ=1.
875  CR=1.
876  CS=1.
877  CT=1.
878  CU=1.
879  CV=1.
880  CW=1.
881  CX=1.
882  CY=1.
883  CZ=1.
884  DA=1.
885  DB=1.
886  DC=1.
887  DD=1.
888  DE=1.
889  DF=1.
890  DG=1.
891  DH=1.
892  DI=1.
893  DJ=1.
894  DK=1.
895  DL=1.
896  DM=1.
897  DN=1.
898  DO=1.
899  DP=1.
900  DQ=1.
901  DR=1.
902  DS=1.
903  DT=1.
904  DU=1.
905  DV=1.
906  DW=1.
907  DX=1.
908  DY=1.
909  DZ=1.
910  EA=1.
911  EB=1.
912  EC=1.
913  ED=1.
914  EE=1.
915  EF=1.
916  EG=1.
917  EH=1.
918  EI=1.
919  EJ=1.
920  EK=1.
921  EL=1.
922  EM=1.
923  EN=1.
924  EO=1.
925  EP=1.
926  EQ=1.
927  ER=1.
928  ES=1.
929  ET=1.
930  EU=1.
931  EV=1.
932  EW=1.
933  EX=1.
934  EY=1.
935  EZ=1.
936  FA=1.
937  FB=1.
938  FC=1.
939  FD=1.
940  FE=1.
941  FF=1.
942  FG=1.
943  FH=1.
944  FI=1.
945  FJ=1.
946  FK=1.
947  FL=1.
948  FM=1.
949  FN=1.
950  FO=1.
951  FP=1.
952  FQ=1.
953  FR=1.
954  FS=1.
955  FT=1.
956  FU=1.
957  FV=1.
958  FW=1.
959  FX=1.
960  FY=1.
961  FZ=1.
962  GA=1.
963  GB=1.
964  GC=1.
965  GD=1.
966  GE=1.
967  GF=1.
968  GG=1.
969  GH=1.
970  GI=1.
971  GJ=1.
972  GK=1.
973  GL=1.
974  GM=1.
975  GN=1.
976  GO=1.
977  GP=1.
978  GQ=1.
979  GR=1.
980  GS=1.
981  GT=1.
982  GU=1.
983  GV=1.
984  GW=1.
985  GX=1.
986  GY=1.
987  GZ=1.
988  HA=1.
989  HB=1.
990  HC=1.
991  HD=1.
992  HE=1.
993  HF=1.
994  HG=1.
995  HH=1.
996  HI=1.
997  HJ=1.
998  HK=1.
999  HL=1.
1000  HM=1.
1001  HN=1.
1002  HO=1.
1003  HP=1.
1004  HQ=1.
1005  HR=1.
1006  HS=1.
1007  HT=1.
1008  HU=1.
1009  HV=1.
1010  HW=1.
1011  HX=1.
1012  HY=1.
1013  HZ=1.
1014  IA=1.
1015  IB=1.
1016  IC=1.
1017  ID=1.
1018  IE=1.
1019  IF=1.
1020  IG=1.
1021  IH=1.
1022  II=1.
1023  IJ=1.
1024  IK=1.
1025  IL=1.
1026  IM=1.
1027  IN=1.
1028  IO=1.
1029  IP=1.
1030  IQ=1.
1031  IR=1.
1032  IS=1.
1033  IT=1.
1034  IU=1.
1035  IV=1.
1036  IW=1.
1037  IX=1.
1038  IY=1.
1039  IZ=1.
1040  JA=1.
1041  JB=1.
1042  JC=1.
1043  JD=1.
1044  JE=1.
1045  JF=1.
1046  JG=1.
1047  JH=1.
1048  JI=1.
1049  JJ=1.
1050  JK=1.
1051  JL=1.
1052  JM=1.
1053  JN=1.
1054  JO=1.
1055  JP=1.
1056  JQ=1.
1057  JR=1.
1058  JS=1.
1059  JT=1.
1060  JU=1.
1061  JV=1.
1062  JW=1.
1063  JX=1.
1064  JY=1.
1065  JZ=1.
1066  KA=1.
1067  KB=1.
1068  KC=1.
1069  KD=1.
1070  KE=1.
1071  KF=1.
1072  KG=1.
1073  KH=1.
1074  KI=1.
1075  KJ=1.
1076  KL=1.
1077  KM=1.
1078  KN=1.
1079  KO=1.
1080  KP=1.
1081  KQ=1.
1082  KR=1.
1083  KS=1.
1084  KT=1.
1085  KU=1.
1086  KV=1.
1087  KW=1.
1088  KX=1.
1089  KY=1.
1090  KZ=1.
1091  LA=1.
1092  LB=1.
1093  LC=1.
1094  LD=1.
1095  LE=1.
1096  LF=1.
1097  LG=1.
1098  LH=1.
1099  LI=1.
1100  LJ=1.
1101  LK=1.
1102  LL=1.
1103  LM=1.
1104  LN=1.
1105  LO=1.
1106  LP=1.
1107  LQ=1.
1108  LR=1.
1109  LS=1.
1110  LT=1.
1111  LU=1.
1112  LV=1.
1113  LW=1.
1114  LX=1.
1115  LY=1.
1116  LZ=1.
1117  MA=1.
1118  MB=1.
1119  MC=1.
1120  MD=1.
1121  ME=1.
1122  MF=1.
1123  MG=1.
1124  MH=1.
1125  MI=1.
1126  MJ=1.
1127  MK=1.
1128  ML=1.
1129  MM=1.
1130  MN=1.
1131  MO=1.
1132  MP=1.
1133  MQ=1.
1134  MR=1.
1135  MS=1.
1136  MT=1.
1137  MU=1.
1138  MV=1.
1139  MW=1.
1140  MX=1.
1141  MY=1.
1142  MZ=1.
1143  NA=1.
1144  NB=1.
1145  NC=1.
1146  ND=1.
1147  NE=1.
1148  NF=1.
1149  NG=1.
1150  NH=1.
1151  NI=1.
1152  NJ=1.
1153  NK=1.
1154  NL=1.
1155  NM=1.
1156  NN=1.
1157  NO=1.
1158  NP=1.
1159  NQ=1.
1160  NR=1.
1161  NS=1.
1162  NT=1.
1163  NU=1.
1164  NV=1.
1165  NW=1.
1166  NX=1.
1167  NY=1.
1168  NZ=1.
1169  OA=1.
1170  OB=1.
1171  OC=1.
1172  OD=1.
1173  OE=1.
1174  OF=1.
1175  OG=1.
1176  OH=1.
1177  OI=1.
1178  OJ=1.
1179  OK=1.
1180  OL=1.
1181  OM=1.
1182  ON=1.
1183  OO=1.
1184  OP=1.
1185  OQ=1.
1186  OR=1.
1187  OS=1.
1188  OT=1.
1189  OU=1.
1190  OV=1.
1191  OW=1.
1192  OX=1.
1193  OY=1.
1194  OZ=1.
1195  PA=1.
1196  PB=1.
1197  PC=1.
1198  PD=1.
1199  PE=1.
1200  PF=1.
1201  PG=1.
1202  PH=1.
1203  PI=1.
1204  PJ=1.
1205  PK=1.
1206  PL=1.
1207  PM=1.
1208  PN=1.
1209  PO=1.
1210  PP=1.
1211  PQ=1.
1212  PR=1.
1213  PS=1.
1214  PT=1.
1215  PU=1.
1216  PV=1.
1217  PW=1.
1218  PX=1.
1219  PY=1.
1220  PZ=1.
1221  QA=1.
1222  QB=1.
1223  QC=1.
1224  QD=1.
1225  QE=1.
1226  QF=1.
1227  QG=1.
1228  QH=1.
1229  QI=1.
1230  QJ=1.
1231  QK=1.
1232  QL=1.
1233  QM=1.
1234  QN=1.
1235  QO=1.
1236  QP=1.
1237  QQ=1.
1238  QR=1.
1239  QS=1.
1240  QT=1.
1241  QU=1.
1242  QV=1.
1243  QW=1.
1244  QX=1.
1245  QY=1.
1246  QZ=1.
1247  RA=1.
1248  RB=1.
1249  RC=1.
1250  RD=1.
1251  RE=1.
1252  RF=1.
1253  RG=1.
1254  RH=1.
1255  RI=1.
1256  RJ=1.
1257  RK=1.
1258  RL=1.
1259  RM=1.
1260  RN=1.
1261  RO=1.
1262  RP=1.
1263  RQ=1.
1264  RR=1.
1265  RS=1.
1266  RT=1.
1267  RU=1.
1268  RV=1.
1269  RW=1.
1270  RX=1.
1271  RY=1.
1272  RZ=1.
1273  SA=1.
1274  SB=1.
1275  SC=1.
1276  SD=1.
1277  SE=1.
1278  SF=1.
1279  SG=1.
1280  SH=1.
1281  SI=1.
1282  SJ=1.
1283  SK=1.
1284  SL=1.
1285  SM=1.
1286  SN=1.
1287  SO=1.
1288  SP=1.
1289  SQ=1.
1290  SR=1.
1291  SS=1.
1292  ST=1.
1293  SU=1.
1294  SV=1.
1295  SW=1.
1296  SX=1.
1297  SY=1.
1298  SZ=1.
1299  TA=1.
1300  TB=1.
1301  TC=1.
1302  TD=1.
1303  TE=1.
1304  TF=1.
1305  TG=1.
1306  TH=1.
1307  TI=1.
1308  TJ=1.
1309  TK=1.
1310  TL=1.
1311  TM=1.
1312  TN=1.
1313  TO=1.
1314  TP=1.
1315  TQ=1.
1316  TR=1.
1317  TS=1.
1318  TU=1.
1319  TV=1.
1320  TW=1.
1321  TX=1.
1322  TY=1.
1323  TZ=1.
1324  UA=1.
1325  UB=1.
1326  UC=1.
1327  UD=1.
1328  UE=1.
1329  UF=1.
1330  UG=1.
1331  UH=1.
1332  UI=1.
1333  UJ=1.
1334  UK=1.
1335  UL=1.
1336  UM=1.
1337  UN=1.
1338  UO=1.
1339  UP=1.
1340  UQ=1.
1341  UR=1.
1342  US=1.
1343  UT=1.
1344  UY=1.
1345  UZ=1.
1346  VA=1.
1347  VB=1.
1348  VC=1.
1349  VD=1.
1350  VE=1.
1351  VF=1.
1352  VG=1.
1353  VH=1.
1354  VI=1.
1355  VJ=1.
1356  VK=1.
1357  VL=1.
1358  VM=1.
1359  VN=1.
1360  VO=1.
1361  VP=1.
1362  VQ=1.
1363  VR=1.
1364  VS=1.
1365  VT=1.
1366  VU=1.
1367  VV=1.
1368  VW=1.
1369  VX=1.
1370  VY=1.
1371  VZ=1.
1372  WA=1.
1373  WB=1.
1374  WC=1.
1375  WD=1.
1376  WE=1.
1377  WF=1.
1378  WG=1.
1379  WH=1.
1380  WI=1.
1381  WJ=1.
1382  WK=1.
1383  WL=1.

```


END

SYMBOLIC REFERENCE MAP (Rm33)

ENTRY POINTS
S TABIJDEF LINE
1REFERENCES
57

VARIABLES ON TYPE RELOCATION

433 A DOUBLE

434 A1 DOUBLE

435 AIP DOUBLE

436 ARS DOUBLE

437 B DOUBLE

438 BT DOUBLE

439 BIP DOUBLE

440 C1 REAL

441 C2 REAL

442 F DOUBLE

1200 FMULT DOUBLE

443 FP DOUBLE

444 FT DOUBLE

445 FMAX REAL

730 FIP DOUBLE

446 G DOUBLE

1206 GMULT DOUBLE

447 GP DOUBLE

448 GT DOUBLE

449 GMAX REAL

1056 GTP DOUBLE

450 I INTEGER

451 IABIJ INTEGER

1372 IMOL INTEGER

1210 JHOL INTEGER

453 K INTEGER

344 SORT3 REAL

454 XFACT DOUBLE

1212 XPI REAL

1402 YPI REAL

FILE NAMES

MODE

OUTPUT

FMT

WRITES

43

66

DEF LINE REFERENCES

26

2036

2037

2038

2039

2040

2041

2042

2043

2044

2045

2046

2047

2048

2049

2050

2051

2052

2053

2054

2055

2056

2057

2058

2059

2060

2061

2062

2063

2064

2065

2066

2067

2068

2069

2070

2071

2072

2073

2074

2075

2076

2077

2078

2079

2080

2081

2082

2083

2084

2085

2086

2087

2088

2089

2090

2091

2092

2093

2094

2095

2096

2097

2098

2099

2100

2101

2102

2103

2104

2105

2106

2107

2108

2109

2110

2111

2112

2113

2114

2115

2116

2117

2118

2119

2120

2121

2122

2123

2124

2125

2126

2127

2128

2129

2130

2131

2132

2133

2134

2135

2136

2137

2138

2139

2140

2141

2142

2143

2144

2145

2146

2147

2148

2149

2150

2151

2152

2153

2154

2155

2156

2157

2158

2159

2160

2161

2162

2163

2164

2165

2166

2167

2168

2169

2170

2171

2172

2173

2174

2175

2176

2177

2178

2179

2180

2181

2182

2183

2184

2185

2186

2187

2188

2189

2190

2191

2192

2193

2194

2195

2196

2197

2198

2199

2200

2201

2202

2203

2204

2205

2206

2207

2208

2209

2210

2211

2212

2213

2214

2215

2216

2217

2218

2219

2220

2221

2222

2223

2224

2225

2226

2227

2228

2229

2230

2231

2232

2233

2234

2235

2236

2237

2238

2239

2240

2241

2242

2243

2244

2245

2246

2247

2248

2249

2250

2251

2252

2253

2254

2255

2256

2257

2258

2259

2260

2261

2262

2263

2264

2265

2266

2267

2268

2269

2270

2271

2272

2273

2274

2275

2276

2277

2278

2279

2280

2281

2282

2283

2284

2285

2286

2287

2288

2289

2290

2291

2292

2293

2294

2295

2296

2297

2298

2299

2300

2301

2302

2303

2304

2305

2306

2307

2308

2309

2310

2311

2312

2313

2314

2315

2316

2317

2318

2319

2320

2321

2322

2323

2324

2325

2326

2327

2328

2329

2330

2331

2332

2333

2334

2335

2336

2337

2338

2339

2340

2341

2342

2343

2344

2345

2346

2347

2348

1 C

SUBROUTINE CFAC

C

COMMON /XFACT/XFACT(150),FT(43),GT(43),FTP(43),GTP(43),
* FMULT,GMULT,JHOL(2),XPI(120),YPI(120),JHOL(100)

C

DOUBLE PRECISION FMULT,FT,FTP,GMULT,GTP,XFACT

C

XFACT(1)=1
DO 100 I=2,150
100 XFACT(I)=XFACT(I-1)*I

C

999 RETURN
END

SYMBOLIC REFERENCE MAP (R=3)

ENTRY POINTS DEF LINE REFERENCES
2 CFAC 2 13

VARIABLES ON TYPE RELOCATION

1204 FMULT	DOUBLE	XFACT	REFS	4	7
430 FT	DOUBLE	ARRAY	REFS	4	7
730 FTP	DOUBLE	ARRAY	REFS	4	7
1206 GMULT	DOUBLE	XFACT	REFS	4	7
602 GT	DOUBLE	ARRAY	REFS	4	7
1056 GTP	DOUBLE	ARRAY	REFS	4	7
22 I	INTEGER	10111 DEFINED	REFS	10	
1372 JHOL	INTEGER	ARRAY	REFS	4	
1210 JHOL	INTEGER	ARRAY	REFS	4	
0 XFACT	DOUBLE	ARRAY	REFS	4	
1212 XPI	REAL	ARRAY	REFS	4	
1402 YPI	REAL	ARRAY	REFS	4	

STATEMENT LABELS DEF LINE REFERENCES

0 100	11	10
0 099	13	

LOOPS LABEL INDEX FROM-TO LENGTH PROPERTIES

13 100	1	10 11	50	INSTACK
--------	---	-------	----	---------

COMMON BLOCKS LENGTH MEMBERS - BYAS NAME(LENGTH)

XFACT	990	0 XFACT (300)
		472 FTP (66)
		646 GMULT (2)
		770 YPI (120)

STATISTICS

PROGRAM LENGTH	230	19
CM LABELED COMMON LENGTH	17368	990
CM LABELED COMMON CM USED	52000	

Appendix I
I-9THIS PAGE IS BEST QUALITY PRACTICABLE
FROM COPY FURNISHED TO DDG

1-800-610-6151

203

11

[illegible]

--	--	--	--	--

--	--	--	--

1

THIS PAGE IS BEST QUALITY PRACTICABLE
FROM COPY FURNISHED TO DDG

VARIABLES ON TYPE DOUBLE

RELOCATION P.P.

DEFN

DEFINED

EXTERNALS

CXP COMPLEX
IABJ INTEGER
IM2HP INTEGER

REFERENCES

1 LIBRARY
3 13
3 10

INLINE FUNCTIONS
CMPL COMPLEX

ARGO 2 INTRIN

DEF LINE REFERENCES

STATEMENT LABELS

100 970
105 000
105 000

DEF LINE REFERENCES

21 10 14
22 10 14

STATISTICS

PROGRAM LENGTH
330000 CHANGED

3320 150

Appendix I
I-14

THIS PAGE IS BEST QUALITY PRACTICABLE
FROM COPY FURNISHED TO DDG

THIS PAGE IS BEST QUALITY PRACTICABLE
FROM COPY FURNISHED TO DDC

Appendix I
I-15

134

SUBROUTINE IPLOT(ICMT,XLIXL,DIL00P,PATL00P)

COMMON /XFACT/XFACT(150),FT(43),GT(43),PT(43),STP(43),
FMULT,GMULT,JHOL(2),XPI(120),YPI(120),JHOL(100)

DOUBLE PRECISION XFACT,PT,GT,STP,FT,FMULT,GMULT
CALL TITLE(MN,100,N
115N,100,12,0.0)

MSG=7.
YMSG=9.
YMSG=25

ENCODE(100,111,IMOL,XLIXL
FORMAT(MIL, 0,0,0,1,0,0,0)

CALL MESSAGE(IMOL,100,XMSG,YMSG)

YMSG=YMSG-25

ENCODE(100,121,JHOL,DIL00P
FORMAT(MN, 0,0,0,1,0,0,0)

CALL MESSAGE(IMOL,100,XMSG,YMSG)

CALL GRAPH(0,1,0,0,2,0)

CALL CURVE(XPI,YPI,ICMT,0)

CALL ENDPL(0)

999 RETURN
END

SYMBOLIC REFERENCE MAP (R03)

ENTRY POINTS 4 IPLOT	DEF LINE 1	REFERENCES 26	RELOCATION F.P.
VARIABLES	SM	TYPE	
1204 DIL00P	REAL		
450 FMULT	DOUBLE		
450 FT	DOUBLE		
730 FIP	DOUBLE		
1206 GMULT	DOUBLE		
602 GT	DOUBLE		
1056 GTP	DOUBLE		
0 ICMT	INTEGER		
1572 IMOL	INTEGER		
1210 JHOL	INTEGER		
0 PATL00P	REAL		
0 XFACT	DOUBLE		
0 XLIXL	REAL		
142 XMSG	REAL		
1212 XPI	REAL		
143 YMSG	REAL		

REFS	17	DEFINED	1
REFS	3	7	
REFS	3	7	
REFS	3	7	
REFS	3	7	
REFS	3	7	
REFS	3	7	
REFS	25	DEFINED	1
REFS	3	15	
REFS	3	23	DEFINED
REFS	3	13	DEFINED
REFS	21	DEFINED	1
REFS	3	7	
REFS	13	DEFINED	1
REFS	15	19	
REFS	15	23	DEFINED
REFS	12	15	
REFS	16	19	20
REFS	12	20	23

VARIABLES ON TYPE REAL ARRAY XFACT RELOCATION DEFINED REFS

1002 YP1 25 10 12 20

EXTERNALS TYPE ARGO REFERENCES

CURVE 25
ENOPL 26
GRAPH 20
MESSAG 15
TITLE 0

STATEMENT LABELS DEF LINE REFERENCES

100 111 PNT 10 13
111 120 PNT 10 17
122 131 PNT 22 21
0 999 INACTIVE 20

COMMON BLOCKS LENGTH NUMBERS - DIAS NAME(LENGTH)

XFACT 999
0 XFACT (300)
072 YTP (06)
006 SMULT (2)
770 YP1 (120)
300 FT (06)
990 STP (06)
000 SMULT (2)
000 TMOU (100)
300 OF (06)
000 PMULT (2)
000 X21 (120)

STATISTICS

PROGRAM LENGTH 1340 100
CN LABELED COMMON LENGTH 17340 990
520000 CN USED

Appendix I
I-16

135

THIS PAGE IS BEST QUALITY PRACTICABLE
FROM COPY FURNISHED TO DDC

Appendix I
I-17THIS PAGE IS BEST QUALITY PRACTICABLE
FROM COPY FURNISHED TO DDC

CYBER LOADER 1.3-452 77/09/22, 14.00.11. PAGE 1

LOAD MAP - J087

FMA OF THE LOAD
LMA+1 OF THE LOAD111
57415

TRANSFER ADDRESS -- J087

5437

PROGRAM AND BLOCK ASSIGNMENTS.

BLOCK	ADDRESS	LENGTH	FILE	DATE	PROCESSOR VER	LEVEL	HARDWARE	COMMENTS
JFACT/	111	1736						
J087	2047	4317	LGO	77/09/22	FTN	4.6 452	666X 1	PROGRAM OPT01 TRACE
JABTJ	6366	472	LGO	77/09/22	FTN	4.6 452	666X 1	FUNCTION OPT01 TRACE
JFACT	7060	23	LGO	77/09/22	FTN	4.6 452	666X 1	SUBROUTINE OPT01 TRACE
JM2P	7103	1246	LGO	77/09/22	FTN	4.6 452	666X 1	FUNCTION OPT01 TRACE
J087	10351	232	LGO	77/09/22	FTN	4.6 452	666X 1	FUNCTION OPT01 TRACE
J087	10603	154	LGO	77/09/22	FTN	4.6 452	666X 1	SUBROUTINE OPT01 TRACE
J087	10757	573	UL-INH18	77/08/26	FTN	4.6 420	666X 1	OPT01
J087	11552	76	UL-INH18	77/08/26	FTN	4.6 420	666X 1	OPT01
J087	11650	41	UL-INH18	77/08/26	FTN	4.6 420	666X 1	OPT01
J087	11711	3	UL-D188PLA	76/03/29	FTN	4.5 410	666X 1	OPT01
J087	11714	70						
J087	12010	50						
J087	12060	72						
J087	12152	43						
J087	12215	5						
J087	12222	13						
J087	12235	4						
J087	12241	4						
J087	12245	2						
J087	12247	70						
J087	12337	11						
J087	12350	24						
J087	12374	1154	UL-D188PLA	76/03/29	FTN	4.5 410	666X 1	OPT01
J087	13550	11	UL-D188PLA	76/03/29	FTN	4.5 410	666X 1	OPT01
J087	13561	4	UL-D188PLA	76/03/29	FTN	4.5 410	666X 1	OPT01
J087	13565	22	UL-D188PLA	76/03/29	FTN	4.5 410	666X 1	OPT01
J087	13607	24	UL-D188PLA	76/03/29	FTN	4.5 410	666X 1	OPT01
J087	13633	2						
J087	13635	624	UL-D188PLA	76/03/29	FTN	4.5 410	666X 1	OPT01
J087	14461	162	UL-D188PLA	76/03/29	FTN	4.5 410	666X 1	OPT01
J087	14643	24	UL-D188PLA	76/03/29	FTN	4.5 410	666X 1	OPT01
J087	14667	43	UL-D188PLA	76/03/29	FTN	4.5 410	666X 1	OPT01
J087	14732	25	UL-D188PLA	76/03/29	COMPASS 3, 2-410			
J087	14757	17						
J087	14776	52	UL-D188PLA	76/03/29	FTN	4.5 410	666X 1	OPT01
J087	15050	710	UL-D188PLA	76/03/29	FTN	4.5 410	666X 1	OPT01
J087	15760	14	UL-D188PLA	76/03/29	FTN	4.5 410	666X 1	OPT01
J087	15774	67						
J087	16063	767	UL-D188PLA	76/03/29	FTN	4.5 410	666X 1	OPT01
J087	17052	133	UL-D188PLA	76/03/29	FTN	4.5 410	666X 1	OPT01
J087	17205	16	UL-D188PLA	76/03/29	FTN	4.5 410	666X 1	OPT01
J087	17223	101	UL-D188PLA	76/03/29	FTN	4.5 410	666X 1	OPT01
J087	17324	7						
J087	17333	117	UL-D188PLA	76/03/29	FTN	4.5 410	666X 1	OPT01

APPENDIX II

Computer program for the Hankel (16) Function
of second kind and one third order.

[illegible]

1 C FUNCTION IABJ(ARG,AI,BI,AIP,BIP)

COMMON /XFACT/XFACT(150),FT(43),GT(43),FTP(43),GTP(43),*
FMULT,GMULT,JMOL(2)

2 C DOUBLE PRECISION A,AI,AIP,ARG,B,BI,BIP,F,FMULT
DOUBLE PRECISION FP,FTP,FP,GMULT,GP,GT,GTP,XFACT

3 C DATA C1,C2,80RT3V,355020530,7390104037,1.732050808/

10 C PRINT 9,9 ARG,ARG

11 C IABJ=1

12 C A=1.

13 C B=1.

14 C F=1.

15 C G=ARG

16 C FP=0.

17 C GP=1.

18 C FTHAX=GTMAX=0

20 C DO 200 K=1,43

21 C A=ARG(30K-2)

22 C B=ARG(30K-1)

23 C FT(K)=A*ARG(30K)/XFACT(30K)

24 C GT(K)=B*ARG(30K+1)/XFACT(30K+1)

25 C IF(DABS(FT(K)).GT.ABS(FTMAX))FTMAX=DABS(FT(K))

26 C IF(DABS(GT(K)).GT.ABS(GTMAX))GTMAX=DABS(GT(K))

27 C F=FT(K)

28 C G=GT(K)

29 C FTP(K)=(3.0K)*A*ARG(30K-1)/XFACT(30K)

30 C GTP(K)=(3.0K+1)*B*ARG(30K)/XFACT(30K+1)

31 C FP=FP+FTP(K)

32 C GP=GP+GTP(K)

33 C PRINT 191,K,A,B,FT(K),GT(K),F,G,FTP(K),GTP(K),FP,GP

34 C FORMAT(13,1X,10D11.3)

35 C CONTINUE

36 C DO 202 I=1,5

37 C IF(1000.*DABS(FT(10+I)).LT.ABS(FTMAX).AND.

38 C 1000.*DABS(GT(10+I)).LT.ABS(GTMAX))GO TO 202

39 C GO TO 204

40 C CONTINUE

41 C GO TO 220

42 C PRINT 205,ARG,F,G

43 C FORMAT(n MORE ACC. REQUIRED IN AIRY CALC.,G,A,B ARG= 01010.3,/,

44 C n F= 0.015.6,/,n G= 0.015.6)

45 C PRINT 206,(1,FT(1),GT(1),101,03)

46 C FORMAT(15,2D15.6)

47 C IABJ=1

48 C GO TO 999

49 C A=C10F-C20G

50 C AIBORT30(C10F+C20G)

51 C AIP=C10F-C20G

52 C BIP=ORT30(C10F+C20G)

53 C PRINT 211,K,A,B,F,G,FP,GP,AI,BI,AIP,BIP

54 C FORMAT(n K,A,B,F,G,FP,GP,AI,BI,AIP,BIP,/,

55 C 13,2X,10D10.3)

56 C RETURN

142
Appendix II
II-5

THIS PAGE IS BEST QUALITY PRACTICABLE
FROM COPY FURNISHED TO DDG

END

SYNOPSIS: DVM: JCHENGL30 21 NOV 68 (REV) 1003

[illegible]

STATEMENT LABELS				DEF LINE		REFERENCES	
260 202	41	37	30				
265 204	43	40					
376 205	44	43					
420 206	47	46					
423 211	55						
310 220	50	42					
352 999	57	49					

LOOPS LABEL				FROM-TO		LENGTH		PROPERTIES	
34 200	0 1	21 36	2018						
237 202	0 1	37 41	248					EXT REFS	
272	0 1	46 46	118					EXT REFS	

COMMON BLOCKS				LENGTH		MEMBERS		DIAS NAME(LENGTH)	
COMMON XFACT	650								

STATISTICS				LENGTH		MEMBERS		DIAS NAME(LENGTH)	
PROGRAM LENGTH	4728	314							
ON-LABELS-COMMON-LENGTH	13130	650							
ON-LABELS-COMMON-LENGTH	13130	650							

COMMON BLOCKS				LENGTH		MEMBERS		DIAS NAME(LENGTH)	
COMMON XFACT	650								

COMMON BLOCKS				LENGTH		MEMBERS		DIAS NAME(LENGTH)	
COMMON XFACT	650								

COMMON BLOCKS				LENGTH		MEMBERS		DIAS NAME(LENGTH)	
COMMON XFACT	650								

COMMON BLOCKS				LENGTH		MEMBERS		DIAS NAME(LENGTH)	
COMMON XFACT	650								

COMMON BLOCKS				LENGTH		MEMBERS		DIAS NAME(LENGTH)	
COMMON XFACT	650								

COMMON BLOCKS				LENGTH		MEMBERS		DIAS NAME(LENGTH)	
COMMON XFACT	650								

COMMON BLOCKS				LENGTH		MEMBERS		DIAS NAME(LENGTH)	
COMMON XFACT	650								

COMMON BLOCKS				LENGTH		MEMBERS		DIAS NAME(LENGTH)	
COMMON XFACT	650								

Appendix II
II-7

144

THIS PAGE IS BEST QUALITY PRACTICABLE
FROM COPY FURNISHED TO DDG

300 FT (06)
550 GTP (06)
600 PHUL T (2)

300 FT (06)
550 GTP (06)
600 JNOL (2)

0 XFACT (300)
472 FTP (06)
600 CHUL T (2)

4728 314
13130 650

520000 CH USED

SUBROUTINE CFACT

COMMON /XFACT/XFACT(150),PT(43),ST(43),PTD(43),STP(43),
PMULT,CMULT,CMOL(2)

DOUBLE PRECISION PMULT,PTPTD,CMULT,ST,STP,XFACT

XFACT(150)
DO 100 I=2,150
100 XFACT(I)=XFACT(I-1)*IRETURN
END

SYMBOLIC REFERENCE MAP (R03)

ENTRY POINTS DEF LINE REFERENCES
2 CFACT 2 13

VARIABLES SM TYPE RELOCATION

1204 PMULT	DOUBLE	XFACT	REFS
054 PT	DOUBLE	ARRAY	REFS
730 PTP	DOUBLE	ARRAY	REFS
1206 CMULT	DOUBLE	XFACT	REFS
002 GT	DOUBLE	ARRAY	REFS
1056 STP	DOUBLE	ARRAY	REFS
22 I	INTEGER	XFACT	REFS
1210 JCOL	INTEGER	ARRAY	REFS
0 XFACT	DOUBLE	ARRAY	REFS

STATEMENT LABELS DEF LINE REFERENCES

0 100	11	10
0 999	INACTIVE	13

LOOPS LABEL INDEX FROM-TO LENGTH PROPERTIES

13 100	1	10 11	58	INSTACK
--------	---	-------	----	---------

COMMON BLOCKS LENGTH MEMBERS - DIAS NAME(LENGTH)

XFACT	650	0 XFACT	13005
		472 PTP	1065
		646 CMULT	12

STATISTICS

PROGRAM LENGTH	235	19
CH LABELED COMMON LENGTH	12125	650
CH LABELED CM USED	520008	

Appendix II
II-8THIS PAGE IS BEST QUALITY PRACTICABLE
FROM COPY FURNISHED TO DDC


```
1 C FUNCTION IN2M2P(ARG,M2,M2P)
2 C COMMON /XFACT/XFACT(150),PT(43),GT(43),PTP(43),GTP(43),
3 C * PMULT,GMULT,JHOL(2)
4 C DIMENSION MFT(43),MGT(43),MFTP(43),MGTTP(43)
5 C COMPLEX ARG,MFT,MGT,MFTP,MGTP,P,G,PP,OP,
6 C * PT,GT,FTP,GTP,MC,MPC
7 C DOUBLE PRECISION A,B,PMULT,GMULT
8 C DOUBLE PRECISION M2,M2P,XFACT
9 C DATA SORTS/1.732050808/
10 C PRINT 0,M ARG,M,ARG
11 C PRINT 0,M M2P,M2P
12 C DO 300 J=1,13
13 C DN 300 I=1,13
14 C X=7,0,18
15 C Y=-7,0,18
16 C IF(X.EQ.0.AND.Y.EQ.0)GO TO 300
17 C ARG=CMPLX(X,Y)
18 C IN2M2P=1
19 C A=1.
20 C B=1.
21 C F=1.
22 C G=ARG
23 C FP=0.
24 C GP=1.
25 C HFTMAX=0.
26 C MGTMAX=0.
27 C DN 200 K=1,43
28 C A=AS(30K-2)
29 C B=BS(30K-1)
30 C MFTN=((-1,30K)0A/XFACT(30K)
31 C MFTK)=HFTN*ARG00(30K)
32 C MGTN=((-1,30K)0B/XFACT(30K+1)
33 C MGTK)=MGTN*ARG00(30K+1)
34 C IF(CABS(MFT(K)),GT,ABS(HFTMAX))HFTMAX=CABS(MFT(K))
35 C IF(CABS(MGT(K)),GT,ABS(MGTMAX))MGTMAX=CABS(MGT(K))
36 C F=F+HFT(K)
37 C G=G+MGT(K)
38 C MFTP(K)=((-1,30K)0A/XFACT(30K)
39 C MGTTP(K)=MFTP(K)*ARG00(30K-1)
40 C MGTTP(K)=((-1,30K)0B/XFACT(30K+1)
41 C MGTTP(K)=MGTTP(K)*ARG00(30K)
42 C PP=PP+HFTP(K)
43 C GP=GP+MGTTP(K)
44 C PRINT 191,K,A,B,MFT(K),MGT(K),P,G,PP,GP,MFTP(K),MGTTP(K),PTP,OP
45 C FORMAT(13,1X,10I1,3)
46 C CONTINUE
47 C DO 202 I=1,5
48 C IF(1000,0CABS(MFT(30+1)),LT,ABS(HFTMAX),AND,
49 C * 1000,0CABS(MGT(30+1)),LT,ABS(MGTMAX))GO TO 202
```

Appendix II
II-9

146

THIS PAGE IS BEST QUALITY PRACTICABLE
FROM COPY FURNISHED TO DDG


```

60 TO 204
CONTINUE
60 TO 220
204 PRINT 205,ARG,P,B
205 FORMAT(MORE ACC. REQUIRED IN INH2P CALC.,P,B ARG 0,2010,317,
  * P,B,2015,0,0,0,0,0,2015,0)
PRINT 206,(I,M,T(1),M,T(2),M,T(3),I,0,0,0,0)
206 FORMAT(15,0515,0)
INH2P=1
60 TO 999
207 F=HULTOP
208 G=HULTOP
F=F+HULTOP
G=G+HULTOP
H2=CABS(MC)
H2=CABS(MC)
H2=CABS(MC)
210 PRINT 211,M,A,B,P,0,0,P,0,P,H2,H2,P,0,0
211 FORMAT(M,A,B,P,0,0,P,0,P,H2,H2,P,0,0,
  * 13,2X,0010,3)
PRINT 301,ARG,MC,MPC
300 CONTINUE
301 FORMAT(13,IN(,2015,0,2M,1))
STOP
999 RETURN
END

```

Appendix II II-10

THIS PAGE IS BEST QUALITY PRACTICABLE
FROM COPY FURNISHED TO DDC

SYMBOLIC REFERENCE MAP (RMS)

ENTRY POINTS DEF LINE REFERENCES

5 INH2P

03

RELOCATION

F.P.

TYPE

SH

DEF LINE

REFERENCES

5 INH2P

03

TYPE

SH

DEF LINE

REFERENCES

5 INH2P

03

TYPE

SH

DEF LINE

REFERENCES

5 INH2P

03

TYPE

SH

DEF LINE

REFERENCES

5 INH2P

03

TYPE

SH

DEF LINE

REFERENCES

5 INH2P

03

TYPE

SH

DEF LINE

REFERENCES

5 INH2P

03

TYPE

SH

DEF LINE

REFERENCES

5 INH2P

03

TYPE

SH

DEF LINE

REFERENCES

5 INH2P

03

TYPE

SH

DEF LINE

REFERENCES

5 INH2P

03

TYPE

SH

DEF LINE

REFERENCES

5 INH2P

03

TYPE

SH

DEF LINE

REFERENCES

5 INH2P

03

TYPE

SH

DEF LINE

REFERENCES

5 INH2P

03

TYPE

SH

DEF LINE

REFERENCES

5 INH2P

03

TYPE

SH

DEF LINE

REFERENCES

5 INH2P

03

TYPE

SH

DEF LINE

REFERENCES

5 INH2P

03

TYPE

SH

DEF LINE

REFERENCES

5 INH2P

03

TYPE

SH

DEF LINE

REFERENCES

5 INH2P

03

TYPE

SH

DEF LINE

REFERENCES

5 INH2P

03

TYPE

SH

DEF LINE

REFERENCES

5 INH2P

03

TYPE

SH

DEF LINE

REFERENCES

5 INH2P

03

TYPE

SH

DEF LINE

REFERENCES

5 INH2P

03

TYPE

SH

DEF LINE

REFERENCES

5 INH2P

03

TYPE

SH

DEF LINE

REFERENCES

5 INH2P

03

TYPE

SH

DEF LINE

REFERENCES

5 INH2P

03

TYPE

SH

DEF LINE

REFERENCES

5 INH2P

03

TYPE

SH

DEF LINE

REFERENCES

5 INH2P

03

TYPE

SH

DEF LINE

REFERENCES

5 INH2P

03

TYPE

SH

DEF LINE

REFERENCES

5 INH2P

03

TYPE

SH

DEF LINE

REFERENCES

5 INH2P

03

TYPE

SH

DEF LINE

REFERENCES

5 INH2P

03

TYPE

SH

DEF LINE

REFERENCES

5 INH2P

03

TYPE

SH

DEF LINE

REFERENCES

5 INH2P

03

TYPE

SH

DEF LINE

REFERENCES

5 INH2P

03

TYPE

SH

DEF LINE

REFERENCES

5 INH2P

03

TYPE

SH

DEF LINE

REFERENCES

5 INH2P

03

TYPE

SH

DEF LINE

REFERENCES

5 INH2P

03

TYPE

SH

DEF LINE

REFERENCES

5 INH2P

03

TYPE

SH

DEF LINE

REFERENCES

5 INH2P

03

TYPE

SH

DEF LINE

REFERENCES

5 INH2P

03

TYPE

SH

DEF LINE

REFERENCES

5 INH2P

03

TYPE

SH

DEF LINE

REFERENCES

5 INH2P

03

TYPE

SH

DEF LINE

REFERENCES

5 INH2P

03

TYPE

SH

DEF LINE

REFERENCES

5 INH2P

03

TYPE

SH

DEF LINE

REFERENCES

5 INH2P

03

TYPE

SH

DEF LINE

REFERENCES

5 INH2P

03

TYPE

SH

DEF LINE

REFERENCES

5 INH2P

03

TYPE

SH

DEF LINE

REFERENCES

5 INH2P

03

TYPE

SH

DEF LINE

REFERENCES

5 INH2P

03

TYPE

SH

DEF LINE

REFERENCES

5 INH2P

03

VARIABLES ON TYPE COMPLEX ARRAY

VARIABLES	ON	TYPE	COMPLEX	ARRAY	REFS	DEFINED	0	2042	44	56	64
554 MPT					REFS	DEFINED	30				
547 MTK		REAL			REFS	DEFINED	30				
540 MTHAX		REAL			REFS	DEFINED	42		32	42	
1030 MTP		COMPLEX		ARRAY	REFS	DEFINED	6		50	47	
551 MTPS		REAL			REFS	DEFINED	47		46		
702 MGT		COMPLEX		ARRAY	REFS	DEFINED	6		2043	56	64
550 MGTK		REAL			REFS	DEFINED	41				
545 MGTMAX		REAL			REFS	DEFINED	41		40		
1156 MGT		COMPLEX		ARRAY	REFS	DEFINED	43		33	43	
552 MGTKP		REAL			REFS	DEFINED	6		51	49	
532 MTK		COMPLEX			REFS	DEFINED	49		40		
0 M2		DOUBLE			REFS	DEFINED	8		79	73	
0 M2P		DOUBLE			REFS	DEFINED	12		74		
553 I		INTEGER			REFS	DEFINED	2054		55	64	
517 IN2M2P		INTEGER			REFS	DEFINED	25				
541 I0		INTEGER			REFS	DEFINED	21		20		
1210 JML		INTEGER		ARRAY	REFS	DEFINED	3				
540 J0		INTEGER			REFS	DEFINED	22		19		
546 K		INTEGER			REFS	DEFINED	36		2046	2040	2040
426 SORT3		REAL			REFS	DEFINED	44		45	3046	3046
542 X		REAL			REFS	DEFINED	72		14		
0 XFACT		DOUBLE			REFS	DEFINED	23		21	46	48
543 Y		REAL			REFS	DEFINED	3		30		

Appendix II-11

THIS PAGE IS BEST QUALITY PRACTICALLY FROM COPY FURNISHED TO DUC

FILE NAMES MODE MIXED

EXTERNALS	CARG	TYPE	ARGO	LIBRARY	2042	2043	2054	74	75
433 191		REAL			REFS	DEFINED	41	64	79

INLINE FUNCTIONS

ARG	TYPE	ARGO	DEF LINE	REFERENCES
1	REAL	1	INTRIN	43
2	COMPLEX	2	INTRIN	72

STATEMENT LABELS

DEF LINE	REFERENCES
0 100	INACTIVE 35
433 191	FMT NO REFS 53
0 200	54
305 202	55
312 204	56
444 205	61
466 206	62
471 211	65
535 220	64
374 300	60
505 301	19
405 999	81
	83

LOOPS LABEL

INDEX	FROM-TO	LENGTH	PROPERTIES
0 J0	19 40	3570	EXT REFS EXT REFS NOT INNER
0 J0	20 40	3520	EXT REFS EXT REFS NOT INNER
0 K	35 54	2130	EXT REFS EXT REFS
0 I	55 59	230	EXT REFS EXT REFS

149

Appendix II
II-12

THIS PAGE IS BEST QUALITY PRACTICABLE
FROM COPY FURNISHED TO ADG

PAGE 8

77/00/16, 00.00.30

FTN 4.00458

73/74 OPTIM TRACE

FUNCTION INCH27

EXT DEFS

PROPERTIES

LENGTH

FROM-TO

INDEX

LABEL

317

MEMBERS - STAS NAME(LENGTH)

LENGTH

COMMON BLOCKS

STACT

300 PT (063)

550 STP (063)

472 PTP (063)

646 CMULT (23)

0 STACT (3003)

0 STACT (3003)

300 PT (063)

9747107120

PROGRAM LENGTH

CM LABELED COMMON LENGTH

13270

13270

650

650

650

650

650

FUNCTION 16A1(800,820,800,PI,PAJ,OILOOP,C1,XNUM,XDEN)

COMPI EX 920

COMPLETION
COUPLE PRECISION H2.H2P.EYP.EYM.800.800.800.800

DOUBLE PRECISION AOP, AOP, AOP, AOP, AOP, AOP, AOP, AOP

DOUBLE PRECISION XMM, XMM, CI, PA3

0-121181

82D=5000EXP(CMPLX(0.2,PI/3),90PA3002

IF(1H2112P(82D,H2,H2P),WE.1)GO TO 970

ЭУРЭНЭ/НЭР

800-800-0100 (1-800-800-0100)

IF(IABIJ(-500,400,500,400,500),NE.1)GO TO 970

04-018917-ME. (4000V.0000V.0000V) CIVILIAN

[illegible]

0000-0000-0000-0000

1-800-4-A-RENTAL

CO TO 000
IDENTIFICATION NUMBER

03

1948150-1

2

RESULTS

Appendix II
II-13

THIS PAGE IS BEST-QUALITY PRACTICABLE
FROM COPY FURNISHED TO DDC

~~SYMBOLIC REFERENCE MAP (R03)~~

ENTRY POINTS	DEF LINE	REFERENCE	RELOCATION
5	1	23	
ISUB1			
VARIABLES	SN	TYPE	
212 A00		DOUBLE	
216 A00P		DOUBLE	
222 A00		DOUBLE	
224 A00P		DOUBLE	
214 H00		DOUBLE	
220 H00P		DOUBLE	
224 B00		DOUBLE	
230 B00P		DOUBLE	
0 C1		DOUBLE	
0 O100P		REAL	
210 EYN		DOUBLE	
206 EYP		DOUBLE	
202 H2		DOUBLE	
204 H2P		DOUBLE	
201 ISUB1		INTEGER	
0 P13		DOUBLE	
0 P1		REAL	
0 S00		DOUBLE	
0 S000		DOUBLE	
0 S20		COMPLEX	
0 S20N		DOUBLE	

CHARS	CH	TYPE	DOUBLE	RELOCATION	F.P.	REFS
0	INUN	DOUBLE			0	DEFINED 1 16

TERMS	TYPE	ARGS	REFERENCES
COMP	COMPLEX	1 LIBRARY	9
INTJ	INTEGER	5	13
INTK29	INTEGER	3	10

LINE FUNCTIONS	TYPE	ARGS	DEF LINE	REFERENCES
CMPL	COMPLEX	2 INTRN		9

STATEMENT LABELS	DEF LINE	REFERENCES
200 070	21	10
205 090	23	19

PROGRAM LENGTH	32000 CH USED
2328	130

Appendix II
II-14

THIS PAGE IS BEST QUALITY PRACTICABLE
FROM COPY FURNISHED TO DDG

A decorative rectangular border with a repeating scroll-like pattern surrounds the central text.

MISSION of Rome Air Development Center

RADC plans and conducts research, exploratory and advanced development programs in command, control, and communications (C³) activities, and in the C³ areas of information sciences and intelligence. The principal technical mission areas are communications, electromagnetic guidance and control, surveillance of ground and aerospace objects, intelligence data collection and handling, information system technology, ionospheric propagation, solid state sciences, microwave physics and electronic reliability, maintainability and compatibility.